Doctoral Thesis

Quantification of diffuse phosphorous inputs into surface water systems

submitted in satisfaction of the requirements for the degree of
Doctor of Science in Civil Engineering
of the Vienna University of Technology, Faculty of Civil Engineering

as part of the
Vienna Doctoral Programme on Water Resource Systems

by

Ádám Kovács, MSc.

Examiners:

Prof. Matthias Zessner-Spitzenberg, MSc. PhD.
Institute for Water Quality, Resources and Waste Management
Vienna University of Technology

Assoc. Prof. Kálmán Buzás, MSc. PhD.
Department of Sanitary and Environmental Engineering
Budapest University of Technology and Economics

Prof. Günter Blöschl, MSc. PhD.
Institute of Hydraulic Engineering and Water Resources Management
Vienna University of Technology

Vienna, April 2013

Dissertation

Quantifizierung der diffusen Phosphoreinträge in die Oberflächengewässer

ausgeführt zum Zwecke der Erlangung des akademischen Grades eines
Doktors der technischen Wissenschaft
eingereicht an der Technischen Universität Wien Fakultät für Bauingenieurwesen

im Rahmen des
Vienna Doctoral Programme on Water Resource Systems

von

Dipl.-Ing. Ádám Kovács

Prüfer:

Ao.Univ.Prof. Dipl.-Ing. Dr.techn. Matthias Zessner-Spitzenberg
Institut für Wassergüte, Ressourcenmanagement und Abfallwirtschaft
Technische Universität Wien

Assoz.Univ.Prof. Dipl.-Ing. Dr.techn. Kálmán Buzás
Institut für Siedlungswasserwirtschaft und Umwelttechnik
Technische und Wirtschaftswissenschaftliche Universität Budapest

Univ.Prof. Dipl.-Ing. Dr.techn. Günter Blöschl
Institut für Wasserbau und Ingenieurhydrologie
Technische Universität Wien

Wien, April 2013

Abstract

Cost-effective management of phosphorus emissions to ensure sustainable agricultural production and good ecological status of water bodies is a highly relevant issue in watershed management. Policy making is often hindered by a lack of information on the locations of emission hotspots in the catchment. This information would allow specific problem areas to be targeted with appropriate management measures and financial support. Carefully planned measures can help to avoid significant changes or realignment of the land management practices which would ensure that implementation costs and farmer resistance are minimized. However, due to the complex environmental processes and interactions among the natural and artificial systems within a catchment one of the major challenges related to managing phosphorus in catchments is predicting how phosphorus applied to the fields will mobilize and reach the streams. Planning cost effective management essentially requires approximation of phosphorous movement at the catchment-scale, and importantly, water quality modeling.

The purpose of this thesis is to contribute to understanding the fate of phosphorus in agricultural landscapes and to support decision making in phosphorus management. The thesis presents a distributed parameter, long-term average phosphorus emission and transport model, known as PhosFate, which can be applied for cost-effective management strategy development at the catchment scale. The model was tested in various hilly medium-sized catchments with significant agricultural coverage. Based on the results the model has the ability to realistically simulate the annual phosphorus river loads at the catchment outlets and internal locations as assessed by cross-validation analyses. Despite some uncertainties that are mostly related to local processes and parameters, the model is considered a useful tool for critical area screening in catchments in respect to phosphorus pollution of the surface water bodies.

PhosFate is able to identify the most significant sources of local phosphorus emissions by spatially distributed emission modeling. Identification of emission source areas is essential for any resource management effort to reduce local soil and phosphorus loss from the agricultural fields. Applying an explicit phosphorus transport model, the responsibility of

each cell in respect to water quality degradation can be assessed. Despite the relatively high proportion of emission source areas, only a few percent of the total area effectively contribute to the river loads. If intervention measures are concentrated on these effective source and transfer zones that have the strongest possibility to reduce river loads, a highly effective management can be achieved without having to change the overall land use practice in the catchment.

The model also provides an optimization algorithm to find the most cost-effective solution to achieve a particular water quality target. Involving cost considerations the method gives policy makers some idea on the value of economic support/subsidies needed to effectively reduce phosphorus pollution of waterways. The optimization algorithm can compare different management alternatives in terms of their cost efficiency and it is feasible to evaluate combined management plans with spatially differentiated practices at differing costs.

The PhosFate model is a screening procedure at the catchment scale. It is able to identify possible hot-spots where improved management activities may be needed. Additionally, it can provide priority lists of the fields to be controlled even with spatially differentiated management practices for various water quality targets. In a next step, it may be useful to perform more detailed analyses (field scale modeling and field experiments) to determine what particular management options are necessary at the local scale.

Kurzfassung

Kosten-effektives Phosphormanagement, welches sowohl der Sicherung einer nachhaltigen landwirtschaftlichen Produktion als auch dem guten ökologischen Zustand von Oberflächengewässern dient, ist ein hochrelevantes Thema im Bereich des Einzugsgebietsmanagements. Politische Entscheidungen werden oft durch einen Mangel an Kenntnis über die relevanten "hot-spots" im Einzugsgebiet beeinträchtigt. Eine bessere Kenntnis über die relevanten Quellgebiete von Phosphoremissionen würde es ermöglichen, geeignete Maßnahmen in spezifischen Problembereichen zu planen und gezielt finanziell zu fördern. Durch sorgfältige Planung könnte die Notwendigkeit bedeutender Veränderungen in der Landnutzung vermieden und trotzdem eine relevante Verringerung der Gewässerbelastung erreicht werden. Dies würde sowohl die Umsetzungskosten als auch den Widerstand der Landwirte reduzieren. Eine wesentliche Voraussetzung für entsprechende Maßnahmenpläne ist die quantitative Erfassung des Phosphortransportes aus den landwirtschaftlichen Flächen in die Gewässer.

Das Ziel dieser Dissertation ist es, zum Verständnis des Verbleibes von Phosphor in landwirtschaftlich geprägten Einzugsgebieten beizutragen und damit Grundlagen zur Entscheidungsfindung für ein optimiertes Phosphormanagement zu schaffen. So wurde im Rahmen der Dissertation ein rasterbasiertes und langfristiges Phosphoremissions- und Transportmodell mit dem Namen PhosFate entwickelt. Mit Hilfe von PhosFate können Grundlagen für die Erarbeitung von kosten-effektiven Maßnahmenstrategien auf Einzugsgebietsebene geschaffen werden. Das Modell wurde in verschiedenen mittelgroßen Einzugsgebieten mit bedeutendem landwirtschaftlichem Anteil getestet. Es konnte gezeigt werden, dass das Modell die jährlichen Phosphorgewässerfrachten an den Auslasspunkten der Einzugsgebiete und auch an anderen Pegeln im Einzugsgebiet realistisch abbilden kann. Trotz einigen Unsicherheiten, die meist mit lokalen Prozessen und Parametern zusammenhängen, kann PhosFate als geeignetes Instrument für die Identifizierung potentiell kritischer Gebiete einer Phosphorbelastung der Oberflächengewässer betrachtet werden.

PhosFate kann zum einen die wichtigsten Quellen der Phosphoremissionen durch eine räumlich verteilte Emissionsmodellierung identifizieren. Die Erkennung der

Emissionsquellen ist eine wesentliche Basis für die Bestrebungen eines Ressourcenmanagements, welches die lokalen Boden- und Phosphorverluste von landwirtschaftlichen Flächen zu reduzieren beabsichtigt. Zum anderen kann PhosFate durch explizite Transportmodellierung den Beitrag jeder Zelle zur Belastung der Gewässer identifizieren und den Eintrag in die Gewässer quantifizieren. Trotz eines relativ hohen Flächenanteils der relevanten Emissionsquellen im Einzugsgebiet tragen nur einige wenige Prozente der Gesamtfläche effektiv zu den Emissionen in die Gewässer bei. Wenn Maßnahmen sich auf die relevantesten Quellen und auf jene Transferzonen konzentrieren, die das stärkste Potenzial zu Frachtverminderung aufweisen, ist ein sehr effizientes Management ohne einen massiven Eingriff in die generelle Landnutzung erreichbar.

Um dies zu nutzen, bietet das Modell ein Optimierungsverfahren an, mit welchem die finanziell effektivste Managementalternative für eine angestrebte Verbesserung der Wasserqualität ausgewiesen werden kann. Die Optimierungsmethode kann auch verschiedene Managementvarianten in Hinblick auf die Kosteneffektivität vergleichen und kombinierte Managementpläne mit räumlich differenzierten Maßnahmen und Kosten evaluieren.

Das Modell PhosFate dient als Evaluierungsmethode auf Einzugsgebietsebene. Es kann die möglichen "hot-spots" in Einzugsgebieten identifizieren, in denen verbesserte Managementaktivitäten für die Reduktion von Sediment und Phosphoreinträgen effektiv sein können. Basierend auf den Ergebnissen von PhosFate können in einem nächsten Schritt vor Ort detailliertere Analysen (lokale Messungen und "field-scale" Modellierung) für die konkrete Maßnahmenplanung auf lokaler Ebene durchgeführt werden.

Acknowledgments

Since this Thesis has a longer history, there is a rather long list of people, who I feel obliged to thank. First of all I would like to say thanks to my first supervisor, Prof. Matthias Zessner-Spitzenberg who invited me four years ago to come to Vienna and join the Doctoral Programme. He has always been very helpful both professionally and personally. He gave me a lot of valuable suggestions in relation to the research topic. And I have really appreciated his kind pressure towards me to speak German since the beginning of my stay in Vienna (even though the Thesis is in English). I am also very thankful to Prof. Helmut Kroiss, the former leader of the Institute of Water Quality Management at Vienna University of Technology for giving me the possibility to join his institute as an assistant. He has been encouraging me to finish this work passionately.

Looking back on the period before Vienna I would like to thank for her support and cooperation to Prof. Adrienne Clement. She is my second supervisor and I am really grateful that she has always supported me on my university career and research work and introduced me to the world of diffuse pollution. I would also like to express many thanks to Prof. László Somlyódy, the former leader of the Institute of Sanitary and Environmental Engineering at Budapest University of Technology and Economics, who has directed me towards water quality management and employed me as a lecturer assistant at his institute.

As the Thesis is part of the Doctoral Programme on Water Resources Systems, I would like to express my gratitude to Prof. Günter Blöschl, Chair of the Programme for letting me take part in the Programme and continuously observing how I was proceeding with my work. Many thanks to Dr. Gemma Carr, who helped me find my way through the labyrinth of the official system of the Doctoral Programme. I am really grateful to Prof. Matthias Zessner-Spitzenberg, Prof. Kálmán Buzás and Prof. Günter Blöschl for their conscientious and thorough work as Thesis reviewers.

I need to thank many other people for their help, cooperation and support related to this dissertation. All the co-authors, former and actual colleagues, project partners have had a great contribution to this work through their questions, opinions and suggestions during our

discussions. Continuous help of the administrative stuff of the institutes and universities I have worked for is also acknowledged.

Special thanks have to be delivered to Dr. Márk Honti, friend and colleague, who had been working with me from the first calculations till the last word of my papers. His contribution to the Thesis with model coding and idea formulation was really excellent and essential.

Finally, I would like to say thanks to my family and friends for supporting me during the last couple of years in this project. I am very thankful to my mother and father for giving me an excellent base from their best and ensuring me a stable and deep family background. Last but not least, I would like to thank my wife Kata for her love and faith in me and for providing me peace and relief at home. Without her support and patience you would not have a chance to read this Thesis.

Contents

1 Introduction 1
1.1 Aim of the Thesis and its research questions 4
1.2 Structure of the Thesis 5
2 Estimation of diffuse phosphorus emissions at small catchment scale by GIS-based pollution potential analysis 7
2.1 Introduction 7
2.2 Methods 8
2.2.1 The MONERIS model 8
2.2.2 Pollution sensitivity analysis by GIS 9
2.2.3 Combination of the two estimation approaches 12
2.2.4 River load calculations 13
2.3 Results and discussion 14
2.4 Conclusions 17
3 Design of best management practice applications for diffuse phosphorus pollution 19
3.1 Introduction 19
3.2 Background 20
3.3 Methods 21
3.3.1 Fate model 22
3.3.2 Design tool 23
3.4 Results and discussion 25
3.4.1 Model calibration and verification 25
3.4.2 Scenario analysis 27
3.5 Conclusions 27
4 Detection of hot spots of soil erosion in mountainous Mediterranean catchments 29
4.1 Introduction 29
4.2 Methods 30
4.2.1 Annual erosion and sediment transport modeling 30

4.2.2 Hot spot identification and optimization ... 31
4.2.3 Case study region: Albania ... 32
4.3 Results and discussion ... 35
4.3.1 Model calibration ... 35
4.3.2 Soil erosion ... 37
4.3.3 Sediment transport ... 39
4.3.4 Management of the source areas and optimized interventions ... 40
4.4 Conclusions ... 43
5 Identification of phosphorus emission hotspots in agricultural catchments ... 45
5.1 Introduction ... 45
5.2 Case study areas ... 49
5.3 Methods ... 51
5.3.1 The PhosFate model ... 51
5.3.2 Hot spot identification and optimization ... 53
5.3.3 Evaluation of the river monitoring data ... 56
5.3.4 Definition of water quality targets ... 57
5.3.5 Model application ... 57
5.4 Results and discussion ... 59
5.4.1 Event load separation and load targets ... 59
5.4.2 Model calibration and validation ... 60
5.4.3 Catchment scale results ... 62
5.4.4 Spatial distributions of the emissions ... 65
5.4.5 Results of the management strategies ... 68
5.4.6 Uncertainties of the results ... 73
5.5 Conclusions ... 74
6 From the regional towards the local scale: a coupled modeling approach to manage phosphorus emissions into surface water bodies of Upper-Austria ... 77
6.1 Introduction ... 77
6.2 Background ... 81
6.3 Methods ... 83

6.3.1 MONERIS model 84
6.3.2 PhosFate model 84
6.3.3 Model application and scenario analysis 86
6.3.4 River load estimations and water quality target for the PP loads 90
6.4 Results and discussion 90
6.4.1 MONERIS results at sub-catchment scale 90
6.4.2 PhosFate results at local (cell) scale 92
6.4.3 Targeted management scenarios 96
6.4.4 Cost-effective optimized management under different management situations 99
6.4.5 Discussion 104
6.5 Conclusions 106
7 Summary and conclusions 109
8 References 113
Appendix A: The PhosFate model 123
A.1 Hydrology 123
A.2 Soil erosion 126
A.3 Soil P forms 128
A.4 P emissions 131
A.4 Flow routing 133
A.5 Sediment transport 134
A.6 DP transport 137
A.7 PP transport 139
Appendix B: Authorship 141

List of figures

Fig. 2.1 Structural scheme of GIS-based sensitivity analysis. 12

Fig. 2.2 Area specific diffuse phosphorus emissions of Hungarian sub-catchments (1998–2000). 15

Fig. 2.3 Comparison of measured and simulated river loads at selected monitoring stations. 16

Fig. 2.4 Cumulative phosphorus river loads at the outlets of the Hungarian sub-catchments (1998–2000). 16

Fig. 3.1 Location of the Zala River catchment. 21

Fig. 3.2 Comparison of simulated and measured annual DP and PP loads in the Zala River. 25

Fig. 3.3 Spatial resolution of long-term average DP (left) and PP (right) emissions in the Zala River catchment. 26

Fig. 3.4 Spatial resolution of long-term average TP fluxes (left) and retention (right) in the Zala River catchment. 26

Fig. 4.1 Albania and its topography. 34

Fig. 4.2 Simulated and reported long-term average net river flow of the Albanian rivers (top); simulated and reported long-term average net SS flux of the Albanian rivers (bottom). 37

Fig. 4.3 Calculated long-term average specific soil loss rates in Albania (left); sediment transport by the main watercourses of Albania (right). 39

Fig. 4.4 Optimization results (load reduction) for the entire Albanian territory(top); optimized intervention locations in Albania(bottom); A, B and C are the easily manageable erosion hotspot zones (the magnified parts show the different spatial arrangement of intervention zones in the Northern and Southern parts of the country). 42

Fig. 5.1 Location of the case study areas (circles and triangles indicate the catchment outlets and upstream gauges, respectively). 50

Fig. 5.2 Scheme of the transport algorithm. 52

Fig. 5.3 Observed and modeled long-term average (1994-200, without extremes) SS (left) and PP (right) event river loads at the monitoring stations of the Wulka and the Zala rivers (one dot represents one station, outlet: calibration, upstream gauges: validation). 61

Fig. 5.4 Observed and modeled SS (left) and PP (right) event river loads of individual years at the outlet of the Wulka (1992-2000) and the Zala (1994-2003) catchments (one dot represents one year). 62

Fig. 5.5 Long-term average area-specific local PP emissions via soil erosion in the Wulka (left) and the Zala (right) catchments..... 66

Fig. 5.6 Local contributions to the long-term average PP event river loads at the outlet (source loads) in the Wulka (left) and the Zala (right) catchments. 67

Fig. 5.7 Achievable reductions of PP event river loads at the outlet at different intervention areas in the Wulka and the Zala catchments (dashed lines represent values for halved and doubled emissions)..... 69

Fig. 5.8 Suggested areas (indicated by black color on the original land use maps) for intervention in order to fulfill water quality management (pollution control) goal according to scenario 2 in the Wulka (left) and the Zala (right) catchments..... 70

Fig. 5.9 Suggested areas (indicated by black color on the original land use maps) for intervention in order to fulfill both water quality and soil phosphorus management goals in the Wulka (left) and the Zala (right) catchment..... 71

Fig. 6.1 Location and hydrography of the Upper-Austrian territory. Test regions: Krems-Ipfbach (R1), Pram-Antiesen (R2), Trattnach-Aschach (R3)..... 83

Fig. 6.2 Observed versus simulated long-term average (2001-2006) total P loads of the gauged Upper-Austrian sub-catchment outlets (left); spatial distribution of the long-term average (2001-2006) P emissions of the water bodies via soil erosion in Upper-Austria, pie diagrams illustrate the relative contribution of the soil erosion to the total P emissions, whilst the lines indicate the exceedance of the EQS for PO_4-P (right). 92

Fig. 6.3 Observed versus modeled long-term average (2001-2006) PP event loads at gauges in the case study sub-catchments (left, circles indicate the gauges used for calibration); local emissions of PP, emissions into the river network and river loads of the case study sub-catchments (right, *: transported local emissions only, not cumulated river loads)..... 94

Fig. 6.4 Spatial distribution of the long-term average (2001-2006) local PP emissions (top) and PP cell loads (bottom). 95

Fig. 6.5 PP event river loads of the test regions according to the different scenarios (left); relative cumulative frequency curves of the relative PP river load reductions and the necessary load reductions (right). 97

Fig. 6.6 PP event load reductions and intervention areas versus total costs according to different optimization alternatives: OPT1-afforestation, OPT2-restricted crop rotation plus buffer zone, OPT3-meadow or pasture establishment plus buffer zone..... 100

Fig. 6.7 Location of the intervention areas in R3 region. 103

List of tables

Table 2.1 Diffuse phosphorus emissions via different pathways of Hungary and their proportion on the total emission for the period 1998–2000. 9
Table 3.1 Examined management scenarios. 24
Table 3.2 Load reduction efficiency of the selected management practices. 27
Table 3.3 Costs of the scenarios. 27
Table 4.1 Areas, total amounts and proportions of the specific soil loss rate classes in Albania. 39
Table 5.1 Main characteristics of the Wulka and the Zala catchments. 50
Table 5.2 Target criteria values (concentrations and loads) and necessary event load reductions for the watershed management. 60
Table 5.3 Long-term average, area-specific SS and PP fluxes of the Wulka and the Zala catchments. 63
Table 5.4 Area demand and event load reductions of the Wulka and the Zala catchments according to different management strategies. 72
Table 6.1 Preferred land use types, their costs and their potential emission reductions. 89
Table 6.2 Annual total costs and load reductions of the targeted scenarios. 98
Table 6.3 Costs, area demand and cost-specific PP event load reductions according to different optimization alternatives. 103

1 Introduction

Phosphorus (P) is a key element in our life. It plays a principal role in the intercellular energy transfer of all living organisms. It is a building block of the Adenosine-triphosphate (ATP) molecules that transport chemical energy within cells for metabolism. P is essential to all forms of life (photosynthesis, cellular respiration, DNA replication) and cannot be substituted by any other element. P is therefore one of the major nutrients for plant organisms and the agricultural sector has long recognized that appropriate P input to cropland is necessary to sustain optimal plant growth and agricultural production. As the both the global population and degree of urbanization rapidly rose in the 20th Century, there was a worldwide shift from smaller farming systems to larger, monocultural and intensively operated agricultural enterprises to provide sufficient food. However, natural stock of P in soils is limited by the P content of the underlying parent rock material, and the weathering rate and release of P into the soil (Campbell *et al.*, 2004).

To overcome the P-deficiency of many soils and to sustain the high demand on agricultural yields, chemical P fertilizers derived from intensive mining of P-rich minerals (*e.g.* apatite) have been applied onto fields in substantial quantities (Campbell *et al.*, 2004). Large amounts of fertilizers have been widely applied without any concern that excess P amounts not utilized by plants are available to move away from the fields. P inputs in excess of crop requirements (typically about 30-70 kg P_2O_5 per year and per hectare) resulted in significant P-surpluses and a generally high P level in agricultural soils. For instance, the estimated mean agricultural P surplus of the OECD countries in 1989 was 15 kg P ha^{-1} a^{-1} (Schröder *et al.*, 2010), ranging between 5 kg P ha^{-1} a^{-1} and 55 kg P ha^{-1} a^{-1} (Austria: 7 kg P ha^{-1} a^{-1}). These processes - to varying extents – continue throughout the world till today, even though as fertilizer prices have strongly increased in the last decades (actual mean price of the phosphate fertilizers is about 2 € per kilogram P and has doubled in the last two decades, WB), significantly lower application rates of P fertilizers have been recorded recently (*e.g.* in Austria application reduced by 60% in the last 20 years to approx. 12 kg P_2O_5 per year and per hectare total agricultural area, AMA; 30% reduction was estimated for the OECD countries in the last decade, Schröder *et al.*, 2010). Recent surplus values of the OECD

countries are also remarkably lower, the mean value reduced to 7 kg P ha^{-1} a^{-1} (Schröder *et al.*, 2010), varying between 20 kg P ha^{-1} a^{-1} and 1 kg P ha^{-1} a^{-1} (Austria: 2 kg P ha^{-1} a^{-1}). These tendencies indicate growing demands in the agricultural sector to reduce the P inputs to the soils and minimize the losses of P resources from the soils. Recent estimates on the available potential P-rock reserves predict that they may become exhausted in about 300 years (Van Vuuren *et al.*, 2010; USGS, 2012) under the recent exploitation rates (*ca.* 150 million tons rock per year, the worldwide P-fertilizer consumption is *ca.* 40 million tons P_2O_5, Pierzynski, 2005; Schröder *et al.*, 2010). Thus, there is concern over long-term future supplies of P because it is a non-renewable resource.

Problems caused by P released from the agriculture (and waste water treatment plants) to the environment – especially to surface waters – are recognized through radical changes in water ecosystems. In water bodies where P is a limiting nutrient, the natural ecosystem is highly sensitive to the amount of P available. Many lakes and seas suffered from eutrophication that severely impairs water quality and ecosystem functioning (substantial algae growth and consequently oxygen depletion, toxicity, pH variations, accumulation of organic substances, change in species composition and in number of pieces) as well as limits or hinders human water uses (recreation, fisheries, drinking water supply) For example, Lake Balaton (in Hungary) in the 1980s became completely green exceeding 200 µg l^{-1} a-chlorophyll concentration due to the significant growth of some specific algae species (*e.g.* the invasive Cylindrospermopsis Raziborskii) as a response to the high external nutrient loads (Somlyódy and Van Straten). In the Black Sea heavy algae blooms were also observed in the 1980s in the north-west coastal region that is affected by the Danube discharge (Kroiss, 2005). Since then several efforts have been made to improve water quality. Point sources were technically improved first by introducing P removal technology, but the P loads and concentrations of many water bodies remained above the favorable values. This emphasized the importance of the diffuse emissions on P pollution, which come from the catchment area mainly via sediment transport and overland flow. Agriculture has been identified as one of the main sources of diffuse P emissions (*e.g.* in case of the Danube Basin, Kroiss, 2005), and the recent river basin management plans related to the EU Water Framework Directive particularly focus on the good agricultural management suggesting best management practices to minimize P losses.

Because of the dual importance of P (essential nutrient and pollutant) it is essential to develop appropriate, multi-aspect P management strategies within our catchments. Their main goal is to meet the interests of both the agricultural sector and water quality protection. Effective strategies should ensure sufficient P is available for optimal agricultural production while simultaneously minimizing P pollution in the receiving water bodies. Such strategies involve two fundamental approaches: 1) lowering P inputs into the agricultural systems through more efficient utilization of P and 2) reducing P transport out of the system. However, practical implementation of management strategies on diffuse P pollution reduction is complicated due to the spatial and temporal variability of the emissions, their different transport pathways and complex and strong relations to hydrology and soil properties. Thus, one of the major challenges related to manage P in agricultural catchments is predicting how P applied to a field will mobilize and even reach a stream or river. This knowledge is essential to identify exactly where phosphorous applications are causing the greatest harm and should be controlled. Appropriate measures are those, which can be implemented without any significant realignment of the land management practice to avoid enormous costs and massive resistance of the farmers. Not all of the source areas effectively contribute to the river loads and the extent of their contribution depends on the transport efficiency of the emitted pollutants within the catchment and towards the outlet. Thus, management efforts to reduce water pollution should be selective if costs are also considered. Interventions should be concentrated on the critical source and/or transfer areas where the highest fluxes to the river net come from and/or where significant direct transfers of pollutants from land to water probably occur. Therefore, only a transport-based management approach can be environmentally and economically effective at the catchment scale. Optimized placement of the interventions is essential in countries, where the extent of the agricultural areas is limited due to the topographical conditions, like *e.g.* cropland in Austria.

Since diffuse P emissions are almost immeasurable at their source or at transport pathways, it is hard to identify their area of origin or locations with significant mass transfer by the tools of classic monitoring systems. Only the river loads can be appropriately detected, however, they show the final response of the entire catchment to the land activities and the causes of that response remain almost completely hidden. Because of the observation difficulties and the complicated interactions and load contributions of the different fields, cost-effective

management of the diffuse P pollution requires watershed level approximation and model simulations. There is a considerable variety of existing catchment scale models at various temporal and spatial resolutions to assess water quality of rivers. The most promising approaches in terms of tracing the critical areas are the spatially distributed models, which divide the study area into small elementary units (cells or small areas with similar hydrologic behavior). They focus more detailed on the local variations of the catchment properties, the contaminations and their management alternatives within the watershed. They are widely used to asses P loads of catchments and evaluate impacts of several management scenarios on the loads. However, there are only a few approaches that could be applied for cost-effective management strategy development at the catchment scale. The main expectations to such a model are 1) the ability of direct modeling of the emissions from catchment, climate and farming properties and explicit routing of the fluxes with simple distributed parameter approach to find the critical areas within the catchment; 2) it should produce comparable results (loads) to the observations and the impact of the improved management practices on the critical areas should directly be related to water quality improvements; 3) it should contain an optimization procedure to rank the hot-spot cells according their load reduction if an intervention occurs, which enables us to select the most effective intervention areas within the catchment and minimize the intervention area; 4) it should concern the costs of the management actions and evaluate combined management plans with spatially differentiated practices at differing costs; and 5) it should have acceptable data demand and reasonable computation time. This Thesis provides a catchment model that fulfills all the criteria above.

1.1 Aim of the Thesis and its research questions

In accordance to the problems discussed before, the main product of this Thesis is a new catchment-scale, distributed parameter P emission and transport model provided for P management purposes. It is called PhosFate and aims to support decision-making in catchment management to effectively reduce P loads of surface water bodies. Applying the critical area concept it attempts to find the most important source and transfer areas, which are principally responsible for the P pollution of rivers and to demonstrate cost-effective management alternatives.

The research questions to be addressed in this Thesis are the following:

- Can the calibrated model parameters be transposed in space to achieve cross-validation?
- What uncertainties can have a spatially distributed catchment-scale water quality model?
- How can we find the main emission sources of P in the catchment where resource management efforts should be concentrated?
- How can we identify the critical source and transfer areas of the catchment, where management practices for water quality should focus?
- How can we achieve a cost-effective management alternative in our catchments?
- What kind of strategies for catchment management for larger basins or administrative units can be recommended based on modeling?

1.2 Structure of the Thesis

This Thesis is the outcome of a cumulative and continuous research work on P emission modeling and management. The story began a couple of years ago, when large scale modeling results for Hungary were spatially distributed and assigned to small catchments based on P pollution potential analysis. This effort was published in Kovács and Honti (2009) in the journal Desalination and is presented in Chapter 2 of this Thesis. In the next step, this inverse modeling task was transformed to a direct approach by developing the catchment-scale P emission and transport model PhosFate. The model was published first in Kovács *et al.* (2009) in Water Science and Technology. This paper is shown in Chapter 3. Using the erosion module of PhosFate, a case study was performed to evaluate the siltation situation of Albania. In this study the model was extended with an optimization algorithm to find the hot-spots of the Albanian catchments, which screens the areas with highest potential to transport suspended solids from land to water. This work was published in Kovács *et al.* (2012) in the e-journal Energy Procedia and is presented in Chapter 4. Chapter 5 contains the paper of Kovács *et al.* (2012) published in Science of the Total Environment. This paper demonstrates substantial improvements for both the model and optimization algorithm. The new model approaches were tested in two agricultural catchments located in Austria and Hungary. Chapter 6 shows an application of the model (with some additional improvements) for management purposes, where cost efficiency of various management alternatives was

evaluated. A paper with this topic has been submitted to the Journal of Environmental Management. After presenting the scientific work, the main conclusions are summarized. Finally, an Appendix has been attached with the algorithm of the PhosFate model.

2 Estimation of diffuse phosphorus emissions at small catchment scale by GIS-based pollution potential analysis

2.1 Introduction

Estimation of non-point nutrient emissions into surface waters is a key issue of management strategies. However, quantification of diffuse contaminations in case of smaller catchments is difficult. Modeling tools to calculate nutrient emissions, especially regarding the fluxes from the diffuse sources have great inaccuracies. Several watershed models can be found in the literature based on either empirical or physical approaches (Donigian and Huber, 1991; Jolánkai *et al.*, 1999; Novotny, 2003). Empirical models have major simplifications and they are mostly lumped parameter methods. These models do not provide detailed information on spatial variability of the emissions. Uncertainties can result from the extension of the empirical equations to areas out of the original calibration range. This type of models can be applied to estimate the order of magnitude of the long-term average emissions. On the other hand, physically based, dynamic models with distributed parameters are theoretically useful approaches to simulate the non-point pollutions due to the detailed mathematical description of environmental processes. However, their applicability depends on the availability of data. The limitations of these models are the absence of data and some uncertain parameters characterizing unclear environmental processes (for example, nutrient retention and retardation on catchment field, in soils and in stream channels). Consequently decreasing watershed scale due to the increased number of processes can often enlarge the uncertainty of the calculations.

River nutrient loads can be also estimated from discharge data and nutrient concentration observations. However, monitoring systems are usually not designed to register long-term concentration time-series at high frequency. Therefore they are not suitable to measure annual average nutrient loads properly. Spatial density of the monitoring stations is also insufficient in many cases to provide enough information from smaller areas. Thus,

application of both modeling tools and measurement systems in case of numerous small sub-catchments is limited due to lack of data.

The uniform water policy of the European Union (OJEC, 2000) prescribes the determination of nutrient emissions affecting the trophic state of water bodies. Introduction of the Directive should change the focus of the water management from larger river basins to smaller catchments (Somlyódy and Hock, 2002). In Hungary, 892 small sub-catchments (each has an area from 10 to 1000 km^2) were designated, for which the annual average nutrient loads should be quantified.

This paper presents a simple distributed parameter method to calculate diffuse phosphorus emissions at small watershed level based on a large scale emission distribution procedure. Applying the method, phosphorus emissions of 892 Hungarian sub-catchments were calculated for the period 1998–2000.

2.2 Methods

Two approaches were combined to quantify phosphorus emissions for small catchments. The first is the MONERIS model (MOdeling Nutrient Emissions into RIver Systems, Behrendt *et al.*, 1999), a large scale empirical method. The other is a sensitivity factor method at cell scale based on the detailed spatial information on catchment properties. By joining the two methods, the spatial distribution of the large scale emissions can be determined. The combination gives the possibility to calculate emissions for every grid cell.

2.2.1 The MONERIS model

The MONERIS model has been developed to calculate nutrient emissions entering river systems at large watershed scale (catchment area larger than 1000 km^2). It is a lumped parameter model for the estimation of long-term averages based on mostly empirical relationships. The application of the model requires detailed statistical, sampling and literature data, default parameters and digital maps about various characteristics of the watershed. It provides long-term average amount of water balance components, nutrient emissions and river loads at the main sub-catchment outlets. The model does not distinguish phosphorus forms. It focuses only on total phosphorus emissions. It separates seven different

pathways, which result in the total amount of phosphorus emissions. Six of these are diffuse sources: atmospheric deposition, overland flow, erosion, tile drainage, groundwater and urban systems. The seventh component is the contamination from point sources. For each pathway the appropriate water balance component (in case of erosion the sediment flux) is computed empirically and after that phosphorus concentration is determined for the water (sediment) flows. Soil phosphorus content is estimated based on the nutrient balance calculations of the agricultural areas. Additionally possible field retention is taken into account along the pathways (*e.g.* sediment deposition on surfaces). Finally, from the total emission values of sub-catchments river loads are computed using an empirical in-stream retention model.

The model was applied to calculate the nutrient emissions of large sub-catchments into the Danube River and its main tributaries for the period 1998–2000 (Schreiber *et al.*, 2003). The Hungarian contribution to the phosphorus emissions of the whole basin was 2913 t P a^{-1}, in which erosion from rural areas was the most important emission pathway (Table 2.1).

Table 2.1 Diffuse phosphorus emissions via different pathways of Hungary and their proportion on the total emission for the period 1998–2000.

Emission component	Rural		Urban		Total	
	t P a^{-1}	%	t P a^{-1}	%	t P a^{-1}	%
Surface runoff	46	1.6	122	4.2	168	5.8
Erosion	1776	60.9	367	12.6	2143	73.6
Groundwater	365	12.5	237	8.1	602	20.7
Total diffuse	2187	75.1	726	24.9	2913	100.0

2.2.2 Pollution sensitivity analysis by GIS

Pollution sensitivity analysis was executed at grid cell level in three phases. The first phase was data preparation. Several digital base maps were used to characterize the catchments of Hungary. In the second step, starting from the base maps, first-order sensitivity factor maps were determined relating to the main transport processes (surface runoff, erosion and base flow) and their phosphorus contents. In the third phase, second-order sensitivity maps concerning to the main emission components were formed from the first-order maps.

Nine digital base maps covering the whole territory of Hungary were used for the estimation

(Fig. 2.1). A (i) digital elevation model was available in 50x50 m grid-format. Polygon maps having 1:100 000 resolutions were used to characterize (ii) the soil and (iii) land use types, as well as (iv) the delineated small sub-catchments. Point data were collected on soil (v) humus and (vi) plant-available phosphorus content (data from 1990) and (vii) annual average amount of precipitation (for the actual time period). Information associated to points was extended by interpolation to the surrounding areas. Yearly mineral fertilizer amounts applied on soils in agricultural use and harvested amounts of agricultural plants from the 1960 to 2000 were collected from statistical database at county level. These (viii) agricultural data were linked to the agricultural areas. Finally, (ix) statistical data of settlements (population and its proportion connected to sewer system) concerning the actual time period were assigned to paved areas. To provide the possibility of uniform parameterization, all maps were converted to raster format with 200x200 m grid resolution. The time period of the maps was also different. Since relative values were used in the calculations and it was assumed that the relative differences are valid for the examined time period also, the temporal variability among the maps was neglected.

Based on the information of the base maps, 10 first-order sensitivity maps were created. Each sensitivity map has relative values between 0 and 1. Base maps with non-numerical data types (*e.g.* soil, land use) were filled up with corresponding parameters found in the literature (see next enumerations). For sensitivity maps created by combination of base maps, appropriate equations were used for the combination (see next enumerations). Relationships between base and first-order maps are presented in Fig. 2.1.

The first-order sensitivity maps are the following:

- surface runoff potential based on topography, soil and land use dependent runoff coefficients and precipitation amount (Batelaan and Woldeamlak, 2004);
- erosion potential according to the Universal Soil Loss Equation (USLE, *e.g.* Neitsch *et al.*, 2002; Novotny, 2003), which distinguishes the erosion capacity of the cells by soil and land use types, slope, humus content and precipitation energy;
- recharge or base flow potential related to saturated hydraulic conductivity of soils and precipitation amount (Rawls *et al.*, 1993; Batelaan and Woldeamlak, 2004);

- phosphorus surplus of soil was determined based on yearly average mineral fertilizer application, humus mineralization (Neitsch *et al.*, 2002), plant uptake (Schreiber *et al.*, 2003), and plant-available phosphorus content (agricultural area), the density of population living without connections to sewer systems (urban area with no-sewer systems) and atmospheric deposition rate (rest of the area, Schreiber *et al.*, 2003);
- dissolved phosphorus (DP) concentration of topsoil according to the Langmuir-isotherm of the soils based on clay, organic matter content and pH value of soils as well as phosphorus surplus (Novotny, 2003);
- particulate phosphorus (PP) concentration of topsoil according to the Langmuir-isotherm of the soils (Novotny, 2003) as well as phosphorus surplus and humus content (Neitsch *et al.*, 2002);
- overland delivery ratio of sediment based on the relief-maximum field travel length ratio of the sub-catchments (no difference between cell values was assumed within the same small sub-catchment, Ouyang and Bartholic 1997);
- phosphorus enrichment ratio related to average clay content of soil and the average field travel distance of the sub-catchments (no difference between cell values was assumed within the same small sub-catchment, Novotny, 2003);
- DP concentration in urban runoff categorized by urban land use classes (Novotny, 2003);
- PP concentration in urban runoff categorized by urban land use classes (Novotny, 2003).

Second-order maps were generated by multiplying the proper first-order maps (Fig. 2.1). These maps already regard the main emission components. Six second-order sensitivity map were prepared differing by the main transporting pathways (surface runoff, erosion and groundwater), and by source areas (rural and urban).

The second-order sensitivity maps are the following:

- DP emission via surface runoff as the product of surface runoff potential and DP concentration of topsoil;
- PP emission via erosion as the product of the erosion potential, PP concentration of topsoil, overland delivery ratio and enrichment ratio;
- DP emission via groundwater as the product of recharge potential and DP concentration of topsoil.

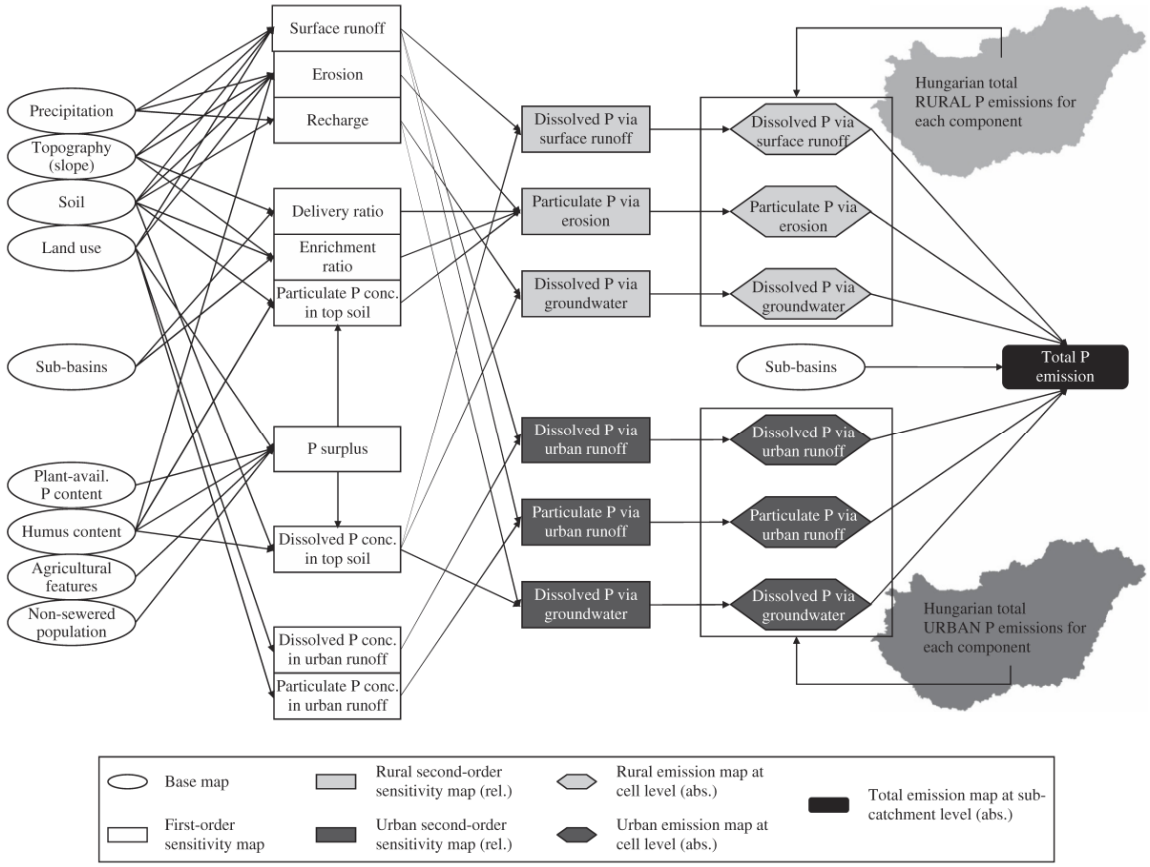

Fig. 2.1 Structural scheme of GIS-based sensitivity analysis.

- DP emission via urban runoff as the product of surface runoff potential and DP concentration in urban runoff;
- PP emission via urban runoff as the product of surface runoff potential and PP concentration in urban runoff;
- DP emission via groundwater as the product of recharge potential and DP concentration of topsoil.

2.2.3 Combination of the two estimation approaches

Combining the approaches absolute values were assigned to the relative factors of the second-order sensitivity maps for each grid cell. The total emission values of each component calculated by MONERIS model were distributed to cell level by weighing the cells according to their pollution potential (calculated by the second-order sensitivity maps):

$$e_{n,i} = \frac{E_{tot,n}}{\sum_{i=1}^{m_n} POT_{n,i}} \cdot POT_{n,i} \cdot \frac{10^3}{A_{cell}} \tag{2.1}$$

where $e_{n,i}$ is the emission value for the component n at cell i [kg P ha^{-1} a^{-1}], $E_{tot,n}$ is the total emission for the component n (result of the large scale modeling, Table 2.1) [t P a^{-1}], $POT_{n,i}$ is the pollution potential for the component n at cell i (relative values of the second-order sensitivity maps), n is the index of the emission components (1-6) [-], i is the index of the cells [-], m_n is the number of the cells with data in the second-order sensitivity map n [-], A_{cell} is the cell area [ha].

The distribution procedure resulted in absolute emission values [kg ha^{-1} a^{-1}] for each component in each cell. Afterwards, individual cells were ordered into sub-catchments and the emissions of cells belonging to the same sub-catchment were summed. In course of summation, additional sources and sinks were neglected. That means, no retention was assumed during the field transport of the DP (surface runoff and groundwater), while emission values via erosion includes field retention (delivery ratio).

2.2.4 River load calculations

To convert of the emissions to river loads, other impacts must have been taken into account. Emissions from registered point sources were calculated using the effluent discharge and nutrient concentration data. In case of non-registered treatment plants, loads were estimated based on the population equivalent of settlements, the inhabitant specific phosphorus output (Schreiber *et al.*, 2003) and the elimination rate of applied treatment technology (Somlyódy *et al.*, 2002). These estimated point source emissions were assigned to the sub-catchments.

Since several river sections and tributaries of larger rivers were defined as an individual water body, it was necessary to sum the point and nonpoint source emissions of water bodies according to the river topology. Fluxes entering the country were neglected in order to calculate the net Hungarian river loads. Finally, since phosphorus cannot be considered as a conservative matter, the transport and retention processes taking place in river systems must be included. Phosphorus retention was estimated by a simple first-order equation (Campbell and Edwards, 2003). The phosphorus loads at catchment outlet including retention were

calculated with the following equation:

$$L_i = \sum_{j=1}^{n} \left[\left(D_j + P_j \right) \cdot exp(-k \cdot s_j) \right] \tag{2.2}$$

where L_i is the phosphorus load at the catchment outlet i [t P a^{-1}], D_j, is the total diffuse emission of sub-catchment j [t P a^{-1}], P_j, is the total point source emission of sub-catchment j [t P a^{-1}], s_j, is the total channel travel distance from the sub-catchment j to the catchment outlet i [m], i is the index of the given catchment outlet [–], j is the index of the given sub-catchment upstream to the catchment outlet i [−], n is the number of sub-catchments upstream to the catchment outlet i [–], k a constant model parameter for phosphorus retention [m^{-1}].

Controlling of load calculations was performed at 50 monitoring stations, which have permanent data with proper frequency and no influence abroad. Measured loads for the period 1998–2000 were determined from river discharge and total phosphorus concentration time-series. To reach the best fit between calculated and measured loads, parameters of base maps as well as Eq. (2.2) were calibrated.

2.3 Results and discussion

DP emissions via surface runoff have a range between 0.01 and 0.3 P kg P ha^{-1} a^{-1}. High specific emission values can be found in areas with remarkable surface runoff amount, high soil phosphorus content and limited soil adsorption capacity. PP emissions via erosion vary between 0.01 and 7.5 kg P ha^{-1} a^{-1}. Regions with steeper slopes, agricultural landscape and higher soil phosphorus content in topsoil have remarkable contribution to the PP emissions. Subsurface emissions have a range from 0.001 and 2 kg P ha^{-1} a^{-1}. Significant emission rates arise from the regions that have a higher recharge rate and low adsorption capacity. Fig. 2.2 presents the calculated total (sum of the three components) diffuse phosphorus emissions for Hungarian water bodies. The total specific emission values range between 0.01 and 7.5 kg P ha^{-1} a^{-1}. The northern and western hilly region of the county shows the highest total emission rates, some lowlands with sandy soils produce considerable emissions as well. The spatial distribution of phosphorus emissions corresponds to the environmental behavior of this

element: it moves towards the river systems primarily by erosion from the steeper slopes under arable cultivation.

After calibration of the parameters R^2=0.8 correlation factor was found as best fit (Fig. 2.3). Considering the complexity of the processes and the inaccuracy of both estimation method and river water quality data, the calculated values fit reasonable the measured ones. Results of river load estimations can be seen in Fig. 2.4. Values vary between 0.01 and 3500 t P a^{-1}. At the main three final outlet of the country (the Danube River, the Tisa River and the Drava River) the sum of river loads is 4910 t P a^{-1}, while the total emission of the country is 7280 t P a^{-1} (the sum of point source emissions was 4367 t P a^{-1}). This difference indicates a value of 2370 t P a^{-1} for river retention, *i.e.* one third of the emissions was retained in the Hungarian river systems.

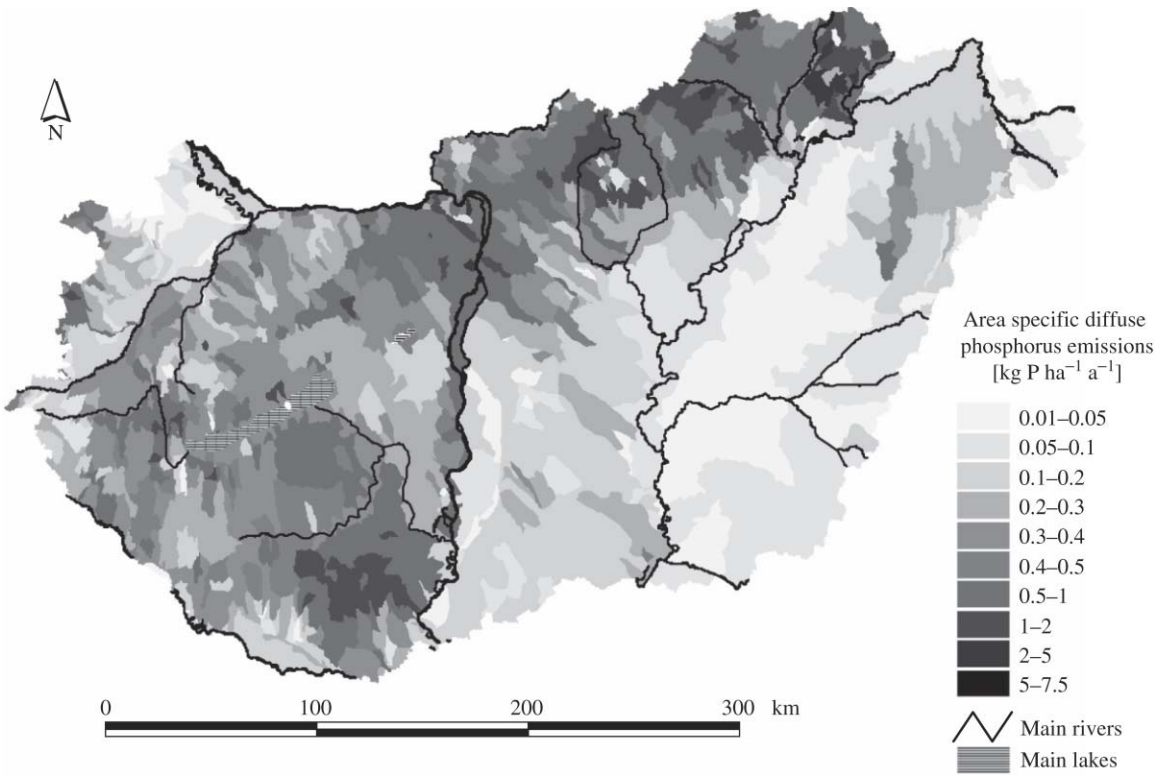

Fig. 2.2 Area specific diffuse phosphorus emissions of Hungarian sub-catchments (1998–2000).

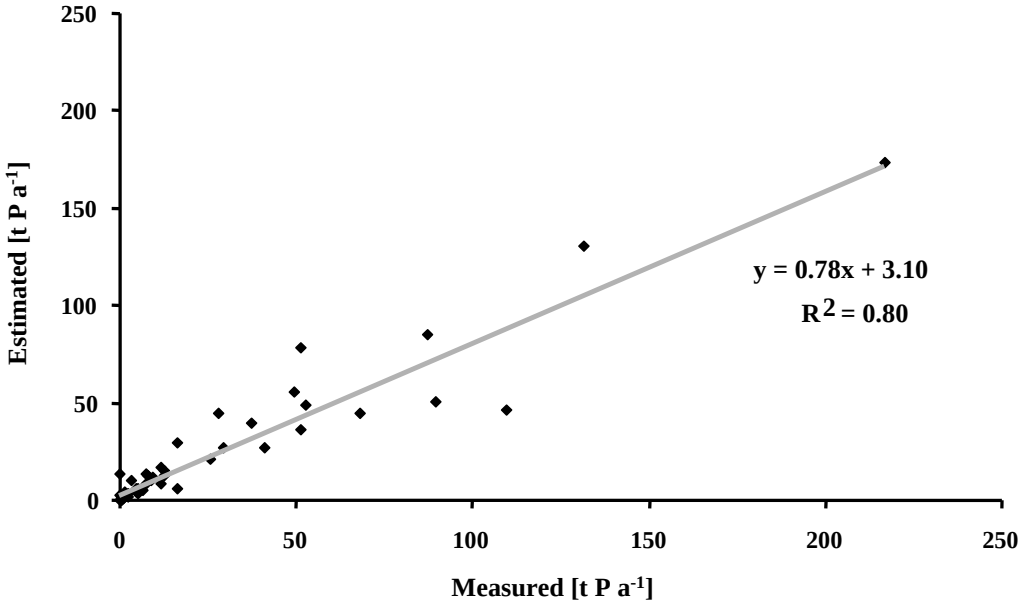

Fig. 2.3 Comparison of measured and simulated river loads at selected monitoring stations.

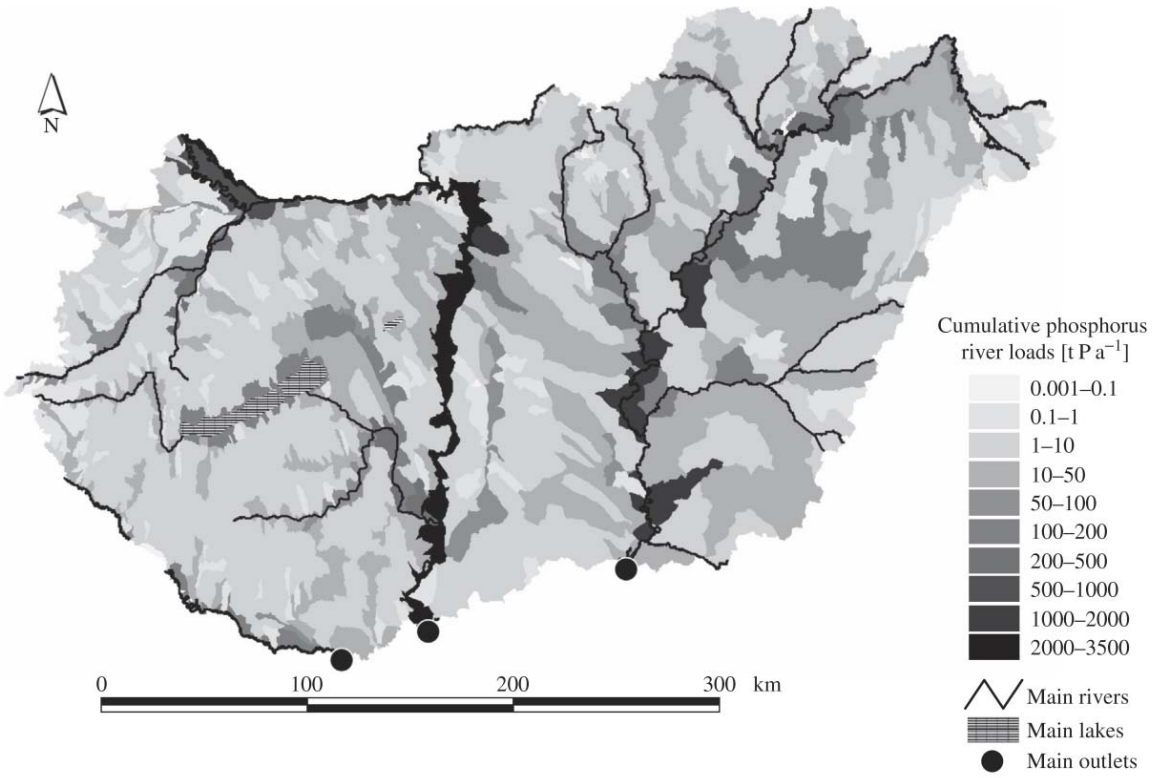

Fig. 2.4 Cumulative phosphorus river loads at the outlets of the Hungarian sub-catchments (1998–2000).

2.4 Conclusions

With the presented method, diffuse phosphorus emissions at small sub-catchment level can be quantified. The main advantages of the approach are the supportable data demand and the simple algorithm. Due to the distributed parameter hot spot analysis can be executed within a given sub-catchment. Based on the calculated emissions and measured runoff values, potential phosphorus concentrations of water bodies and their risk of eutrophication can be identified. Besides the implementation of WFD, this method can support strategic decisions in water management. However, due to the absence of refined process description the method is not capable to execute detailed analyses and dynamic simulations. Although the method requires large scale emission estimates or measurements to calculate the spatial distribution of diffuse loads, the data requirements of these are more feasible to provide than that of a detailed simulation with high spatial resolution in numerous sub-catchments.

The distribution procedure was applied to 892 Hungarian sub-catchments for the period 1998–2000. Areas having remarkable erosion potential contribute at greatest amount to the diffuse phosphorus emissions of surface water bodies. Specific emissions vary between 0.01 and 7.5kg P ha^{-1} a^{-1}. After considering point source emissions as well as river retention, cumulative phosphorus river loads were determined at the sub-catchment outlets. At 50 outlets the results were checked by measured fluxes. Reasonable correspondence was found between the observed and simulated loads (R^2=0.8). The results indicate the method to be applicable to determine the diffuse phosphorus emissions at small sub-catchment scale.

3 Design of best management practice applications for diffuse phosphorus pollution

3.1 Introduction

Best management practices (BMPs), as measures and activities to control the diffuse water pollution have become a cornerstone of watershed management plans. Numerous BMPs reducing the diffuse phosphorus (P) emissions and loads have been published (Ritter and Shirmohammadi, 2001; Novotny, 2003; Campbell *et al.*, 2004). Interventions have two main groups, source and delivery control. Source control includes minimizing the introduction of pollutants into the environment and preventing mobilization of pollutants. Delivery or transport control tries to reduce the transfer of pollutants from soil to water bodies. Efficiency of applied practices has been evaluated in different case study areas (Campbell *et al.*, 2004).

However, design of BMPs in complete catchments extending to several thousand square kilometers cannot miss the quantification of the pollutant fluxes. Since diffuse emissions are immeasurable at source, their regulation must be based on modeling. Catchment simulation models are able to calculate diffuse emissions as well as their transport at the field and in the stream network. After calibration and validation, the models can be used for scenario analyses according to different management plans including various BMPs.

Several watershed models can be found in the literature based on either the empirical or the physical approach (Donigian and Huber, 1991; Novotny, 2003). Empirical models have major simplifications and they are mostly lumped parameter and long-term average methods. These models do not provide detailed information on spatial and temporal variability of the emissions. Physically based, dynamic models with distributed parameters are theoretically the most useful approaches to simulate the non-point pollutions due to the detailed mathematical description of environmental processes. However, their applicability is often limited by the availability of data.

Besides modeling, practical application of BMP concept must be accompanied by a cost–benefit analysis and economic feasibility study as well as legal regulation. There are BMP

alternatives at nearly the same emission reducing efficiency, therefore costs can play an important role in decision making. There can be areas with high economic or natural value, where land use form should not be changed. Finally, farmers should be interested in changing their management practices by economic and/or legal programmes.

This paper presents the PhosFate (Phosphorus Fate) design tool for planning BMPs based on a distributed parameter, long-term (annual) average P fate model calculating diffuse P emissions and their surface transport and an interactive BMP design tool. The tool was applied in the Hungarian Zala River catchment to evaluate the impacts of different management practices on the water quality.

3.2 Background

Lake Balaton, which is the greatest shallow lake in the Central European region, is sensitive to eutrophication (Somlyódy and Hock, 2002). First signs of heavy eutrophication occurred during the seventies due to the increased nutrient loads reaching the high priority recreational lake (the highest algae biomass reached a value of 200 mg chl-a m^{-3}, Somlyódy and Hock, 2002). Since then several investments have been conducted to protect the water quality. Most of the wastewater treatment plants on the watershed were expanded with P removal technology. In addition, since the early 1990's, an artificial wetland area (Kis-Balaton reservoir) was constructed close to the lake inlet. It was intended to retain nutrients transported by the main influent Zala River, which carries most of the nutrient loads of the lake. Due to the control of point sources, the major portion of P emissions is now associated with diffuse sources. Since the current P load is about two times higher than the desirable value, future water quality management of the lake must reduce the non-point pollution (Somlyódy and Hock, 2002). Consequently the region is a highly feasible area to study the impacts of diffuse loads.

The Zala River catchment is located in the western, hilly part of Hungary (Fig. 3.1). The area of the selected part of the watershed (upstream of Kis-Balaton reservoir) is 1528 km^2. The elevation range is between 90 and 325 m above the Baltic Sea level. The area has moderate slopes (the average value is 4.2%). The long-term average discharge and P load at the outlet is 4.4 m^3 s^{-1} and 34 t P a^{-1}, respectively. The dominant physical soil type is loam having poor

to moderate hydraulic conductivity. The area is sensitive to soil erosion by water (the estimated average soil loss from agricultural lands is about 15 t ha^{-1} a^{-1}). The majority of the watershed is agricultural area, in particular arable land, which is 54% of the catchment. Forests are relatively important, covering approximately one third of the whole catchment.

Fig. 3.1 Location of the Zala River catchment.

3.3 Methods

To calculate diffuse P emissions and impacts on them due to the management change, a complex environmental engineering tool has been developed. The PhosFate tool supports decision makers to design BMPs in catchments to reduce non-point P emissions. The tool has two main parts: (a) a simple phosphorus (P) fate model to calculate diffuse P emissions and their surface transport and (b) an interactive tool to design BMPs in small catchments. The fate model aims to calculate diffuse P emissions at their source area. It is a conceptual, distributed parameter model. It utilizes raster maps at 100x100 m resolution. The input base maps are the digital elevation model, the soil and land use type, soil humus content and precipitation. Maps having non-numerical data were filled up with corresponding parameters collected from the literature (see the references below). The outputs are long-term averages of non-point source P fluxes via surface pathways. The time step is one year.

3.3.1 Fate model

For each cell a simple water balance (surface runoff and percolation out of the soil zone) is calculated based on precipitation data and physical properties (slope, land use and soil type) (Rawls *et al.*, 1993; Batelaan and Woldeamlak 2004). Erosion is computed by the USLE-equation adjusted to local conditions. The R-factor is calculated from precipitation amount and an average distribution of the different rainfall intensities (Salamin, 1982; Novotny, 2003). Other factors in USLE were derived according to soil, land use, slope and management practices applied (Salamin, 1982; Neitsch *et al.*, 2002; Novotny, 2003).

Soil P-content is calculated based on long-term agricultural data, soil humus content as well as atmospheric deposition. Because of the accumulation of P in topsoil, a cumulative P balance calculation was executed to determine the current soil P content. The starting year was 1960, when the fertilizer application rate was very low. For each year the P balance was computed as a summation of inputs and losses. Only the inorganic P is monitored, organic P in humus substances is assumed to be slowly varying. Inputs are the applied fertilizer, manure and humus mineralization (Németh, 1996; Neitsch *et al.*, 2002) and atmospheric deposition (Schreiber *et al.*, 2003). Outputs are the harvested P amount (Schreiber *et al.*, 2003) and losses via runoff, erosion and leaching. Since meteorological data for the past (back until 1960) were not available, for each year the average precipitation conditions were used. In each year, the P surplus was partitioned between particulate (PP) and dissolved (DP) phase according to Langmuir-isotherm determined by soil properties (clay and humus content and pH value) (Novotny, 2003). In case of P deficit (negative balance), adsorbed P amounts were reduced and a new equilibrium was computed. The balance calculation can be also used for future fertilization conditions. In case of paved areas, event mean concentrations were used to characterize the P-content of urban runoff according to the urban land use types (Novotny, 2003).

By multiplying the actual amount of the surface runoff and the soil loss with the proper actual P concentration, emission values for the current time period are calculated for each cell via runoff and erosion. In the case of erosion, enrichment of fine particles is also taken into account based on the soil clay content. Total cell emissions are determined by summing the emissions of the different pathways.

The method is appropriate to discover the areas, which are mainly responsible for diffuse P emissions. The fate of emitted P is further examined by a surface transport model to determine the fluxes arising from the emission sensitive areas. Since P moves towards water bodies primarily by erosion and runoff, subsurface loads were neglected. After filling up the local depressions, flow directions are determined for each cell based on the cell elevation values. In this way flow paths (field and channel) are assigned. After determining the flow lines, average flow velocity of runoff and travel time is computed for each cell by the Manning-equation (Fread, 1993; Borah and Bera, 2003). Roughness coefficients are determined based on land use type and channel characteristics (Neitsch *et al.*, 2002; Liu and DeSmedt, 2004). Time averaged hydraulic radius for each cell was estimated by a power function of the drained area upstream of the cell (Liu and DeSmedt, 2004). Field and river retention are computed based on the average travel time in the cell and a constant retention coefficient. No retention is assumed in the case of DP. Combining the cell emissions with the transport algorithm, P fluxes at any points within the catchment can be quantified.

3.3.2 Design tool

Based on the fate model, an interactive design tool was developed to plan BMPs in the catchments and simulate their possible impacts on diffuse P fluxes. There are many BMP alternatives and their combinations, which can be effective in reducing diffuse P contamination. In this tool the land use management is the targeted group of application. It includes land use change, cultivation method change, establishment of buffer zones and wetlands. Land use conversions (*e.g.* reforestation, pasture or wetland development from agricultural land, *etc.*) affect the soil water balance as well as the erosive potential. Cultivation changes (*e.g.* tilling direction, conservation tillage, strip-cropping, mulching, *etc.*) have impact on the soil loss values. These are source controlling interventions by reducing runoff and soil loss. Buffer zones, swales and constructed wetlands are transport controlling measures; they are implemented to retain pollutants during their transport in field and river bed. Their impact appears in reducing flow velocity. The tool provides an interface for the users to introduce various BMPs in the examined catchment, and helps to simulate their impacts by running the emission and the transport model according to the designed modifications. Besides load reducing efficiency, expected costs of intervention can be also

computed.

The presented modeling tool was applied for the Zala River catchment for the period 1994–2002. Model calibration was executed in the first four years, the rest of the examined period was used for model validation. The verified model was built into the interactive BMP design tool for executing scenario analysis. Different management scenarios were worked out and their effects and costs evaluated and compared to each other. Table 3.1 presents the examined scenarios. In Scenario I the sensitive areas were completely reforested. Scenario II means establishment of 50–50 m wide riparian buffer zones at the margins of the main channels. In the third and fourth scenario the sensitive areas were protected by erosion controlling activities (Scenario III: contour plow and strip-cropping, Scenario IV: mulching). Finally, Scenario V is a mixture of the previous ones: it includes forestation and erosion control at the sensitive cells as well as buffer zones close to the river beds. Delineation of the sensitive cells assigned for forestation was carried out based on the suitability of soils for forestation and the environmental sensitivity of the areas (Ángyán *et al.*, 1997).

Interventions were planned in the erosion sensitive areas as well as the riparian zones. Sensitivity to erosion was defined as soil loss value greater than 1 mm a^{-1} (approximately 15 t ha^{-1} a^{-1}). For each scenario the DP and PP loads were computed using the long-term average meteorological conditions and compared to the present values. Besides this, total costs of the interventions and the specific P-removal costs were assessed. Annual costs of the different management practices were collected from the "New Hungary" Rural Development Plan (Tar, 2006, Table 3.1).

Table 3.1 Examined management scenarios.

Scenario	Applied management practice	Area specific cost [USD ha^{-1} a^{-1}]
I	Forestation	250
II	Riparian buffer zone	250
III	Contouring and stripcropping	130
IV	Mulching	170
V	Forestation + riparian zone + mulching	170 / 250

3.4 Results and discussion

3.4.1 Model calibration and verification

Calibration and verification results are presented in Fig. 3.2. To extract diffuse loads arising on the surface, the measured DP and PP loads were separated into strongly variable (surface loads) and slowly variable (subsurface and point source fluxes) categories based on the main flow components. Flow separation was executed by a base flow filtering technique (Arnold *et al.* 1995). After parameter adjustment for the first four years the simulated and measured values fit reasonably in the verification period. Strong correlation was found between the calculated and the observed values (DP: R^2=0.94, PP: R^2=0.90). In the fourth and sixth year the PP simulation has higher inaccuracy. Despite the simple hydraulic algorithm the model well simulates the annual P loads via runoff and erosion.

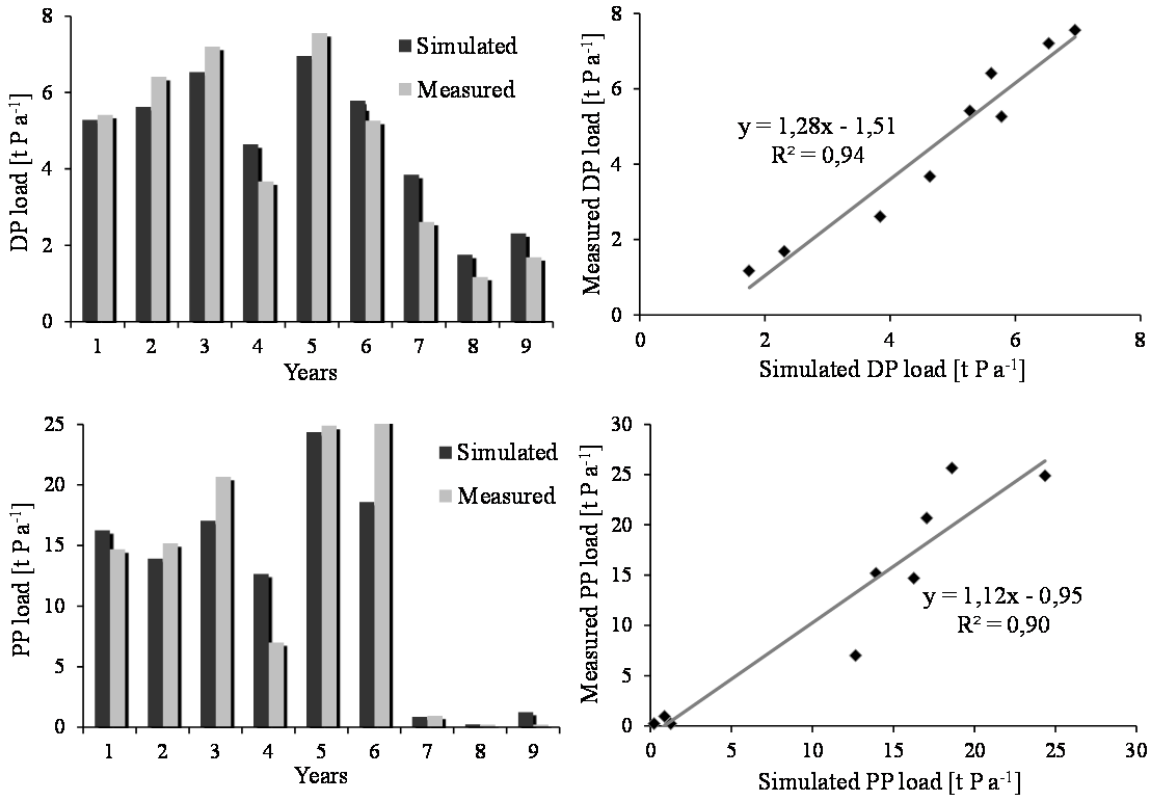

Fig. 3.2 Comparison of simulated and measured annual DP and PP loads in the Zala River.

Fig. 3.3–3.4 show the spatial resolution of the long-term average (1994–2002), yearly area specific DP and PP emissions as well as the outflowing fluxes and the local retention. Areas having higher slopes and agricultural cultivation produce remarkable phosphorus emissions due to their greater runoff and soil loss amounts. TP fluxes are increasing as the water flows down, especially in the mail channel. High rates of local retention were found in forest areas and local depressions.

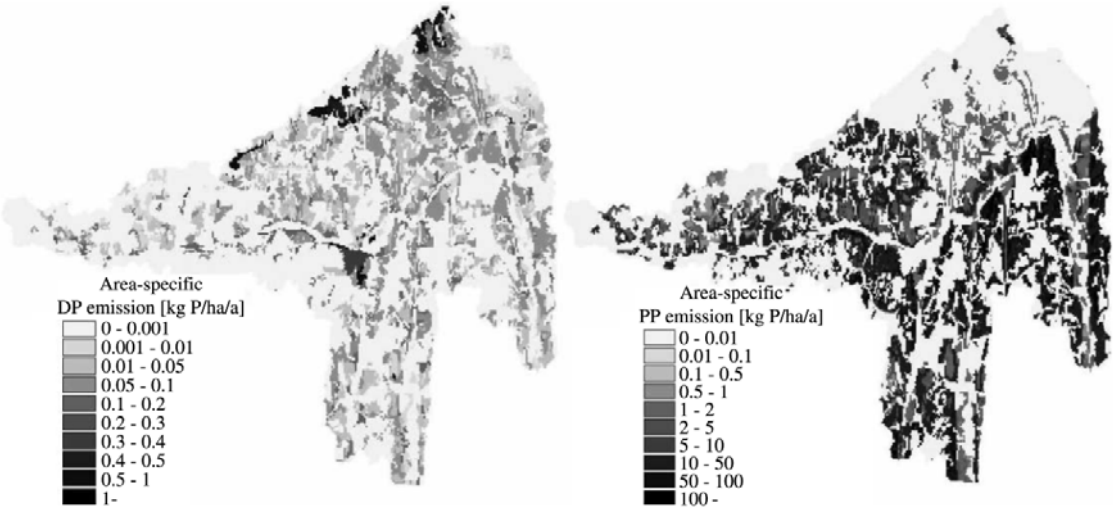

Fig. 3.3 Spatial resolution of long-term average DP (left) and PP (right) emissions in the Zala River catchment.

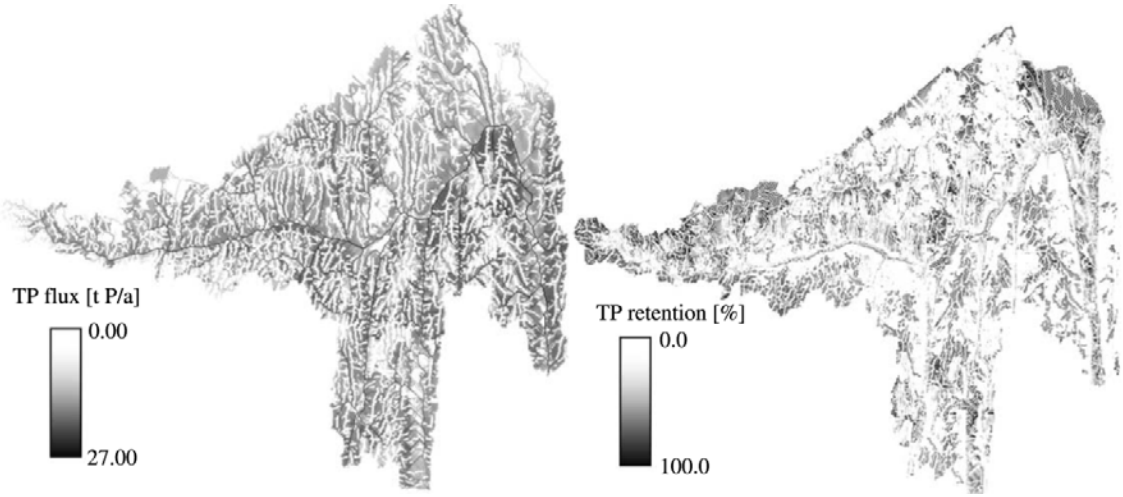

Fig. 3.4 Spatial resolution of long-term average TP fluxes (left) and retention (right) in the Zala River catchment.

3.4.2 Scenario analysis

Comparison of the load reducing efficiency of the planned BMPs can be seen in Table 3.2. The most effective interventions are the combined scenario and forestation. Mulching and strip-cropping can also remarkably reduce the loads. Riparian zones only do not provide sufficient P retention. Costs of the BMPs were also compared (Table 3.3) based on specific costs including losses due to the decreasing agricultural products, deployment and technological costs, *etc*. Forestation has the highest specific and total costs, but it has the best efficiency in load reducing. Buffer zone has the lowest P-specific charges, however, its load reducing capacity is weaker. Erosion control measures have acceptable charges accompanied by effectiveness in P emission reduction. The combined intervention can also be suitable solution if enough financing is available.

Table 3.2 Load reduction efficiency of the selected management practices.

Scenario	DP load [t P a^{-1}]	PP load [t P a^{-1}]	TP load [t P a^{-1}]	Reduction [%]
Present	5.030	21.850	26.880	
I	4.525	4.196	8.721	67.6
II	4.771	11.700	16.471	38.7
III	4.937	7.644	12.580	53.2
IV	4.940	6.031	10.971	59.2
V	4.603	3.615	8.219	69.4

Table 3.3 Costs of the scenarios.

Scenario	Area [ha]	Total cost [Million USD a^{-1}]	Specific P-removal cost [USD (kg P)$^{-1}$ a^{-1}]
I	21600	5.400	297
II	3950	0.988	95
III	21600	2.808	196
IV	21600	3.672	231
V	15500 + 8100	4.660	250

3.5 Conclusions

With the developed PhosFate tool, annual diffuse P emissions via surface pathways at local level can be quantified. The main advantages of the approach are the supportable data

demand and the simple algorithm. Based on the calculated emissions the most important source areas can be identified. By the transport model P fluxes can be determined at arbitrary point within the catchment. The model was successfully calibrated and validated in the Hungarian Zala River catchment. Besides emission and load computation, this method can support strategic decisions in water management. The model was built into an interactive design tool to plan various BMPs in the catchment. Applying the tool, impacts of different land use and cultivation method changes can be easily examined even in complex watersheds. P load reducing capacity and P-removal costs are assessed together. In the pilot area buffer zone establishment was found the most cost effective solution, however, its total P-reduction is the lowest. Forestation is the most effective practice, but at high charges. Combining the buffer zone in the erosion sensitive areas with forestation and/or erosion controlling measures, acceptable technical and economical efficiency can be achieved.

4 Detection of hot spots of soil erosion in mountainous Mediterranean catchments

4.1 Introduction

Soil erosion is almost immeasurable at source; it is hard to identify the area of origin and complicated to manage due to their spatial and temporal variability, complex transport pathways and strong relations to hydrology and soil properties. Because of these characteristics, management of the agricultural soil loss and reservoir siltation problem essentially needs watershed level approximation and model simulations. It is especially necessary, if the river monitoring system is underdeveloped or water quality data are not available. Evaluation of different management scenarios is usually based on model simulations as well. Strategic analyses and decisions related to national water quality management programs or management plans of larger river basins are usually based on larger scale models (Schreiber *et al.*, 2003; Schilling *et al.*, 2011; Zessner *et al.*, 2011a). Local water quality investigations and practical measures rely on smaller scale modeling results.

Local erosion rates in themselves are quite rarely evaluated in respect of water quality. River sediment loads and concentrations (or sediment volume) arising from the local soil losses at the sub-catchment outlets or impoundments are usually used to evaluate the siltation status. However, the desired river load reductions caused by the planned interventions as the overall management results of the whole catchment have to be finally addressed to local fields within the watershed. Soil loss reduction with the same rate in the whole catchment or areas having erosion rates over a certain threshold value would be an equitable solution, but it surely would not provide a cost-effective management. Not all of the source areas effectively contribute to the river loads and the extent of their contribution depends on the transport efficiency of the eroded materials within the catchment and towards the outlet. Management efforts should be concentrated on the critical source areas where transfer of pollutants from land to water probably occurs (Campbell *et al.*, 2004). Therefore, only a transport-based management approach can be environmentally and economically effective.

We present a simple modeling approach, which calculates soil erosion and suspended sediment (SS) transport within a catchment. The model is able to find the most significant source areas contributing to the river loads and provides an optimized, cost-effective management alternative to reduce soil erosion even in the absence of detailed environmental data.

4.2 Methods

The catchment-scale phosphorus (P) emission model PhosFate (Kovács *et al.*, 2008) was applied to evaluate the SS fluxes of the pilot areas. PhosFate was developed for watershed management purposes. The model is appropriate to support decision-making in watershed management. It allows planning best management practices (BMPs) in catchments and simulating their possible impacts on immissions based on the critical source area concept. The model was validated in several types and sizes (from a few to ten thousands of km^2) of well-monitored catchments in Central Europe (Hungary, Austria and Switzerland, *e.g.* Kovács *et al.*, 2008; Honti *et al.*, 2010). The good performance in both arid and wet regions on all spatial scales showed the model's ability to predict the hot spots of erosion and diffuse P pollution in unmonitored catchments. PhosFate is a semi-empirical, long-term average, distributed parameter model. The model computes the main elements of the hydrologic cycle, the soil erosion, local P emissions and SS and P transport in the terrestrial areas and throughout the stream network. The model is able to predict climate change impacts on emissions as well.

4.2.1 Annual erosion and sediment transport modeling

Soil loss is estimated using an adopted version of the Universal Soil Loss Equation (USLE, Wishmeier and Smith, 1978). Parameters of USLE are related to meteorological data (rainfall intensities and heights within the simulation period) and various digital maps about catchment properties (topography, slope, physical soil type, topsoil humus content, land use classes, land management practices). Area-specific annual soil loss values were calculated for every cell. The parameters of USLE were determined according to the literature (Novotny, 2003; Randle *et al.*, 2006) and were kept unchanged during the modeling.

Exceptions are the simulation period dependent rainfall energy factor (as a proxy of the meteorological properties, which can represent climate change impacts) and the erosion protection factor, which can vary according to the desired agricultural practice.

SS transport is computed by joining the individual cells according to the flow tree. Each cell is characterized as either field or channel cell based on a threshold value of upstream catchment area. The outflowing flux from each cell is the difference between the inflowing flux plus the soil loss and the net sediment retention via settling. Net sediment deposition is computed from the inflowing load value with an exponential function of the cell residence time.

Residence time depends on the average flow velocity, which is calculated for both overland and channel flow with the Manning-equation (Fread, 1993). Average hydraulic radius is estimated with a power function of the upstream catchment area of the given cell (Liu and DeSmedt, 2004). Manning roughness parameters are related to the land use classes (Fread, 1993; Liu and DeSmedt, 2004). Deposition rate of the retention formula was calibrated. Different deposition parameter is used for the terrestrial and in-stream transport. Thus, sediment load can be calibrated with two adjustable parameters only, which should be adapted to local conditions. Reservoirs are considered for the channel transport as well, whereas reservoir residence time is calculated from the inflowing discharge and the operation volume. Discharge is calculated according to the long-term water balance model WetSpass (Batelaan and Woldeamlak, 2004). Results of the calculations are the spatial distribution of the soil loss and the SS load values at any arbitrary point within the catchment, the SS retention pattern of the catchment and the cell residence time and travel time values to the outlet.

4.2.2 Hot spot identification and optimization

To identify the cells, which are possible candidates for interventions, a tolerable soil loss value was determined (10 tons per hectare and years in this study). Management scenario analysis was executed according to several individual intervention methods: i) forestation, ii) grassland development, iii) contour planting, and iv) soil stabilization in those agricultural areas, where the computed specific soil loss rate is higher than the tolerable value. Buffer

zone implementation was also examined, all watercourses with an upstream catchment area higher than 10 km^2 were protected by a forest zone along the channel.

To achieve an optimal management (highest reduction in emissions at the lowest cost), not all emission source areas have to be addressed by the interventions, because they contribute differently to the river loads. Tracking the transport pathways from each cell, the most promising locations for an intervention can be selected. The cells, which succeed to send the biggest amount of eroded material to the stream network, can be considered as ideal subjects to source control (reduction of local erosion). The latter layer indicates the main transmitters, which probably have limited rate of erosion, however, they transport significant amounts of SS coming from their immediate vicinity. These are the best places for transport control, *i.e.* to establish retentive zones (mostly along streams). Ranking the cells on both maps, a priority sequence can be derived for the interventions, which forms the basis for an optimized intervention calculation. The optimization can be governed by two objective functions (either load reduction efficiency at fixed available cost or cost efficiency at fixed pollution limit). The two intervention types (source and transport control) must be harmonized during the calculations. If a highly erosive cell is treated by intervention, the relative importance of their downstream neighbors also reduces. Similarly, by the allocation of a buffer zone, the effective contribution of the upstream neighbors declines. Thus, the importance ranking of cells must be updated after each intervention act in a specific cell.

The algorithm of calculation is the following:

1. Estimate to achievable gain for each cell.
2. Intervene (change land use) in the cell with the highest possible gain.
3. Actualize the model calculations in the affected region (up- and downstream neighbors of the intervention cell).
4. If the budget is spent, finish the procedure, else repeat from the beginning (1).

4.2.3 Case study region: Albania

Albania (Fig. 4.1) has a total area of 28 750 km^2, is located between the coasts of the Adriatic and Ionian seas and the Balkanian mountain chains. It has a dense river network with seven

main rivers, which flow from East to West. Catchments of river Buna, Drini and Vjosa have considerable part lying in the neighboring countries, thus, the total hydrographical catchment area of the Albanian rivers is 43 300 km^2, *i.e.* one third of the total catchment is out of the country.

Soil loss via water erosion in Albania is a widespread phenomenon. Soil loss is 2-3 times higher in Albania than in other Mediterranean countries and 10 to 100 times greater than in many other European countries. The typical Mediterranean climate is one of the most aggressive ones in terms of erosion (heavy rainfall intensities, high rainfall amounts, drought as a permanent phenomenon, *etc.*). This together with the topographic (Fig. 4.1) and soil conditions (steep slopes, silty soils, and low humus content) already classifies about more than 50% of the total area in Albania as naturally erosive. This is amplified by the anthropogenic impacts (forest cutting, cultivated steep slopes, up-down cultivations, bare soils after harvesting, overgrazing, absence of erosion protection measures) resulting in significant soil loss rates. Consequently, coastal areas and terrestrial reservoirs are highly subjected to increased SS loads and thus, to accelerated siltation.

Local measurements on hydrology and erosion are extremely scarce and mostly historical. However, the international scientific literature contains several estimates on the erosion and sediment transport in the Mediterranean region. Nevertheless, the various authors report a wide range of soil loss and sediment transport level of the country. Bockheim (2001) states a national average soil erosion rate of 27.2 tons per hectare and year, which results in an annual sediment flux of 60 million tons carried by the Albanian watercourses. Grazhdani and Shumkab (2007) presents an estimation of soil erosion for the whole country, they computed a soil loss rate more than 10 tons per hectare and year for a remarkable part (in the center and south) of the country and even more than 100 tons per hectare and year at three smaller regions also in the south. Bruci *et al.* (2003) reports a soil loss range of 20-100 tons per hectare and years for Albania and they computed for the north, middle and south-east region of the country an annual average agricultural erosion rate of 15, 53 and 37 tons per hectare and year, respectively.

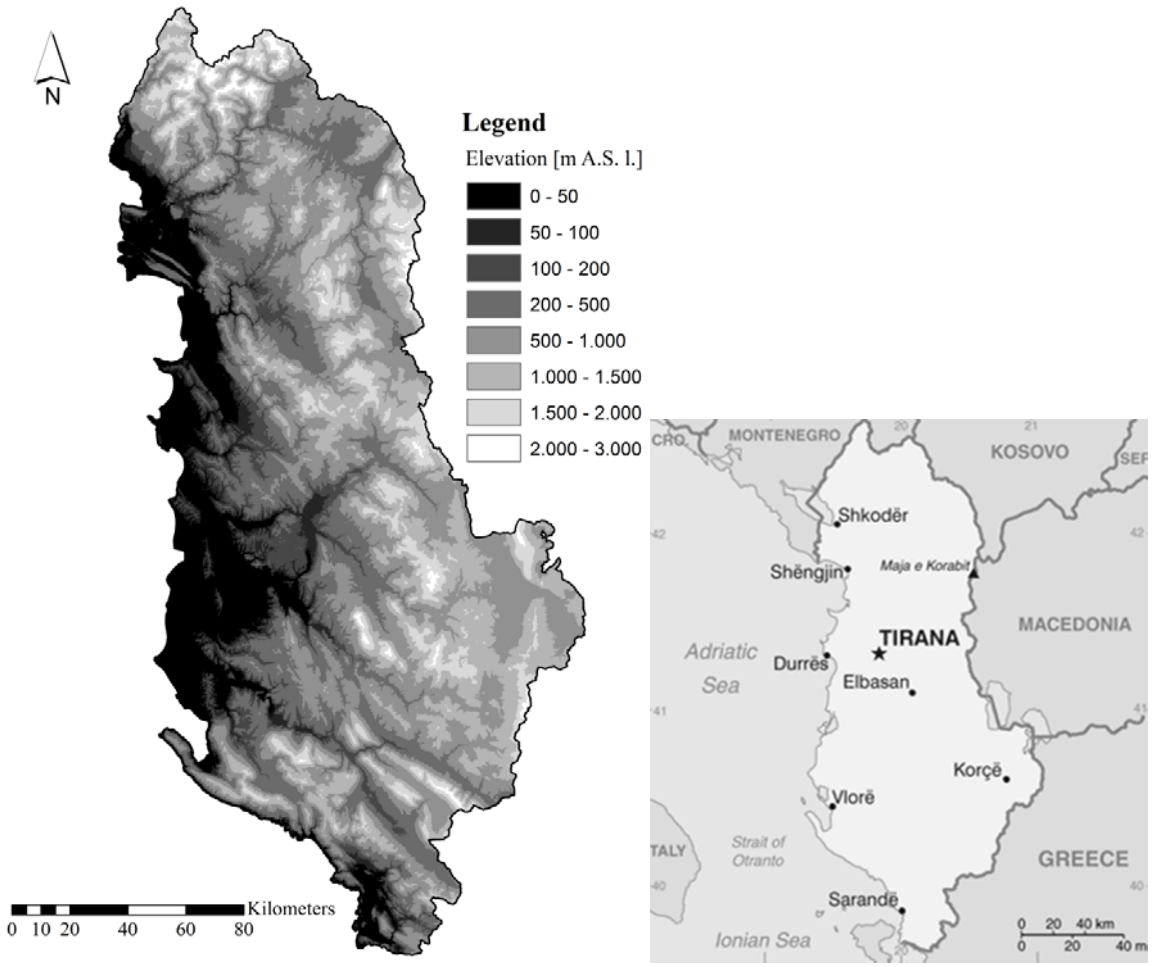

Fig. 4.1 Albania and its topography.

Poulos and Collins (2002) reports about 83 million tons per year SS fluxes transported by the main Albanian rivers into the Adriatic and Ionian seas. Pano *et al.* (2004) published a lower average load entering the seas with a value of 52 million tons per year, however, the fluxes can vary in a wide range between 30 and 120 tons per hectare and years. From the literature data net SS loads were determined which consider the SS loads generated in the Albanian territory only (*e.g.* Drini and Vjosa rivers flow from abroad into the country, but the input data cover only the Albania part of their watershed). The main rivers were used for the model calibration. Their discharge can significantly vary according to the current climatic conditions. River flow can reduce by 40-50% in dry years and increase by 40-70% in wet years. Variation of SS flux is wider, it is from 40% up to 140% according to the climate.

The erosion module of the PhosFate model was applied for the whole territory of Albania considering long-term average conditions. To perform a countrywide assessment on erosion and sediment transport a GIS database was compiled according to the model demands. The necessary digital maps (*e.g.* topography, soil characteristics, humus content, land cover and vegetation) and climate data (rainfall, meteorology) were collected from different international data sources. Besides these, river monitoring data on discharge and SS loads as well as results of other erosion studies were also collected from the literature to calibrate the model and execute comparisons. Data for the modeling were collected from international databases and publications on the erosion and its related and important fields.

4.3 Results and discussion

4.3.1 Model calibration

Modeled versus „measured" (determined from the literature data) long-term average net (generated in Albania) river flow and SS load values are presented in Fig. 4.2. Parameters of the hydrological module of PhosFate, the USLE equation and the transport algorithm were adjusted manually in order to achieve a reasonable fit with the measured ones. Special key factor of the erosion in Albania is the overgrazing of the pastures and woodlands. Pastures, sparsely vegetated areas and the semi-agricultural lands were considered as potential candidates for overgrazing. Their plant coverage parameter was set close to the values of croplands and bare soils (the same was assumed for orchards to take into account grazing effect between the plantations or trees).

Discharge simulations fit quite well the observed data, there are small relative inaccuracies (about 30% overestimation) in case of Ishmi, Erzeni and Semani. In case of SS load, the picture is a bit more problematic. The order of magnitude of the observed loads are well predicted by the model, however, some remarkable deviations can be recognized. In Mati and Ishmi there is a quite significant model error by 60% over- and 50% underestimation, respectively. Erzeni, Drini and Vjosa have also some local differences (30-40%) compared to the estimated values.

Uncertainties in the modeling procedure have three clear sources. The first main source is the input data set. Several maps have low resolution, as they were acquired from global datasets so the small-scale heterogeneities cannot be considered. Besides this, statistics data are usually missing or scarcely available in questionable quality. The second source of uncertainty is the model itself with its assumptions, mathematical approximations and simplifications. The backbone USLE equation is highly empirical, therefore its parameters may differ in a new region. Precise setting of USLE-factors should be based on local conditions. The third component of uncertainties is the reference data set, which was considered as "reality" when the model was calibrated. Due to the overwhelming weight of large-scale estimates in the dataset, the uncertainties in the reference data regarding local soil loss and sediment transport are surely immense. Occasional river sediment fluxes measurements and sediment trap data were the only possibilities to check the performance of any soil erosion calculations. The local measurement of soil loss is very difficult, it can cover only a small field, it requires special equipment plus it has remarkable costs, thus, it had not been applied in the study region.

Considering these uncertainties and the availability of the data, the computed results are satisfying. More detailed information could significantly improve the model performance at local scale and provide the possibility to refine the model parameters or apply more sophisticated approaches. However, despite the limitations and uncertainties of USLE, its improved or revised forms are widely used as long-term soil loss estimator and engineering tool for choosing BMPs to control erosion (Nearing *et al.*, 2001)

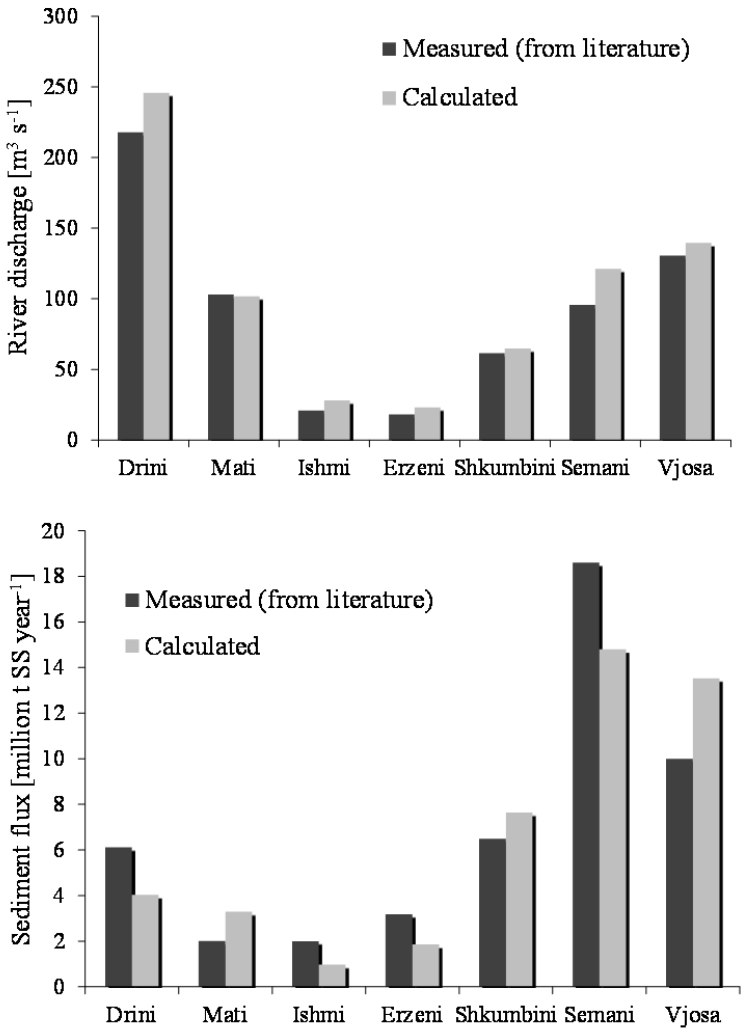

Fig. 4.2 Simulated and reported long-term average net river flow of the Albanian rivers (top); simulated and reported long-term average net SS flux of the Albanian rivers (bottom).

4.3.2 Soil erosion

The calculated soil loss rates of Albania are shown in Fig. 4.3 left. There is remarkable soil loss in the whole territory, but it is especially significant in three main regions, which are located in the north, in the central part of the country and in the south. In these regions, similarly to Grazhdani and Shumkab (2007), high soil loss rates can be found with values more than 10 tons per hectare and year, but values even more than 100 tons per hectare and years appear also quite frequently. Countrywide average soil loss rate is 31.5 tons per hectare

and year, which is far above the tolerable limit of 10 tons per hectare and year, but it fits the average rate reported by Bockheim (2001). The average rate means totally 90.5 million tons soil eroded annually in the country. Distribution of the higher soil loss classes is demonstrated in Table 4.1, 78% of the territory produces tolerable erosion, and 22% (6399 km^2) has higher soil loss rate than the tolerable limit. However, this 22% of the total area is responsible for the majority (93%) of the soil erosion. 76% of the source areas (4875 km^2) is agricultural land. The natural areas (1523 km^2) cause the background SS loads of the river system.

Moderate slopes up to 7% do not generate high soil losses for both specific and total values. Over 7% slope the soil loss values ate increasing and reaching a value more than 40 tons per hectare and year. Over 24% the specific value is slightly rising only, however, due to the high share of the steep regions in the country, the total soil loss volume is much higher in the steepest class (about 57 million tons per year) than in the others. 63% of the total soil loss comes from the steepest regions of the country, while below 12% steepness the contribution to the total erosion is very low.

Extremely high soil loss rates (60-130 tons per hectare and year) were calculated for the mixed agricultural land and the orchards/vineyards located on high slopes. This results in an enormous total soil loss (82 million tons per year) from the total agricultural sector. The mixed lands (especially the semi-natural lands), the grasslands, the sparsely vegetated areas probably used as intensive pasture and they candidate for overgrazing, which leads to high erosion rate. Besides this, it is important to note, that the special monthly distribution of the rainfall in Albania highly strengthens the impacts of erosion, because most of the rainfall events occur in the winter half-year, when agricultural soils are often uncovered. The naturally covered areas remain at low erosion rates at the country level. 92% of the total soil loss comes from the agriculture (or areas affected by the agriculture, *e.g.* overgrazed natural lands), while 8% can be considered as background erosion.

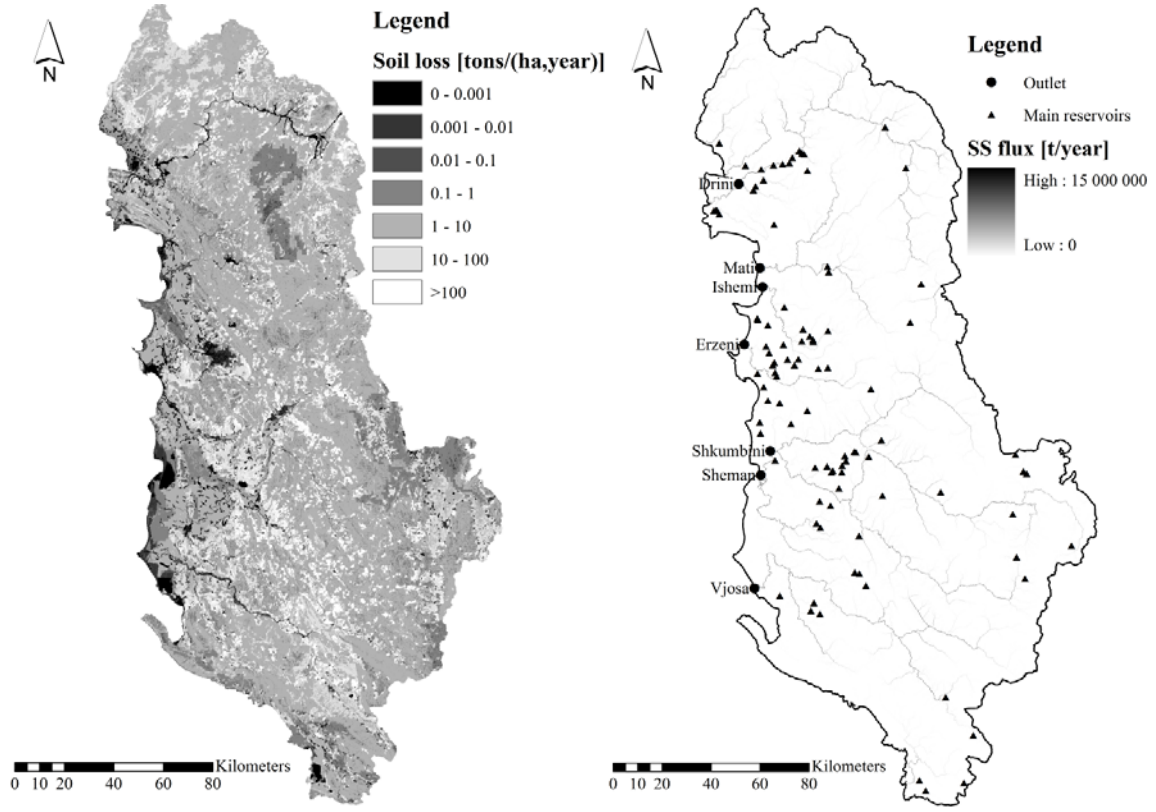

Fig. 4.3 Calculated long-term average specific soil loss rates in Albania (left); sediment transport by the main watercourses of Albania (right).

Table 4.1 Areas, total amounts and proportions of the specific soil loss rate classes in Albania.

Soil loss rate $t\ ha^{-1}\ year^{-1}$	Area km^2	Area proportion %	Total soil loss $10^6\ t\ year^{-1}$	Soil loss proportion %
<1	6556	23	0.2	0.3
1-10	15795	55	6	7
10-100	4122	14	13	14
>100	2277	8	71	79

4.3.3 Sediment transport

Despite the huge total soil loss (90.5 million tons per year) generated in the country, only *ca.* 55 million tons SS is transported by the rivers into the seas annually (Fig. 4.3 right). Consequently, about 40% of the eroded soil material cannot reach the seas because of the

retention while sediment is transported from the source to the recipients. Considerable sediment retention via settling can occur either on the terrain when the surface runoff velocity reduces (decreasing slope, changing land cover) or in the river systems when the flow velocity drops due to hydraulic alterations of the channel (reservoirs, vegetated channels, sections with slow velocity and flow on the floodplain).

In total, 53 million tons per year SS flux is transported out of the country. The highest sediment loads are carried by the river Semani and Vjosa into the seas. About 18% of the SS fluxes discharged from the sub-catchments into the river systems are retained in the river channels, mainly in the reservoirs. The highest sediment retention occurs in river Drini, which has a huge reservoir at Fierze (its surface area is about 70 km^2), where majority of the sediment load is retained. Without the reservoir the river would carry almost 20 million tons annually. Reservoirs have significant impacts in Mati and Ishmi rivers as well. Remarkably sediment retention can be recognized on the terrestrial field also, it is about 21% of the total soil loss in average (slightly varying among the sub-catchments). At country level, 59% of the eroded soil volume is transported to the seas, the sediment retention is equally distributed between the field and the reservoirs.

4.3.4 Management of the source areas and optimized interventions

Among the BMP alternatives forestation and proper grassland management are very efficient, almost 90% of the original soil loss is remains on the field if forestation or grassing is applied. They have almost similar reduction efficiency, there is no considerable difference between their impacts, excepting if grassland is used as pasture. Poaching by animal hoofs and overgrazing can highly reduce the efficiency of the grassland. In case of forest, a certain time period is needed for developing a dense forest, so in the first couple of years the forests remain at lower efficiency until reaching their maturity. Buffer zones along the streams have only small impacts on soil loss at country level (7%) because the interventions consider the riverside zones instead of the source areas. Agricultural soil protection without any soil stabilization is limitedly successful only (17%), however, if it is accompanied by vegetative soil stabilization (*e.g.* mulching on the bare soil or grassing between the permanent crop rows/fruit trees), the efficiency approximates the value of the forests (74%). Decrease of the sediment flux due to the interventions is similar to the soil loss reductions for the source

control measures. However, buffer zones can provide remarkable SS retention by filtering their fluxes when they pass the zone. Buffer zones are insufficient as individual intervention, however, they can enhance the source controls with an additional transport control, consequently the intervention areas at the source can be reduced. Management an agricultural area of 4875 km^2 (17% of the country area) can produce impressive soil loss reduction, however it does not consider cost efficiency.

The optimization method was applied for the whole country. The objective was set to reach the highest load reduction with intervening on maximally 4.5% of the total area. The load reduction was efficient (Fig. 4.4 top). The achievement of the intervention varied from 50% (Erzeni) to 68% reduction (Vjosa) among the watersheds. Similarly, the spatial distribution of intervention locations was not homogeneous in the country (Fig. 4.4 bottom). There were 3 main zones where a significant proportion of interventions concentrated. These areas are the hotspots for erosion and sediment loads on the country level. In the lower Drin watershed the optimal intervention zones covered large, uninterrupted areas on the catchments of some tributaries. However, in the middle and Southern mountainous parts the erosion hotspots formed several independent smaller zones, which are harder to manage. This shows that the manageable erosion-sensitive areas are easier to delimit in some northern parts, while this property shows a much higher spatial variability in the rest of Albania.

Erosion has a very high spatial heterogeneity in the whole country, just like in other parts Europe. This highlights the fact that management should first identify the small-scale locations where best management practices can effectively reduce both erosion and the siltation of the surrounding stream network. Simultaneously, this high variability makes it possible to implement very effective (50-80% reduction) prevention measures by the application of best management practices on a minor proportion (around 5% instead of 17%) of the total catchment areas. Certainly, as erosion is more intense on agricultural areas, the affected proportion of cropland and orchards is higher, typically 10-15% of this category is affected by measures. But the variety of BMP methods allows continuing agricultural production in these zones with minor modifications that reduce erosion.

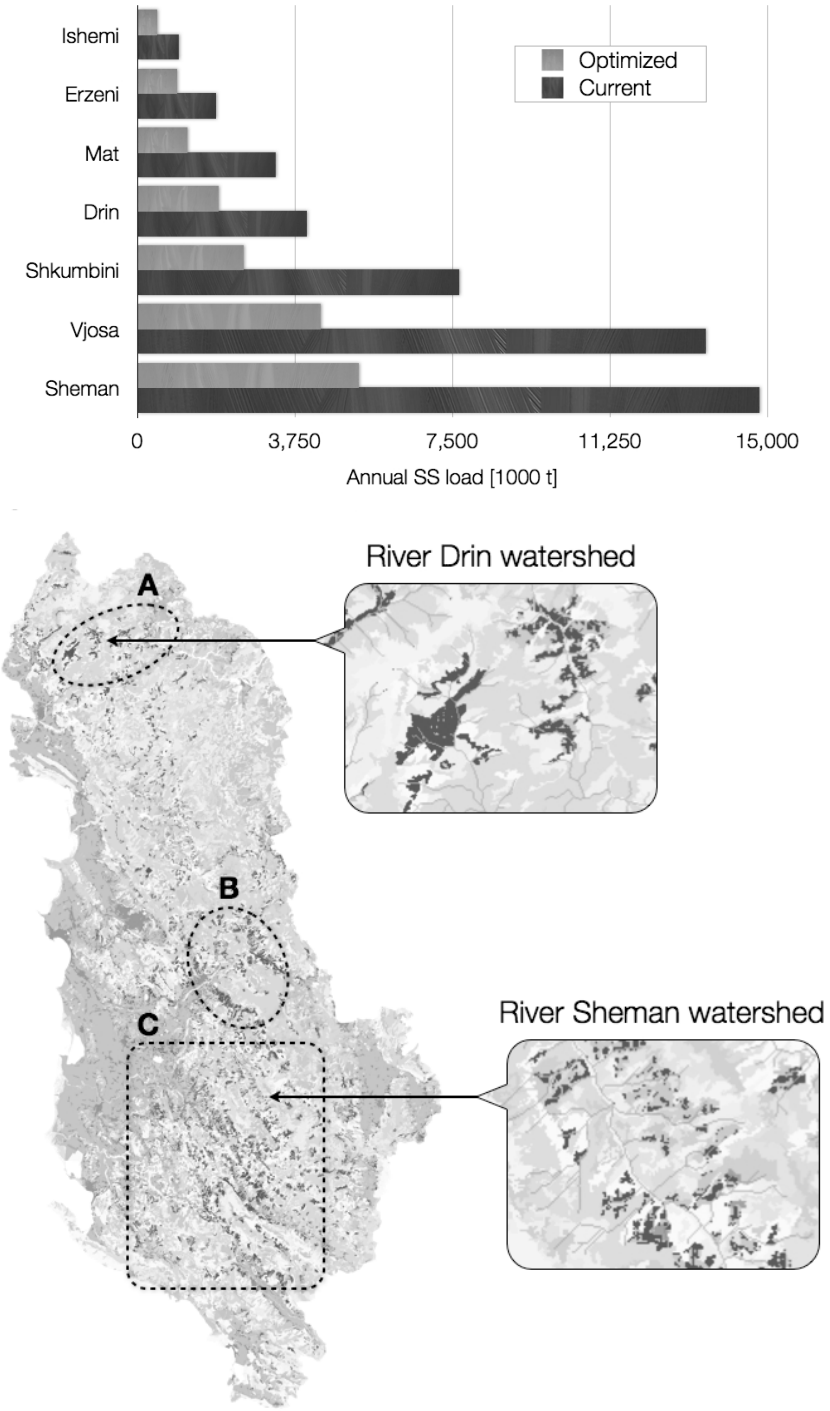

Fig. 4.4 Optimization results (load reduction) for the entire Albanian territory (top); optimized intervention locations in Albania (bottom); A, B and C are the easily manageable erosion hotspot zones (the magnified parts show the different spatial arrangement of intervention zones in the Northern and Southern parts of the country).

4.4 Conclusions

Countrywide average soil loss is about 30 tons per hectare and year. 22% of the country area has higher soil loss rate than the tolerable value (10 tons per hectare and year). This 22% is responsible for the majority (93%) of the soil erosion. Main source sector is the agriculture, which generates *ca.* 90% of the total soil loss, especially agricultural lands located on high slopes. The main Albanian rivers transport considerable SS loads to the seas, *ca.* 60% of the total soil loss amount can reach the coastal zones. According to both international experience and an adapted model application, the erosion potential is highly variable in Albania, too. Hotspots that contribute most to the soil loss and the siltation of streams are frequently separately positioned small areas.

Management scenarios can effectively reduce the local soil loss and the sediment fluxes as well. Both natural vegetative cover and agricultural cultivation with erosion control can be successful. If intervention measures are concentrated on the highly contributive areas, an immensely effective management can be achieved without having to transform the overall land use practice on most of the catchments. Introducing BMPs on a carefully selected few percent of the total area can cut the total amount of erosion and also the transported material fluxes by half or even more.

5 Identification of phosphorus emission hotspots in agricultural catchments

5.1 Introduction

Diffuse phosphorus (P) emissions are almost immeasurable at source and consequently it is hard to identify their area of origin. Management of diffuse P pollution is complicated to implement due to the spatial and temporal variability of the emissions, their different transport pathways and complex and strong relations to hydrology and soil properties. Because of these characteristics, cost-effective management of the diffuse P pollution requires watershed level approximation and model simulations (Campbell *et al.*, 2004) unless a strong emission-based principle is applied (*e.g.* emission regulations), which might be costly and of limited acceptance. Model simulations are especially necessary to understand processes taking place in the catchment if the river monitoring system is underdeveloped or water quality data are scarce. Besides the assessment of existing pollution patterns, mathematical models can be used to assist in the evaluation of management practices to be applied in the catchment (Mostaghimi *et al.*, 2001). Lumped screening models are able to identify the sub-catchments, which have a clear water quality problem related to diffuse emissions, and they can evaluate the role of different pathways and sources of pollution. However, more detailed examinations on the spatial distribution of the emissions and local planning of management practices are limited due to the spatial aggregation used in these models. Spatially distributed catchment models, which divide the study area into small elementary units, focus more detail on the local variations of the catchment properties, the contaminations and their management alternatives within the watershed.

The application of models with different spatial scales depends on the management goals. Strategic analyses and decisions related to national water quality management programs or management plans of larger river basins are usually based on larger scale models (Schreiber *et al.*, 2003, ICPDR, 2009, Schilling *et al.*, 2011, Zessner *et al.*, 2011a). Local water quality investigations and implementation of practical measures rely on field studies and smaller scale modeling results (field scale models, *e.g.* CREAMS, Knisel, 1980 or EPIC, Williams *et*

al., 1983). Watershed scale water quality models (*e.g.* WEPP, Flanagan and Livingston, 1995; EUROSEM, Morgan *et al.*, 1998; ANSWERS-2000, Bouraoui and Dillaha, 2000; SWAT, Neitsch *et al.*, 2002; AnnAGNPS, Bingner and Theurer, 2003) usually use the principles of the process-based field scale models by extending them to complex land use and management situations (Shirmohammadi *et al.*, 2001). The so called index-based approaches attempt to identify the critical pollution areas within the catchment. These pollution screening assessments are often followed by field scale model applications to determine best management practices for the polluted areas (Shirmohammadi *et al.*, 2001).

In case of a distributed parameter model, the selected element (grid) scale can significantly influence the model performance. A major source of error in catchment models comes from the incompatibilities between model scale, database scale and the scale of the heterogeneity of the environmental processes (Zhang *et al.*, 2004). The most common issue is that the parameters or input data are measured at one particular scale (or more) and then they are inputs into a model constructed at another scale. Therefore, some assumptions on the upscaling are needed. The choice of the grid scale (resolution) determines how the variability is represented in the model (Grayson and Blöschl, 2000). Differences from element to element are represented explicitly, whilst heterogeneity within an element is represented implicitly. Fluxes generated in a single element can be explicitly routed in the catchment, however, the related model variables in a grid are affected by the fluxes of the surrounding cells besides the local characteristics (Zhang et al., 2004). Sub-element (implicitly represented) variables can be conceptualized in four ways: (i) assuming zero variation of the parameter values, (ii) using effective parameters, which reproduce the bulk behavior of the cell, (iii) applying distribution functions rather than a single value and (iv) direct parameterization of sub-grid variability (Blöschl and Sivapalan, 1995).

Recent model applications to assess spatial variability of the soil loss or P emissions or spatial risk assessments often rely on the Universal Soil Loss Equations (USLE, Wischmeier and Smith, 1978) or its improved versions (*e.g.* the Revised USLE, (RUSLE), Renard *et al.*, 1997). Van Rompaey *et al.* (2001) developed a new model (SEDEM) to calculate annual sediment yield of river systems, which contains the RUSLE approach (for erosion rates) and a routing function (for sediment transport). They concluded that accuracy of sediment yield predictions using distributed model is significantly higher than that of a lumped regression

model. De Vente *et al.* (2008) applied and compared three sediment yield models with different basic concepts (empirical, physically based and index-based) at regional scale. They state that for the prediction of erosion rates at the regional scale, the use of simple models with limited data requirements seems preferable and provides the best results. Tetzlaff *et al.* (2013) presented an application of an adopted version of USLE extended with a sediment delivery ratio to identify areas having risk potential for sediment input to surface waters. The paper suggests that based on the results, delineation and ranking of sub-areas vulnerable to soil loss and sediment transfer become feasible, followed by target-oriented investment to conduct detailed studies and programs of measures.

Another direction in this research field is to focus on the transport efficiency of the areas and the possible transport routes of the sediment within a catchment under different land use and topographic conditions. These approaches examine the connectivity of the hydrological (sediment transport) systems and determine spatial linkages between the sediment source areas and the recipients through catchments. Using connectivity analyses the effective catchment area can be determined, which has a contribution to the river loads. Examples of this approach can be found in *e.g.* Fryirs *et al.* (2007), Borselli *et al.* (2008) or Aurousseau *et al.* (2009). Phosphorus Index approaches attempt to identify the areas within the catchment, which have potential risk of P movement to water bodies (Campbell and Edwards, 2001). The index is determined by assessing different factors on P availability at the sources (*e.g.* fertilizer and manure rates and application forms, availability for plants), transport possibilities (*e.g.* runoff and soil loss rates, travel distance) and the affecting management properties. P-Index model applications are presented by *e.g.* Bechmann *et al.* (2007), Drewry *et al.* (2011) or Ulén *et al.* (2011).

Water quality targets that are used to evaluate the pollution status of water bodies are usually related to in-stream concentrations (*e g.* requirements based on the European Water Framework Directive (EU WFD), OJEC, 2000). The overall results of the watershed management can be realized as river load (concentration) reductions at several stream monitoring gauges. However, the required management practices to reduce river loads have to finally be addressed to relevant sources within the watershed. Emission reductions with the same rate in the whole catchment or areas having emissions (or soil loss rates) over a certain threshold value would be an equitable solution, but it surely would not provide a cost-

effective management with respect to river water quality. Not all of the source areas effectively contribute to the river loads and the extent of their contribution depends on the transport efficiency of the emitted pollutants within the catchment and toward the outlet. Thus, management efforts to reduce water pollution should be selective if costs are also considered. Interventions should be concentrated on the critical source and/or transfer areas where the highest fluxes to the river net come from and/or where significant direct transfers of pollutants from land to water probably occur (Campbell *et al.*, 2004). Therefore, only a transport-based management approach can be environmentally and economically effective. Besides this, persuasion of the local stake-holders on the necessity of the management actions and the practical execution of the management plans including adequate technical implementation and financial subsidies can probably be realized on a smaller proportion of the catchment area.

Since P usually moves from the sources toward the water bodies in particulate form via overland sediment transport generated by runoff (Campbell and Edwards, 2001), the paper concentrates on the fate of suspended sediment (SS) and particulate phosphorus (PP) within the catchment. The paper presents an enhanced catchment-scale modeling approach by improving its earlier versions. The new model functions focus on SS and PP transport modeling and their optimized management. The model is able to find the most significant source areas contributing to the river loads and provides an optimized, cost-effective management alternative to reduce P emissions. The advantage of the model as compared to other more complex approaches is that information requirements are restricted to data easily available in many countries throughout Europe and beyond and application is neither limited by time and money consuming data acquisition nor calibration procedures. The simple, well-structured methodology contains sets of empirical and physically-based equations with limited number of variables and parameters. Although the model is not able to follow P load time-dynamics by focusing on the spatial variability of the emissions and loads within the catchment, it is easy to recognize likely hot-spot regions and evaluate efficiency of management practices. The model was applied to test the improved algorithms in two pilot areas, which have similar catchment properties (topography, soil, land use, climate), however, they show different SS and PP load observations. Comparative study was executed

in respect to the river loads, spatial distribution of the emissions and management scenarios to reduce SS and PP fluxes.

5.2 Case study areas

The study was performed in two hilly catchments with significant agricultural coverage and dominance of diffuse P emissions. The Wulka River is located in the eastern part of Austria, whilst the Zala River catchment can be found in Western-Hungary (Fig. 5.1). Both watersheds are well monitored (many monitoring stations at high frequency), which provided a proper data set for the model calibration and validation. Since both of the rivers are the main inflows of high-priority lakes (Wulka: Lake Neusiedler, Zala: Lake Balaton), examination of PP river loads is of high concern due to the remobilization capability of the PP settled in the lake. The main watershed characteristics are summarized in Table 5.1. Long-term average (between 1994 and 2000, omitting data of the extreme years) PP concentrations of Wulka and Zala are 0.24 mg P l^{-1} and 0.19 mg P l^{-1}, respectively. Total phosphorus (TP) values are 0.39 mg P l^{-1} (Wulka) and 0.28 mg P l^{-1} (Zala). Since these measured PP and TP concentrations are high in comparison to any water quality standards, reduction of PP river loads is a reasonable management task. Further reason of selection of these two areas was that despite the general properties of the catchments their measured area-specific SS loads show a clear difference, which encourages executing a comparative assessment.

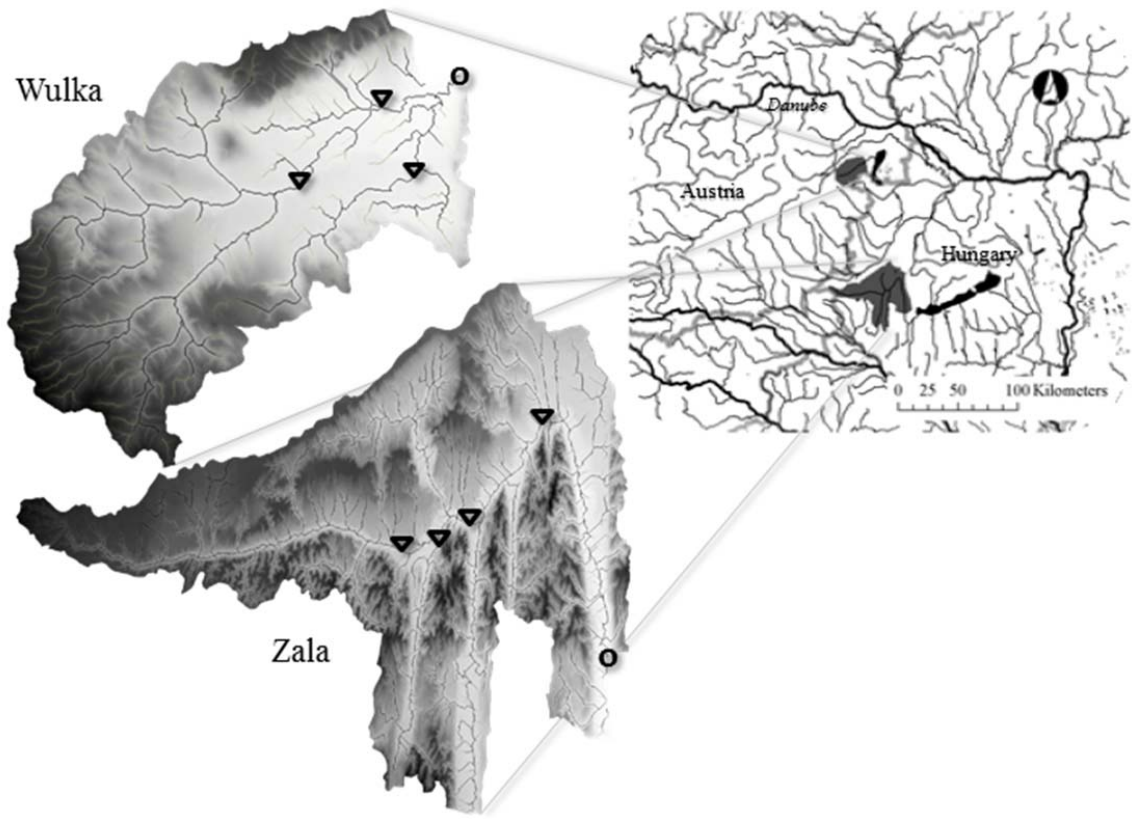

Fig. 5.1 Location of the case study areas (circles and triangles indicate the catchment outlets and upstream gauges, respectively).

Table 5.1 Main characteristics of the Wulka and the Zala catchments.

Attribute	Unit	Wulka	Zala
Area	km^2	373	1480
Mean slope	%	8.0	6.5
Dominant soil type	-	silty, loamy soil	loamy soil
Share of cropland	%	54	49
Share of pastures	%	12	9
Share of forests	%	28	36
Average precipitation	$mm\ a^{-1}$	625	658
Long-term P surplus	$kg\ P\ ha^{-1}$	615	490
Mean discharge	$m^3\ s^{-1}$	1.1	5.6
Mean SS load	$t\ SS\ ha^{-1}\ a^{-1}$	0.13	0.07
Mean PP load	$kg\ P\ ha^{-1}\ a^{-1}$	0.23	0.23
Mean TP load	$kg\ P\ ha^{-1}\ a^{-1}$	0.37	0.33

5.3 Methods

5.3.1 The PhosFate model

The catchment-scale P emission model PhosFate (Kovács *et. al*, 2008) was developed for watershed management purposes. It is appropriate to support decision-making in watershed management. It allows planning best management practices (BMPs) in catchments and simulating their possible impacts on the phosphorus loads based on the critical source area concept. PhosFate is a semi-empirical, long-term average, distributed parameter model. Its spatial units are raster cells (with a size of *e.g.* 50 x 50 m), the time scale is one year or more. It was originally planned to evaluate the point/non-point ratio of the P emissions and to assess the efficiency of different management scenarios in comparison to the present state. The model computes the main elements of the hydrologic cycle, soil erosion, local P emissions and P transport in the terrestrial areas and throughout the stream network. The model was validated in several types and sizes (from a few to ten thousands of km^2) of well-monitored catchments in Central Europe (Hungary, Kovács *et. al*, 2008; Honti *et. al*, 2010; Albania, Kovács *et. al*, 2012a; Austria and Switzerland, ongoing research projects). Model applications showed good performance in both arid and wet regions.

The recent version of the model builds on the earlier attempts (Kovács and Honti, 2008; Kovács *et. al*, 2008) by either adapting or improving their algorithms. However, significant extensions have been recently implemented in the model as well. PhosFate includes water balance modeling and flow routing, enhanced calculation of emissions and transport of SS, PP and dissolved P (DP), calculation of impacts of point sources and reservoirs and an optimization algorithm to reveal relevant emission sources. Since the paper focuses on the fate of the SS and PP fluxes, only the relevant parts of the whole methodology are presented. The scheme of the SS and PP transport calculations is demonstrated in Fig. 5.2. The overall model concept is to build up the catchment from elementary cells to represent the spatial heterogeneity of the watershed. Sub-grid variability is conceptualized by either assuming no variability in the cells or applying effective parameters. Soil loss rates (with USLE) and PP emissions (based on agricultural P surplus data and the soil loss) are computed for every single cell independently according to their own properties. Then the individual cells are

connected by the flow tree and a cumulative transport is calculated with an explicit routing using mass balance equations. SS and PP retention is calculated as a function of the cell residence time.

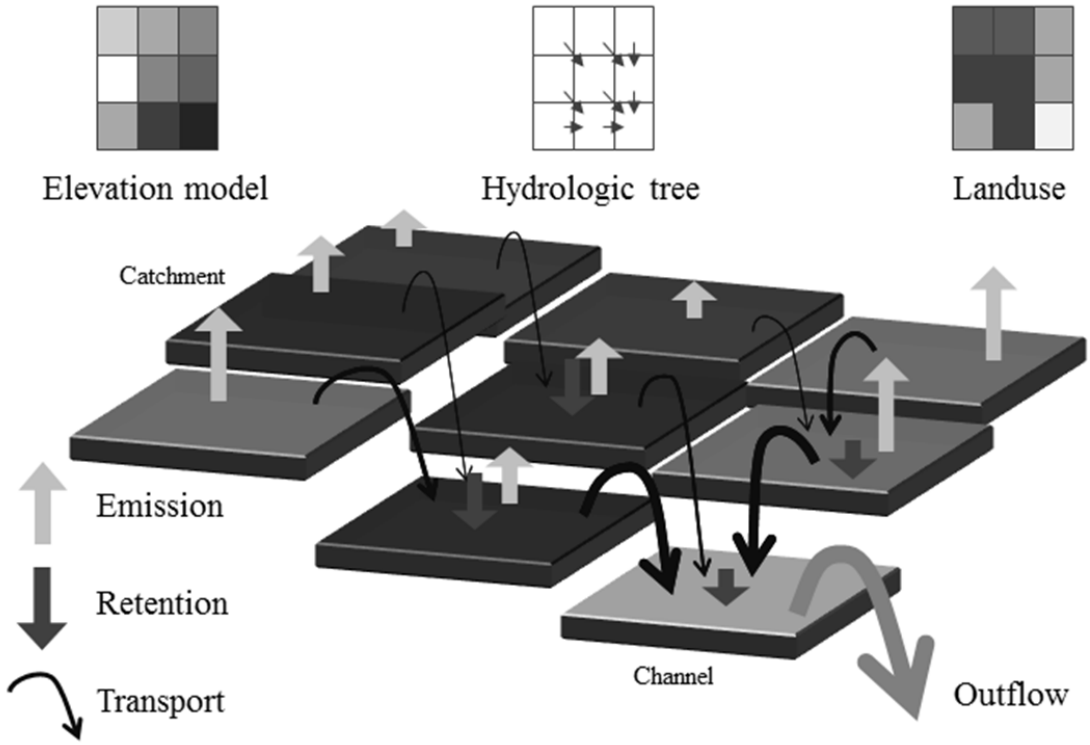

Fig. 5.2 Scheme of the transport algorithm.

A detailed methodology of the model is described in Appendix A. The most important modifications of the emission and transport modeling are the introduction of a dual function (riparian zone and water body) for the channel cells, the enhanced calculation of the SS and PP retention in the terrestrial areas and the separation of the field and in-stream retention parameters. Main inputs of the model are digital maps (elevation, soil type, land use and humus content), statistical data (agricultural P surplus), meteorological data (rainfall records) and point information (reservoir volume). Results of the calculations are the spatial distribution of the soil loss and PP emissions, the SS and PP load values at any arbitrary point within the catchment, the SS and PP retention patterns of the catchment and the cell residence time and travel time values to the outlet.

The optimization algorithm – as the most important model improvement in comparison to the earlier versions – is presented in the following.

5.3.2 Hot spot identification and optimization

To achieve an optimal management (high reduction in PP and SS exports from the catchment at low intervention cost), not all emission source areas have to be addressed by the interventions because they contribute differently to the river loads. PhosFate calculates all processes in a spatially explicit manner. In this way, any modeled quantity can be monitored with the resolution of the input data. Each cell has its contribution to the total river loads and some cells transport remarkable mass fluxes coming from their upstream neighbors in the hydraulic hierarchy. Tracking the transport pathways from each cell, the most promising locations for an intervention can be selected. The selection is driven by the load contribution efficiency of the cells determined by the model. Those cells, which succeed to send the biggest amount of emitted material to the stream network, can be considered as ideal subjects to source control (reduction of local emission via *e.g.* land use change or erosion protection). On the other hand, there are cells that transport significant amounts of P to the rivers coming from their immediate vicinity (even though they can have low rate of own emission). These are the best places for transport control, *i.e.* to establish forest or grassy retention zones (mostly along streams). Some of the cells produce and transmit considerable fluxes as well (*e.g.* arable land adjacent to a stream). The optimization can be governed by two objective functions. The first option is cost efficiency at fixed pollution limit, *i.e.* how to reduce the amount of PP transport into the stream network to a prescribed limit with the most effective intervention methods (covering as few cells as possible). The second one is load reduction efficiency at fixed available cost, *i.e.* how to intervene on a specified number of cells with the biggest gain in load reduction.

The selection method of the hot spots is based on the transport algorithm. Assuming a unit emission value (*e.g.* 1 kg P a^{-1}) in each cell and routing the emissions to the outlet, the proportion of the local emissions that can reach the outlet can be determined. Similarly, the transportable amount of the inflowing flux of the cells can be calculated, *i.e.* what flux can be conveyed from the entering flux of the given cell to the outlet. Although the cumulative relative retention downstream of a local cell is the same for the emission and the inflowing

flux, the retention in the cell itself is different (Eq. (A.46) in Appendix A), which makes it reasonable to differentiate between the two relative contributions. Since the equations are linear for the absolute fluxes, multiplying these relative loads with the cell emission and inflowing flux values, absolute transportable fluxes can be generated. Since these processes are executed for each cell, they result in two new layers called the "source load" map and "transfer load" map. Optimization is based on these two maps by estimating the achievable load reductions on both layers if an intervention is implemented. Utilizing the source load and transfer load maps the impact of a local intervention on the load at the outlet can be directly and locally evaluated. Ranking the cells according to their achievable load reduction (gain) caused by an intervention, a priority sequence of the cells can be derived for the interventions, which forms the basis for an optimized watershed management.

The calculation of the achievable gain is the most performance-demanding part of the algorithm. We assigned a possible intervention type to all non-urban field cells of the catchments. This assignment could theoretically consider the present land use, slope and soil conditions and management practices, but the high number of the applicable alternatives at a specific location would highly complicate the procedure. Therefore, for the optimization we selected two specific options, managed grasslands without over-grazing for any arable land and forestation for everything else. These measures can be considered as almost ideal management practices with high soil loss reduction efficiency and increased roughness. Therefore, we do not specify whether it is source or transport control, simply a potential measure (land use change) is applied that is able to reduce both source and transfer loads. As a first step, we calculated the alternative local SS and PP emissions for each cell based on its intervention land use category. Knowing the (usually decreased) local load and the (usually higher) Manning's coefficient in case of intervening at a specific cell enables us to estimate the exact improvement in the source load and transfer load maps based on Eq. (A.46) in Appendix A. The relative retention (deposition related to the inflowing load or the local emission) after an intervention can be computed as a function of the present relative retention and the Manning's coefficients:

$$1 - ret_{SS,i,m} = \left(1 - ret_{SS,i,o}\right) \cdot exp\left(-k_{SS} \cdot K_{topo,i} \cdot \left(n_{i,m} - n_{i,o}\right)\right) \tag{5.1}$$

where $ret_{SS,i,m}$ is the modified relative retention at cell i after an intervention [-], $ret_{SS,i,o}$ is the original relative retention at cell i [-], k_{SS} is the sediment deposition rate [s^{-1}], $K_{topo,i}$ is a topographic constant at cell i as a function of the cell flow length, slope and hydraulic radius [$m^{1/3}$], $n_{i,m}$ is the modified Manning's coefficient at cell i [s $m^{-1/3}$] and $n_{i,o}$ is the original Manning's coefficient at cell i [s $m^{-1/3}$].

This procedure results in new source load and transfer load maps that show the transportable amount of the local emissions/inflowing fluxes of a single cell if the local emission and the roughness is modified according to the management practice applied in the specific cell. The modified maps are compared to the original ones by calculating their differences, which define the possible gain of each cell. Finally, the two difference maps are summed to get the total achievable gain (amount of PP load reduction at the outlet via source and transport control together). Since the two gains are summed, there is no differentiation between the two kinds of control means (source and transport), their aggregated impact on the river loads is the decisive factor. Intervention is executed in that cell with the highest total gain. Channel cells (with grassy riparian zones) are not involved in the procedure. Since intervening in a cell affects the future possible gain in the connected field cells both upstream (through the improvement in retention from the passing PP and SS flux) and downstream (through the decrease in the local PP and SS loads), the modified source load, transfer load and gain maps need to be updated in these regions after carrying out the actual intervention in the cell with the best gain. These sequential updates make the procedure iterative. Since the change of the source load and transfer load values can be finally traced back to that of the Manning values (Eq. (5.1)), the calculation is relatively fast. Unit-costs of the interventions are not differentiated, the number of cells (the area) designated for interventions simply determines the costs. Cells designated by the algorithm are the possible hot-spots in the catchment where further management efforts should focus on.

The iterative algorithm of calculation is then the following:

1. Estimate the achievable gain for each cell.
2. Intervene (change land use) in the cell with the biggest possible gain.
3. Actualize the model calculations in the affected region (up- and downstream neighbors of the intervention cell).

4. If the budget (maximum area for interventions) is spent or the load target is achieved, finish the procedure, else repeat from the beginning (1).

It is possible to refine the method by differentiating between various land use conversions in respect to specific costs. Designating advisable land use classes at certain locations of the catchment (*e.g.* vulnerable soils, steep slopes, riparian zones or fertile soils) for particular conversions (*e.g.* erosion protection in arable land, change of arable land to grassland, pasture to forest or riparian zone to forest) with different area-specific costs the optimization can be executed more specifically. In this case, the total achievable gain of a cell has to be divided by the costs defined for the conversion applied in order to get gain values related to unit costs (*e.g.* kg P a^{-1} load reduction per €).

5.3.3 Evaluation of the river monitoring data

SS and PP river fluxes generated by soil erosion were determined by analyzing the measured discharge and concentration time series of the gauging stations. At the outlets where daily discharge and water quality data were available, the simple annual averages closely represented the mean loads. However, they still included the fluxes from point sources and autochthonous materials transported by base flow. Applying a flow separation technique (Arnold *et al.*, 1995) for the daily discharge time series, the river fluxes at base flow conditions were analyzed. This routine provides base flow time series from the total discharge data at daily time step using an automated frequency signal analysis technique. The relationship found between the base flow rates and river mass fluxes was extended to the periods with surface runoff contribution as well. In this way, base load contribution was assigned to every day. Then the determined "base loads" were subtracted from the total measured values resulting in "event loads", and finally the daily values were summed up to annual ones. Annual average event loads were considered as soil erosion induced fluxes for the model calibration. At the other upstream stations having weekly, biweekly or monthly values, the simple annual means are highly uncertain due to the insufficient number of the samples. Thus, separation of the base loads was executed only for a long-term period to provide enough number of observations and the derived long-term event loads at the upstream cross-sections were applied to check the spatial plausibility of the model.

5.3.4 Definition of water quality targets

According to the implementation of the EU WFD in Austria and Hungary, the bioregion-related, type-specific environmental quality standard of the good status for orthophosphate-P (PO_4-P) is 0.2 mg P l^{-1} (BMLFUW, 2010) and 0.05 mg P l^{-1} (in case of a downstream lake, VM, 2010), respectively (the Austrian value refers to the 90th percentile, whilst the Hungarian to the mean). However, there is no standard value of the PP, which would be necessary for a management strategy of it. Therefore a PP concentration limit was introduced to provide target value for the management. Assuming same proportion of PO_4-P and PP in the long-term TP concentration, the PP criteria is equal to that of the PO_4-P (as it is set in the Hungarian regulation). Applying both the national PO_4-P criteria values (the Austrian one has to be converted to an annual mean that is approx. 0.15 mg P l^{-1}) and their average, three mean PP criteria values were determined (scenario 1: 0.15 mg P l^{-1}, scenario 2: 0.10 mg P l^{-1} and scenario 3: 0.05 mg P l^{-1}). Multiplying these concentration criteria values with the mean discharge rates, mean PP load criteria were calculated.

Assuming no change in the long-term hydrologic cycle and base load characteristics, the separated base load values of PP can be kept fixed independently on the management practices implemented. Subtracting these base values from the mean total load criteria numbers, target values for the event loads were determined which should be met after the management actions.

5.3.5 Model application

Digital maps of the pilot catchments were collected from open data sources and national data sets. Elevation models were available for both watersheds at 50 m grid size. Land use maps were clipped from the Corine Landcover map (100x100 m raster, EEA). Soil maps were generated by combining national topsoil data and a European soil database (1 km x 1 km raster, EC JRC). P surplus data were taken from former scientific projects related to nutrient management (daNUbs Project, Kroiss, 2005; STOBIMO Project, Zessner *et al.*, 2011b). They were distributed to the agricultural fields (arable land, orchard, vineyard and pasture) of the catchments. Meteorological, hydrological and water quality observations were collected from the national monitoring databases. Spatial interpolation of the rainfall gauges was

executed using the Thiessen-polygon technique. All input maps were finally converted to 50 m gird size (spatial units of the calculations).

Exact determination of the R-factor requires precipitation records at high (at least hourly) frequency. Since such data were not easily available for the pilot areas, the annual R-factors were related to the annual surface runoff volumes as proxies of the high intensity rainfall events instead of rainfall intensities. Long-term average R-factor was estimated from the summer half-annual rainfall volume according to Strauss *et al.* (1995), and annual values were simply estimated from the long-term one using the relative differences of the annual and long-term surface runoff amounts. Surface runoff volumes were determined by applying the flow separation method mentioned before that analyses the measured daily discharge time series (Arnold *et al.*, 1995). Since CM-factor is a highly time-varying parameter (especially for agricultural land), its annual average value was calculated as a weighted mean of CM-factors for summer and winter conditions (representing high and low soil protection by vegetative cover, respectively). Proportions of the summer and winter half-annual surface runoff volumes on the total one were considered as weighting factors.

The model was applied in the test watersheds for different simulation periods (1992-2000 for the Wulka watershed, 1994-2003 for the Zala watershed). Accuracy of the modeled channel network was checked by visual inspection of satellite pictures on the spring sections in Google Maps. Calibration of the model was executed for long-term average SS and PP loads at the outlets. During the model calibration, the field and in-stream retention parameters of the two catchments were set as similar as possible due to the strong similarity of the watershed characteristics. To ensure the consistency of the parameters, calibration in both catchments was done for the overlapping simulation period (1994-2000). The extremes (high load in 1996 in Wulka, low load in 2000 in Zala) were not taken into account in the averages, because they were not considered representative for long-term means. Subsequent spatial validation was done at upstream cross sections for the averages (1994-2000). Additionally, the annual variability of the simulation periods was examined at the outlet for individual years (including the extremes). However, since calibration was performed for the overlapping period, only the years outside the calibration period (Wulka: 1992-1993, Zala: 2001-2003) can be considered as independent validation years. The model results for the

single years within the calibration period (1994-2003) contain only the random errors of the computations, the systematic error was eliminated by the calibration.

Based on the calibrated model, management scenarios were evaluated for long-term average conditions according to different management strategies. In the first step, the source areas were managed (soil nutrient management) only by implementing managed grasslands in areas with soil loss higher than 10 tons SS per hectare and year (that is around a generally suggested maximum tolerance limit for soil loss, Morgan, 2005). Since a certain amount of the calculated local gross soil loss is deposited at the source cells, the tolerance limit applied for management was related to the net soil loss values (exported flux out of the cells, *i.e.* gross soil loss minus deposition). In the next step, the areas with the highest gain in respect to water quality at the outlet were selected and managed using the optimization algorithm (water quality management). Starting always at the cell with the highest gain and covering more and more parts of the catchment with interventions, the decreased PP loads and the load reduction efficiencies of the specified intervention areas were calculated. Additionally, the area demand of the scenarios was determined. Finally, a combinative management procedure that considers both water quality and soil nutrient management together was executed.

5.4 Results and discussion

5.4.1 Event load separation and load targets

Separation of the base loads in the Wulka catchment resulted in long-term SS and PP event loads of 0.09 t SS ha^{-1} a^{-1} and 0.15 kg P ha^{-1} a^{-1}, respectively. Share of the event SS and PP loads from the total amounts (presented in Table 5.1) is 67% and 66%, respectively. It varies among the simulation years between 60% and 88% for SS and 51% and 91% for PP. In the Zala catchment, the determined SS and PP event loads are 0.06 t SS ha^{-1} a^{-1} and 0.14 kg P ha^{-1} a^{-1}, respectively. The proportion of the event loads are 82% and 59%. Lower share of PP event loads in Zala is a consequence of the fact that considerable loads from point sources contribute to the total PP loads. Variability between the simulated years is wider and ranges from 36% to 89% and from 6% to 66%. This is due to the stronger meteorological fluctuations of the simulation period modeled in Zala.

Mean total PP load targets (determined from the mean discharge and criteria concentrations) are reported in Table 5.2. Subtracting the base load values (0.07 kg P ha^{-1} a^{-1} and 0.09 kg P ha^{-1} a^{-1} in the Wulka and Zala catchments, respectively) from the total load criteria numbers resulted in event load target values of 0.07 kg P ha^{-1} a^{-1} and 0.09 kg P ha^{-1} a^{-1} (scenario 1) and 0.02 kg P ha^{-1} a^{-1} and 0.030 kg P ha^{-1} a^{-1} (scenario 2). These targets were used for quality evaluation and management planning of PP event loads in the Wulka and Zala catchments, respectively. PP event load reduction is needed by 55% and 86% in the Wulka catchment and by 36% and 80% in the Zala catchment according to scenarios 1 and 2, respectively (Table 5.2). In case of scenario 3 (the most rigorous limit), the calculated targets became negative (Table 5.2), which indicates that management of erosion induced event loads without involving the base load regulation (*e.g.* point sources) is not enough to meet the 0.05 mg P l^{-1} mean concentration limit. Therefore, only scenarios 1 and 2 were henceforward examined in this study.

Table 5.2 Target criteria values (concentrations and loads) and necessary event load reductions for the watershed management.

Scenario	Target	Unit	Wulka	Zala
-	Base load	kg P ha^{-1} a^{-1}	0.07	0.09
1	Concentration	mg P l^{-1}	0.15	0.15
	Total load	kg P ha^{-1} a^{-1}	0.14	0.18
	Event load	kg P ha^{-1} a^{-1}	0.07	0.09
	Reduction	%	55	36
2	Concentration	mg P l^{-1}	0.10	0.10
	Total load	kg P ha^{-1} a^{-1}	0.09	0.12
	Event load	kg P ha^{-1} a^{-1}	0.02	0.03
	Reduction	%	86	80
3	Concentration	mg P l^{-1}	0.05	0.05
	Total load	kg P ha^{-1} a^{-1}	0.05	0.06
	Event load	kg P ha^{-1} a^{-1}	-0.02	-0.03
	Reduction	%	118	124

5.4.2 Model calibration and validation

Fig. 5.3 and 5.4 show the comparison of the modeled and measured SS and PP loads. Long-term averages at the outlets could be almost perfectly calibrated (Fig. 5.3). Checking the

results at the upstream stations, the simulated fluxes fit the measured long-term averages. Model errors are usually lower than 30%. There are two outliers in both catchments with an error of more than 30%, which are smaller tributaries. These more significant deviations in tributaries are probably caused by the some specific local conditions, which are not caught by the model (neither the input data nor the methodology). They usually have stronger influence on the transport at smaller scale than at larger one.

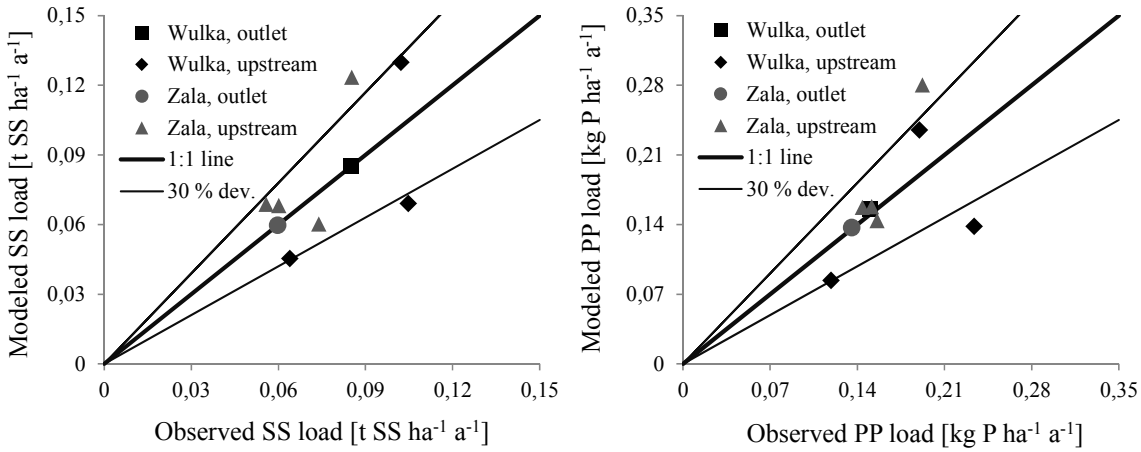

Fig. 5.3 Observed and modeled long-term average (1994-200, without extremes) SS (left) and PP (right) event river loads at the monitoring stations of the Wulka and the Zala rivers (one dot represents one station, outlet: calibration, upstream gauges: validation).

Regarding the annual loads at the two outlets (Fig. 5.4), small modeling errors for SS can be recognized. In Wulka, all deviations are less than 30%, whilst in Zala there are two years with remarkable errors (60% and 82%). This can be explained by analyzing the SS load-surface runoff relationships. In Wulka, there is a strong relationship (direct proportionality) between the SS load and the runoff volume, thus the model is reasonably able to estimate the observed values since R-factor of USLE was estimated from the runoff volumes. However, the relationship of SS load and runoff is more complicated in Zala where despite the generally existing direct proportionality there are remarkable exceptions with even reverse proportionality. That means in these years the R-factor can only uncertainly be estimated from the runoff volume only. This uncertainty is caused by the simple approach for the R-factor estimation, which does not take into account the impact of the rainfall intensities. Coefficient of determination (R^2) of the SS-results is 0.97. For PP, the deviations are a bit

higher, which is a consequence of the constant enrichment ratio applied and the cumulative computation errors (R-factor, SS transport and P enrichment). Nevertheless, there is a reasonable fit between the simulated and observed values. Deviations from the observed values are usually lower than 30% except the problematic years discussed by SS loads and some individual years with unexpected measured PP fluxes. These latter probably represent measuring inaccuracies and cause lower R^2 value of 0.89 for P. Thus, acceptable model performance can be achieved by calibrating a few model parameters.

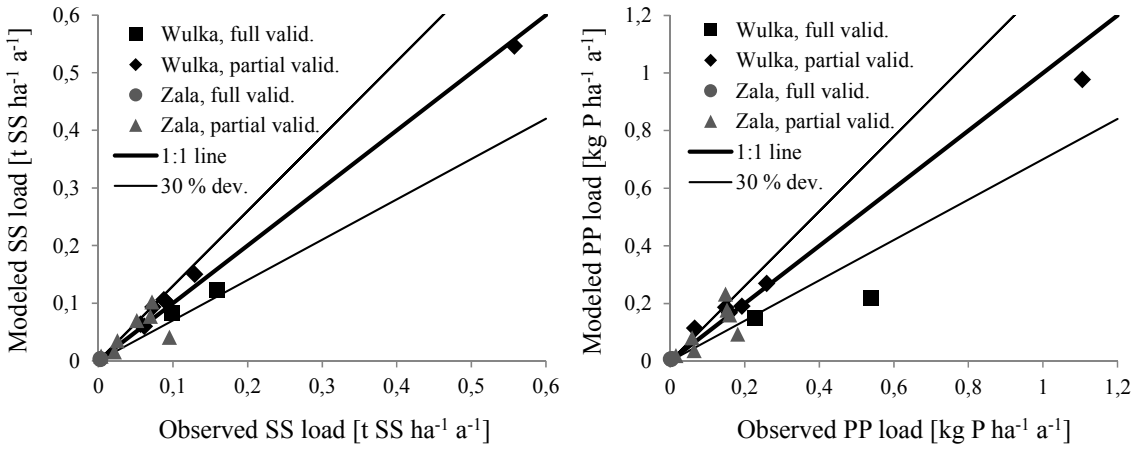

Fig. 5.4 Observed and modeled SS (left) and PP (right) event river loads of individual years at the outlet of the Wulka (1992-2000) and the Zala (1994-2003) catchments (one dot represents one year).

5.4.3 Catchment scale results

From Fig. 5.3 and 5.4 it is obvious that the area-specific SS and PP event loads are higher in the Wulka catchment, although the local specific soil loss rates are lower. This phenomenon indicates significant sediment and PP retention in the Zala watershed, which was also found by Zessner *et al.* (2004) based on water quality data analysis during high flow events. Table 5.3 summarizes the calculated long-term average local emission rates, the transported fluxes (yields) entering the main channel network (taking into account field retention) and the exported fluxes (loads) out of the watershed (considering in-stream retention). About two and half times higher average soil loss and PP emission rate was calculated for the Zala catchment (5.69 t SS ha^{-1} a^{-1} and 4.34 kg ha^{-1} a^{-1}, respectively) than that of the Wulka (2.15 t

SS ha^{-1} a^{-1} and 1.89 kg ha^{-1} a^{-1}). This significant difference is more surprising if we consider that the mean slope is larger in the Wulka than in the Zala. Since the meteorological factors are very similar, the difference is mainly caused by inadequate agricultural practices paired with unfavorable slope and soil conditions in the Zala watershed. Analysis of the slope distribution of the arable lands shows that the area proportion of fields at slopes higher than 12% is two times higher in the Zala catchment (15% in Zala, 7% in Wulka). These fields are responsible for the highest soil loss rates.

Table 5.3 Long-term average, area-specific SS and PP fluxes of the Wulka and the Zala catchments.

Component	Unit	Wulka	Zala
Soil loss	t SS ha^{-1} a^{-1}	2.15	5.69
Field retention	t SS ha^{-1} a^{-1}	2.06 (95.5 %)	5.61 (98.6 %)
Sediment yield	t SS ha^{-1} a^{-1}	0.10	0.08
In-stream retention	t SS ha^{-1} a^{-1}	0.01 (11.8 %)	0.02 (25.0 %)
Sediment event load	t SS ha^{-1} a^{-1}	0.09	0.06
PP emission	kg P ha^{-1} a^{-1}	1.89	4.34
Field retention	kg P ha^{-1} a^{-1}	1.71 (90.7 %)	4.16 (95.8 %)
PP yield	kg P ha^{-1} a^{-1}	0.18	0.18
In-stream retention	kg P ha^{-1} a^{-1}	0.02 (11.7 %)	0.04 (25.0 %)
PP event load	kg P ha^{-1} a^{-1}	0.16	0.14

Similarly, high differences can be seen by the absolute field retention values, thus, the sediment yields of the two areas are close to each other. Retention is more intense in the Zala catchment. It can be explained by analyzing the land use forms of the riverside zones. They were defined as 100m wide corridors in both perpendicular directions from the channel cells. In the Zala catchment, these corridors show a dominance of natural vegetation (55% of the zone area) and less arable land coverage (35%). In the Wulka catchment, the situation is the opposite. The higher share of natural vegetation of the riverside zones in the Zala catchment is a reasonable explanation why the area-specific retention values are differing. In relative terms, 95.5% and 98.6% of the eroded soil material is retained in the catchments of Wulka and Zala, respectively. During the model calibration process the field and in-stream retention parameters were set as similar as possible due to the strong similarity of the pilot areas. Thus, higher retention in the Zala catchment is a consequence of its catchment properties, such as

the natural vegetative zones around the channel network, longer surface runoff lengths and the higher threshold value of drained cells, which defines a stream. This latter is an *a priori* decision of the modeler and the higher value for Zala (400 cells or 100 ha) has been justified by the visual checking in Google Maps. Nevertheless, using the same threshold value for the Zala catchment than that of the Wulka (200 cells), the model computes significantly lower field retention and higher sediment yield entering the river network. This would lead to a necessity to raise the in-stream retention parameter in Zala, which would cause remarkable in-stream retention of SS and would not fit the measured values at the upper stations. Therefore different threshold values and similar retention parameters were set which ensure reasonable fits to the measured loads. The higher threshold value of Zala indicates that the initial stretches of the tributaries are at natural conditions, not or only slightly regulated and convey a little water permanently or only the surface runoff, thus, their retention capability is higher than that of a stretch downstream having permanent flow. Because of the high sensitivity of the river threshold value on the results, it is crucial to determine the threshold value as precise as possible. However, further investigations are needed to absolutely clarify the retention nearby the watercourses and to more explicitly define stream channels in the model.

Comparing the in-stream retention values, considerable difference can be found between the catchments. In the Zala catchment, 25% of the SS remain in the system with a majority of it in the small reservoirs located on the tributaries. In the Wulka catchment where no considerable reservoir exists (except one sediment detention basin near the outlet, but it seems to be less effective based on the analysis of measured water quality data up and downstream), the retention is less (11.7%). In total, only 4% (0.09 t SS ha^{-1} a^{-1}) and 1% (0.06 t SS ha^{-1} a^{-1}) of the total soil loss can be transported out of the Wulka and Zala catchments, respectively. Even though SS load of the Wulka catchment is one and a half times higher than that of the Zala catchment, there is almost no difference between their PP loads. For P, the retention values are lower and the exported proportion is higher (8% and 3%, respectively) due to the P enrichment in the SS. Enrichment is more intense in the Zala catchment, which resulted in almost the same area-specific PP load (0.16 kg P ha^{-1} a^{-1} and 0.14 kg P ha^{-1} a^{-1}).

The calculated sediment delivery ratios (SDR) are low (Wulka: 4% and Zala: 1%), but they still lie in the ranges reported by the literature. For example, a catchment area-SDR function was published by Novotny (2003) based on analysis of watersheds with various sizes. For catchments of a size between 100 km^2 and 1000 km^2, SDR values of 3% - 20% are shown. SDR is decreasing with the increasing size of the drainage area. De Vente *et al.* (2008) evaluated 61 catchments (30 km^2 - 13 000 km^2, the mean size is 1000 km^2) and computed SDR ratios (with a combined RUSLE-sediment transport approach) between 0.4% and 55% (most of them are lower than 10%). Tetzlaff *et al.* (2013) computed an SDR range of 0.5% - 78% (mean: 18%) for 450 sub-catchments of a large catchment. These approaches have similar soil erosion algorithm (USLE or its revised versions) as compared to the PhosFate model, however, they contain different sediment delivery methods (sediment transport capacity by De Vente *et al.* (2008); sediment delivery area concept by Tetzlaff *et al.* (2013); retention calculation based on residence time in PhosFate).

5.4.4 Spatial distributions of the emissions

Spatial distribution of the long-term average PP emissions is demonstrated in Fig. 5.5, which highlights the most important source regions within the catchments. The middle part of the Wulka catchment produces the highest local emissions via soil erosion. South-western regions are mainly covered by forests, whilst agricultural fields on moderate slopes can be found in the east. In the Zala watershed, the source areas are mostly located in the middle and in the southwest. However, they are more evenly distributed within the catchment. 4.8% of the catchment area of Wulka has higher gross (locally mobilized) soil loss value than the selected threshold value of 10 tons SS per hectare and year. These source areas produce 49% of the total PP emissions within the catchment. Changing the threshold value to 2 tons SS per hectare and year (typically suggested for sensitive areas with highly erodible soils, Morgan, 2005), the proportion of the catchment area exceeding the limit is 26%. The share from the total emitted PP amount is 87%. In the Zala catchment, 13% of the total area generates higher soil loss than the limit value of 10 tons SS per hectare annually and it has a share of 85% from the catchment-wide PP emissions. In case of the lower threshold value, the area proportion is 29% and the relative contribution to the total emissions is 97%. That means, only a few percent of the catchment territory is responsible for a remarkable share of the soil

loss of the catchment that is associated with the highest PP emissions as well. Only about 30% of the catchment area produces almost the total P emissions generated by soil erosion. This highly indicates how important the recognition of the source areas within the catchment is. Identification of the local hotspots has an important role in resource management planning in order to reduce nutrient losses from the soils.

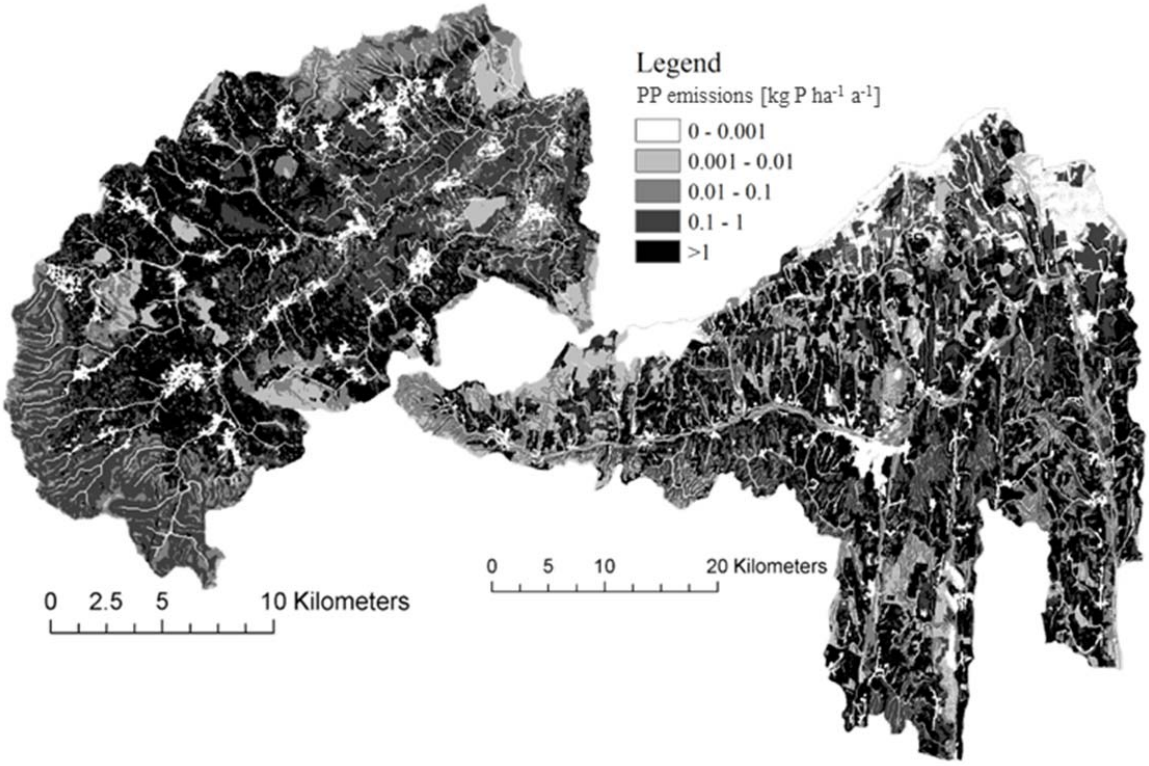

Fig. 5.5 Long-term average area-specific local PP emissions via soil erosion in the Wulka (left) and the Zala (right) catchments.

As it was discussed before, pollution problems cannot be described with the local emission rates only. The transport of pollutants within the catchment also plays a key role in assessing and managing water quality. Fig. 5.6 shows the long-term average contributions of the local cells to the river loads (source loads) or in other terms the remaining fluxes of the cell emissions passed the transmission which can be exported out of the catchment (sum of the cell values is equal to the load at the outlet). The most effective source areas are mainly located along the channel network and in the closer neighborhood of the channels. Comparing the emission and source load maps only a small proportion of the black areas

(high rates) of the emission maps are shown as black on the source load maps as well. That means that only those cells are effective sources which are located in the direct vicinity of channels or are lying farther on and have sufficiently high emission rates to produce load contributions and/or the retention along the overland flow pathways is less intense.

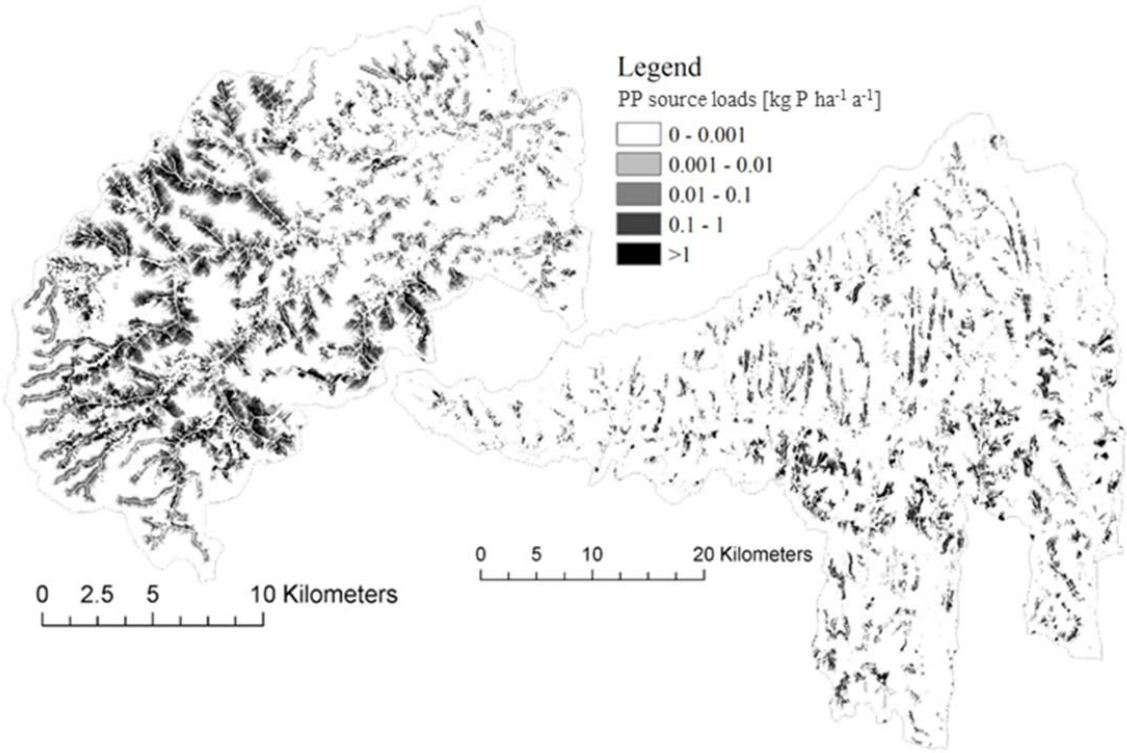

Fig. 5.6 Local contributions to the long-term average PP event river loads at the outlet (source loads) in the Wulka (left) and the Zala (right) catchments.

In the Wulka catchment, only 2.8% of the catchment area transports 75% of the total loads at the outlet (cell loads higher than 1 kg P ha^{-1} a^{-1}), whilst only 12% of the territory is responsible for 96% of the transported flux (cell loads higher than 0.1 kg P ha^{-1} a^{-1}). In Zala, these numbers are 2.2% - 88% and 6.1% - 98%. These values - in comparison to the proportion values reported by the emission rates – emphasize that recognition of the effective source areas is crucial toward an efficient watershed management. These really active source areas – together with the transfer areas - are decisive factors for water quality management to achieve good status of the water bodies.

5.4.5 Results of the management strategies

Management of the source areas (soil nutrient management) affected 2.5% and 11.7% of the total area of the Wulka and the Zala catchments, respectively. Since net soil loss is considered, the proportions of the areas with an erosion rate over the threshold are lower than it was before in the case of gross erosions. Source controlling based on soil loss tolerance limit resulted in a PP load reduction at the outlet of 52% and 88% in the Wulka and the Zala watersheds, respectively. That means, both management scenarios (36% and 80% PP load reduction desired) are executable in the Zala catchment via source controlling in 11.7% (17328 ha) of the total area. In Wulka, only the higher concentration limit that needs a PP load decline of 55% can be nearly achieved via management of the erosive areas. However, it would affect a smaller agricultural area (2.5% or 948 ha) only.

Fig. 5.7 shows the achievable highest PP load reduction at a specific intervention area as a result of the optimized water quality management. Managing a few, but properly selected cells, remarkable decline in PP loads can be realized. As the intervention area increases, the specific efficiency decreases since the cells with the highest gain have already been managed (the shape of the area-load reduction function is a saturation type curve). Management can be more effective in the Zala catchment, 36% reduction (scenario 1) can be already attained with management on 0.1% of the catchment area (148 ha), whilst intervening on 0.75% of the total area (1110 ha) causes a reduction higher than 80% (scenario 2). In the Wulka catchment, 0.5% of the area (186 ha) is necessary to attain 55% reduction (scenario 1) and management of 2.5% catchment area (932 ha) can produce 86% load decrease (scenario 2). Intervention applied on 3% (1119 ha, Wulka) and 1.5% (2220 ha, Zala) of the catchment area would bring a PP load decline of 90%. That means, the same high load reduction (about 90%) can be achieved at much smaller intervention area, if optimized transport and source control are applied together (*e.g.* 1.5% instead of 11.7% in the Zala catchment).

Sensitivity of the emission calculations are presented in Fig. 5.7, where the dashed lines correspond to load reduction curves if the original emission values of the entire catchments are doubled and halved. Load reduction efficiencies are minimally changing as consequences of these modifications, the maximum deviation is 10%. That means, despite the remarkable change of the emissions, the achievable flux reductions are slightly varying, hence the area

demand of the interventions and the designation of the hot-spots are less sensitive to the precision of the emission calculations (if the distribution of the emissions are not changing).

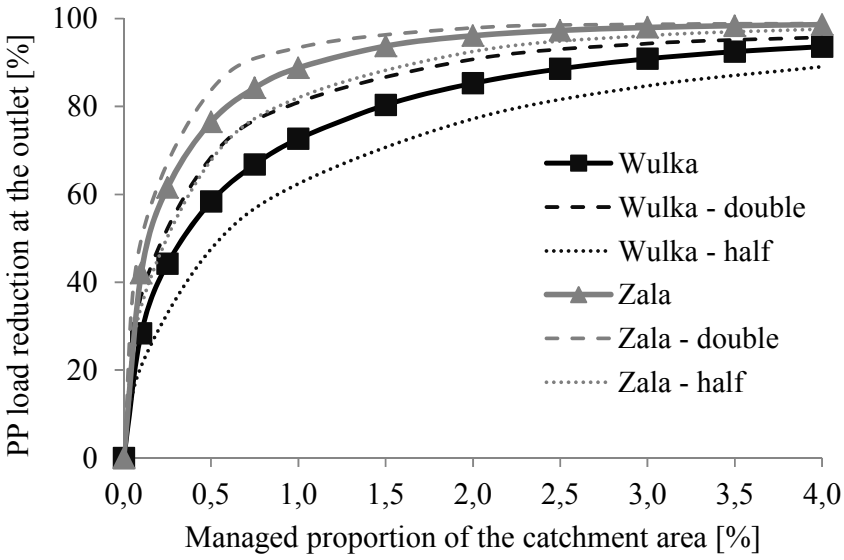

Fig. 5.7 Achievable reductions of PP event river loads at the outlet at different intervention areas in the Wulka and the Zala catchments (dashed lines represent values for halved and doubled emissions).

Fig. 5.8 presents the location of the necessary interventions with respect to water quality targets (according to scenario 2). Hot-spots lie most frequently along the channels (buffer zones) passing the erosive regions of the catchments and additionally some highly erosive slopes are also intervened (source control). Almost all of the designated cells are arable lands or orchards. Since their share on the total area is about 50% in both areas, approx. the double values of the catchment proportions are valid for the cropland.

Combinative management was possible in the Wulka watershed only, because in the Zala catchment soil nutrient management accomplishes the water quality targets as well (on 11.7% of the total area). However, in the Wulka catchment, the lower water quality criteria (scenario 2) cannot be met via source controlling alone. Applying source controlling (soil nutrient management) at 2.5% of the total area (as it was evaluated before) and executing an additional optimized management of the effective hot-spots, the stricter water quality limits can also be fulfilled. This resulted in an additional 1.5% of the catchment area that should be managed. Thus, in total, intervention on 4% of the area of the Wulka catchment can realize

the water quality goal as well. Fig. 5.9 shows the recommended areas for an intervention (Wulka: 4% or 1492 ha, Zala: 11.7% or 17328 ha), which can ensure the realization of both management aspects. Relating the area demand to the arable lands, 7.4% (Wulka) and 23.9% (Zala) are concerned.

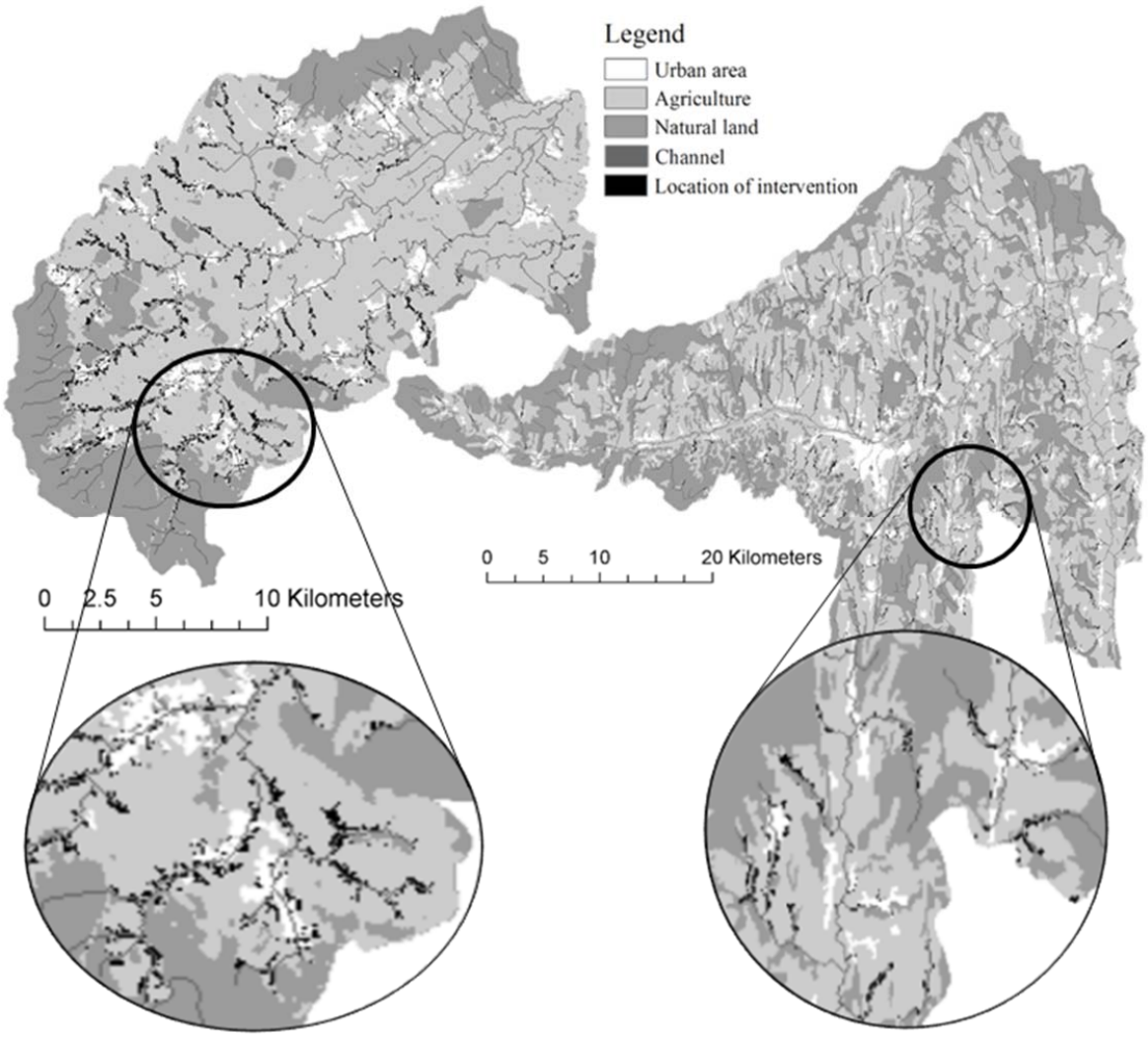

Fig. 5.8 Suggested areas (indicated by black color on the original land use maps) for intervention in order to fulfill water quality management (pollution control) goal according to scenario 2 in the Wulka (left) and the Zala (right) catchments.

Table 5.4 summarizes the main results of the management strategies. Soil nutrient management (over 10 tons SS per hectare and year net erosion rate) is quite effective regarding water quality management as well. However, it would need high area demand

where the original land use should be managed to reduce soil (and phosphorus) losses. If soil nutrient losses are generally not concerned and water quality improvement is the main management goal, impressive river load reductions can be achieved with relatively few intervention cells. However, in this case, higher amount of the phosphorus stock of the topsoil is mobilized and transported from the fields. The combinative approach can fulfill both management purposes with reasonable area demand.

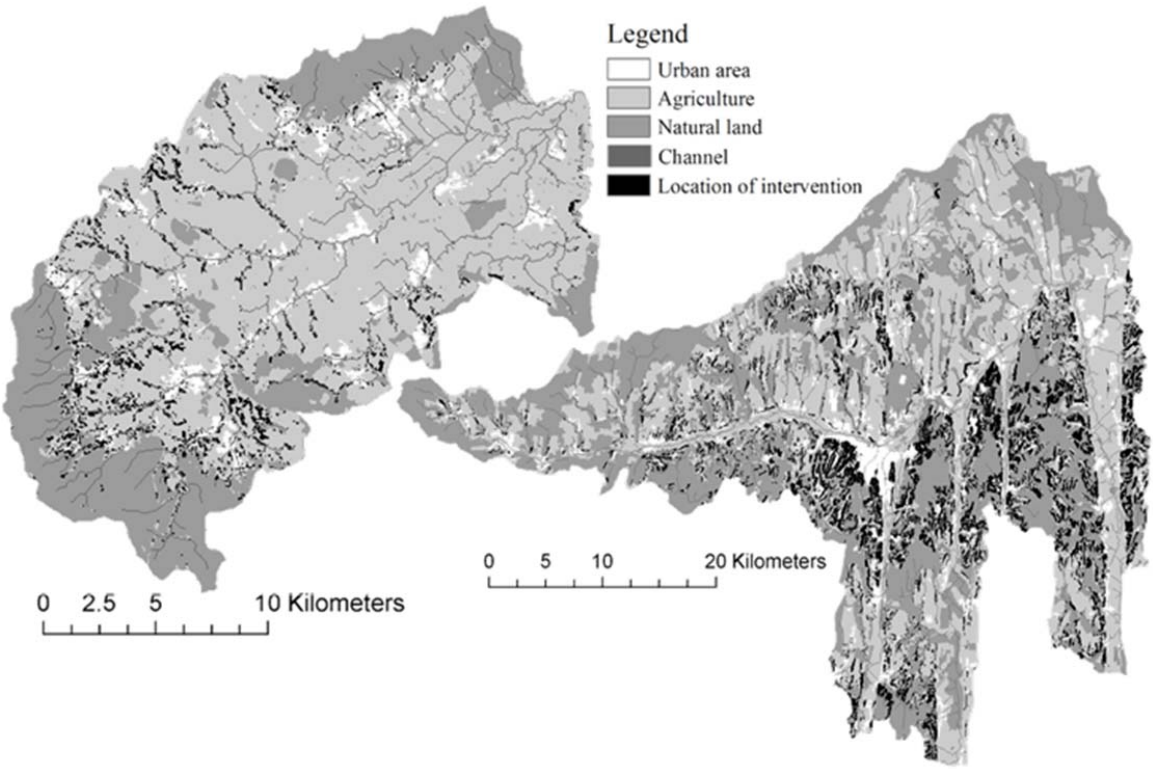

Fig. 5.9 Suggested areas (indicated by black color on the original land use maps) for intervention in order to fulfill both water quality and soil phosphorus management goals in the Wulka (left) and the Zala (right) catchment.

Other studies focus also on the hot-spot identification. Drewry *et al.* (2011) evaluated the risk of P-losses of a catchment using a P index approach. About 33% of total area is considered to be at moderate risk, whilst only 0.03% of the catchment was characterized as an area with high risk. Bechmann *et al.* (2007) tested a P-index model at the sub-catchment scale and they found relatively acceptable correlation between the P-indices and the measured river concentrations of the-sub-catchments. Using a catchment-scale sediment connectivity

approach, Fryirs *et al.* (2007) concluded that the proportion of the effective catchment area (with a potential to contribute to sediment river loads) on the total area is between 3% and 73% for the different pilot sub-catchments, and the proportion depends on the spatial distribution of the buffers and barriers within the sub-catchments.

Table 5.4 Area demand and event load reductions of the Wulka and the Zala catchments according to different management strategies.

Management	Component	Unit	Wulka	Zala
Soil nutrient management	Area	ha	948	17328
	Load reduction	%	52	88
Water quality management	Area (scen. 1)	ha	186	148
	Load reduction (scen. 1)	%	55	36
	Area (scen. 2)	ha	932	1110
	Load reduction (scen. 2)	%	86	80
Combined management	Area (scen 2)	ha	1492	not necessary
	Load reduction (scen. 2)	%	86	not necessary

The novelty of the PhosFate model in comparison to the other approaches, which attempt to identify hot-spots or risk areas, is that it contains the advantages of both the index-based and connectivity procedures. Direct modeling of the emissions (source factors) and the explicit routing of the fluxes (transport factors and connectivity) with simple distributed parameter approach allow one to find the effective areas within the catchment. In addition, the model produces comparable results (loads) to the observations and the impact of the improved management practices on the critical areas can directly be related to water quality improvements. Finally, the optimization procedure ranks the hot-spot cells according to their gain if an intervention occurs, which enables us to select the most effective intervention areas within the catchment and minimize the intervention area. Lumped or semi-distributed parameter models are widely used for water quality assessments as well (*e.g.* SWAT application by White *et al.*, 2010), but they cannot show the possible location of the hot-spots within the sub-catchment or hydrological response units.

Theoretically, the selected critical areas (either source or transmission areas) could be verified by some additional monitoring investigations at hillslope or sub-regional scale (*e.g.* sediment yield measurements at hillslope scale or water quality sampling of the upstream

tributaries). Temporal and financial limitations of this study did not allow us to execute detailed measuring programs. However, despite the limitations of the applied soil loss model (USLE), its improved or revised forms are widely used as long-term or annual soil loss estimator and engineering tool for evaluation management actions to control erosion, especially at regional or hillslope scale (Nearing *et al.*, 2001; Novotny, 2003).

5.4.6 Uncertainties of the results

Model results are likely sensitive to the accuracy of the input data. Data inaccuracies and low resolution of some of the input data (*e.g.* missing spatial objects, aggregated soil or land use classes with average parameter values or estimated management practices) as well as uncertainties in the model structure can lead to uncertainties in runoff pathways, emission rates and consequently, retention parameter values. These can result in uncertain load reduction efficiencies and hot-spot identification. Also, the model does not account for the time-dependency of the emissions and the transport. In addition, the scale problem may confound the results as many of the processes occur at the sub-grid scale (*e.g.* rill flow hydraulics, rill detachment, sediment resuspension). Representation of the sub-grid variability by either assuming zero variability (*e.g.* soil properties or topography) or applying effective parameter values (*e.g.* roughness or crop management factors) is also uncertain.

Resolution of the data is probably not the main source of the inaccuracies (except some spatial data at low resolution). Amore *et al.* (2004) applied the USLE and the WEPP models for different catchments at hillslope scale with different subdivision of the hillslopes. They concluded that a finer subdivision, even though it approximates better the field scale conditions, is not necessarily needed for a better model performance.

Because of the presented uncertainties, many of which are local, we consider the present modeling study as a screening procedure at regional (catchment) scale. The results of the optimization can help identify the most important regions within a catchment in respect to water quality management. These are possible hot-spots or critical areas of the catchment, where practical management activities could be of interest. However, the results do not specify the precise location and kind of the necessary management practices within the screened critical areas. For the possible hot-spots identified by the procedure it may be useful

to conduct more detailed, process-based modeling supported by field experiments. Investigations at local scale can ascertain what practical management actions are needed at a particular location. Nevertheless, screening procedures can effectively support national or basin scale management programs, which can concern many smaller water bodies with limited financial funds, by determining priority areas for implementation of the watershed management action plans.

5.5 Conclusions

The enhanced version of the catchment-scale P emission model PhosFate was successfully applied in two hilly medium-sized catchments with significant agricultural coverage. Even though the model does not specifically address the dynamics of the mass fluxes, it is able to reasonably simulate the annual SS and PP loads. Cross-validation for several upstream gauges was also acceptably executed. Besides river load modeling, a new optimization algorithm is presented. It attempts to identify the most effective source and transmission areas, which probably have the highest load reduction efficiency if an intervention is implemented.

The main finding is that despite the higher proportion of emission source areas only a few percent of the total area is responsible for the majority of the river loads. This small proportion can be further reduced if the most important transfer areas are revealed as well. The area demand of the interventions can be minimized by managing those parts with the strongest possibility to reduce river loads (either source or transfer areas). That means if intervention measures are concentrated on the highly contributive areas, a highly effective management can be achieved without having to transform the overall land use practice in the catchments. Introducing BMPs on a carefully selected few percent of the total area can significantly cut the total amount of emissions and also the transported material fluxes. Combining source controlling with the optimization algorithm, goals of both soil nutrient and water quality management can be simultaneously fulfilled at a reasonable proportion of the catchment area.

The presented modeling study is considered as a screening procedure at regional (catchment) scale. The model is able to identify the possible hot-spots where improved management

activities may be of interest. In a next step it may be beneficial to perform more detailed analyses (field scale modeling and field experiments) to determine what management options are necessary at local scale.

6 From the regional towards the local scale: a coupled modeling approach to manage phosphorus emissions into surface water bodies of Upper-Austria

6.1 Introduction

Phosphorous (P) as a nutrient is essential for growing the food we eat, but it can also be a pollutant, and can seriously damage the ecology of rivers, lakes, estuaries and even oceans inducing eutrophication. This dual importance of P makes it essential to develop appropriate, multi-aspect P management strategies within our watersheds. Their main goal is to meet the interests of both the agricultural sector and water quality protection. Effective strategies should ensure sufficient P is available for optimal agricultural production while simultaneously minimizing P pollution in the receiving water bodies. Such strategies involve two fundamental approaches: 1) lowering P inputs into the agricultural systems through more efficient utilization of P and 2) reducing P transport out of the system (Campbell and Edwards, 2001). This paper is concerned with the second approach and will explore how P movement into surface water bodies can be minimized.

One of the major challenges in managing the use of P in agricultural catchments is predicting and controlling how P applied to a field will reach a stream or river. This knowledge is essential to identify exactly where phosphorous applications are causing the greatest harm and should be controlled. Since diffuse P emissions and the fluxes of P movement through the system are difficult to detect with classic monitoring methods, spatially distributed parameter models are widely used to recognize the most important source and transfer locations. There is considerable research scope how modeling methods can be applied to identify and evaluate management strategies at various catchment scales (review of models can be found in Shirmohammadi *et al.*, 2001; Novotny, 2003; Radcliffe and Cabrera, 2007). Recently, there is a shift towards model-based approaches as primarily methods to simulate

effectiveness of best management practices (BMPs) on P load reduction (Gitau and Veith, 2007). Such works typically test individual or combined management scenarios under various location-specific conditions with regards to their emission and/or load reduction potentials (*e.g.* impact analyses of different single or multiple agricultural BMPs). Even though the model predictions can be inaccurate due to some uncertainties (*e.g.* uncertain local processes and parameters) and lack of appropriate input data and control measurements, model outputs can be considered adequate to make relative comparisons or ranking between effectiveness of BMPs (Gitau and Veith, 2007). Examples that tested individual management strategies (*e.g.* conservation tillage, crop rotation, contour strip cropping, pasture establishment) can be seen in Mostaghimi *et al.* (1997), Vache *et al.* (2002), Leonea *et al.* (2008), White *et al.* (2010), Vigiak *et al.* (2012) using existing watershed scale models. Besides these, there are specialized models to evaluate the efficiency of vegetated filter strip and riparian buffer zones (Muñoz-Carpena *et al.* 1999; Lowrance *et al.*, 2000).

Determining appropriate management strategies to reduce the risk of P pollution is a highly challenging issue. One possibility is to decrease the amount of P in the soil that is not utilized by the plants. Controlling P application on the fields (*e.g.* fertilizer and manure management) helps to avoid excessive application rates that increase the soil P content. Since the most important transport media of P is the surface runoff (mainly in particulate form, attached to the eroded soil particles, Westermann, 2005), best management practices (BMP´s) that control runoff/soil erosion and sediment transport are feasible measures to prevent P pollution of surface waters due to land activities. Many source and transport controlling measures (structures or procedures) and their combinations are suggested, for example contour strip cropping, conservation tillage, crop residue mulches, buffer zones, grass filter strips and wetlands (Mostaghimi *et al.*, 2001; Campbell *et al.*, 2004). Appropriate measures are those which can be implemented without any significant realignment of the land management practice and they should be concentrated on critical areas, where P pollution is likely to occur (Campbell *et al.*, 2004).

Persuasion of farmers about the necessity of management changes is often difficult, especially if they are not directly concerned by water quality problems but they are obligated to implement practices (Collins *et al.*, 2007; Parker *et al.*, 2009). Changes in agricultural practice are also perceived to be costly (Löwgren, 2005). Besides the implementation costs

(*e.g.* afforestation) the farmers might have to face profit losses if either they switch to growing other crops with lower market price than they did before (*e.g.* conversion of arable land to grassland or restriction of particular crop types to grow) or they might have even extra costs due to the construction and maintenance of any structural measure (*e.g.* diversion terraces, check dams). Regulation and enforcement through controls and fines is often counterproductive as mandatory actions might be executed at lower technical quality because of the farmer´s disapproval (Campbell *et al.*, 2004). Therefore, incentive programs can be more effective that make the necessary practice changes financially advantageous, *e.g.* costs of the practice changes are often supported by state subsidies. National and international programs (*e.g.* ÖPUL in Austria, BMLFUW 2007; Common Agricultural Policy, CAP in the European Union, EC AGRI) exist to subsidize management actions to ensure sustainability in the agricultural sector (*e.g.* by reducing P emissions via erosion control). However, the management strategies supported through these programs often make limited impact in terms of water quality protection, because they are not related to the critical source and transfer areas of P (for example they are simply targeted according to the field slope). Thus, specifically targeted subsidy programs that focus on P hot-spots could raise the effectiveness and economic efficiency of strategy implementation regarding water quality protection.

Modeling approaches can also potentially be applied to determine appropriate and cost-effective management strategies based on their ability to identify P hot-spots (critical source and transfer areas). However, only a few studies considered costs of BMPs and cost efficiency at the catchment scale (Gitau and Veith, 2007). Since for the most cost-effective management alternative the complete range of BMPs, their local effectiveness and their interactions within a catchment should be considered, the number of possible location scenarios is enormous and exponentially rising with the increasing number of the fields. Therefore optimization techniques have recently been applied to determine scenario effectiveness at reasonable computation resources.

Srivastava *et al.* (2002) linked an optimization algorithm to the model AnnAGNPS (Bingner and Theurer, 2003) to optimize diffuse pollution control strategies. They used a genetic algorithm as optimization method to optimize the selection of BMPs on a field-by-field basis for an entire watershed in order to maximize pollution reduction and net monetary return.

They found that the genetic algorithm was able to identify BMP schemes that reduced pollutant load by as much as 56% and increased net annual return by 109%. Veith *et al.* (2004) compared the efficiency of BMP scenarios of a uniform simple targeting strategy and that of an optimized strategy. They also applied genetic algorithm for the optimization coupled with an USLE-typed (Wishmeier and Smith, 1978) soil erosion and sediment transport model. Their results showed that optimized placement scenarios had lower cost than the targeting strategy solution for equivalent sediment reduction. Gitau *et al.* (2004) presented a method that considers both water quality and economic concerns and determines cost-effective farm- or watershed-level scenarios through optimization. They combined three existing tools: a genetic algorithm, a watershed-level nonpoint-source model (Soil and Water Assessment Tool, SWAT, Neitsch *et al.*, 2002) and a BMP planning tool.

Bekele and Nicklow (2005) developed an integrative decision-making framework and computational model to assess the role of landscapes in reducing sediment, phosphorous and nitrogen yields while maximizing gross margin earned. The computational model operates at either the watershed scale or a more local, hydrologic response unit (HRU)-scale and is based on the coupling of a hydrologic and environmental simulation model, SWAT, and a multi-objective evolutionary algorithm. Maringanti *et al.* (2009) developed an optimization methodology to select and place BMPs in a watershed to provide solutions that are both economically and ecologically effective. They combined an optimization model, consisting of a multi-objective genetic algorithm and a watershed simulation tool (SWAT) to minimize total pollutant load from the watershed, and net cost increase. Qui and Altinakar (2010) presented a new approach which attempts to combine computational modeling of upland watershed processes (using the AnnAGNPS model extended with a channel module) and modern heuristic optimization techniques ("tabu search" heuristic method) to address the water-land use interrelationship in its full complexity. The best land use allocation is decided by a multi-objective function that minimizes sediment yields and nutrient concentrations as well as the total operation/implementation cost, while the water quality and the production benefits from agricultural exploitation are maximized.

Critical source identification and targeted management of these sources is also a recent topic. Meals *et al.* (2008) combined mass-balance modeling and geographic analysis to identify high-risk areas for P export. Their model DISPLA evaluates changes over time and space in

P export in response to management interventions targeted specifically to critical P source areas. Rao *et al.* (2009) determined the effectiveness of BMPs using the Variable Source Loading Function (VSLF, Schneiderman *et al.*, 2007) model, which captures the spatial and temporal evolutions of the variable source areas in the landscape that produce the majority of the runoff. Giri *et al.* (2012) evaluated the performance of different targeting methods to identify priority areas, compare pollutant reduction in priority areas defined by all targeting methods and determine BMP relative sensitivity index to rank targeting methods. Ghebremichael *et al.* (2013) developed a modeling framework integrating appropriate hydrologic and farm scale tools to design and implement specific targeted management strategies that are both environmentally and economically sustainable in agricultural watersheds. The modeling framework identifies critical source areas for pollutant generation at a watershed scale (using the SWAT model) and plans targeted measures at both watershed and farm scales.

This paper examines how modeling approaches can inform P management strategy at both the federal state and catchment scale. It presents a coupled modeling approach to support P management strategy development. Starting with a regional scale assessment, problematic sub-catchments are identified. Then focusing on these sub-catchments, a spatially distributed model is applied to reveal the hot-spot areas with a high potential to cause P pollution. Finally, several targeted management actions are assessed in terms of P load reduction and cost-effective management alternatives are also suggested using an optimization algorithm. The paper explores how decision makers in P management can be supported by a simple distributed parameter P transport model to find cost-effective BMP implementations and adopt subsidizing policy at the catchment scale without a substantial restructuring of the actual land management.

6.2 Background

Based on the results of national-scale surveys (BMLFUW, 2009) related to the European Water Framework Directive (OJEC, 2000), approximately 15% of Austrian surface water bodies are at the risk of not achieving good ecological status by 2015 due their high nutrient concentrations originating from their sub-catchments. The actual status of P emissions into

Austrian water bodies has been evaluated by catchment-scale modeling (Zessner *et al.*, 2011b). Soil erosion and point sources were found to be the most important contributing pathways to the P loads of the rivers. Hilly sub-catchments with significant agricultural coverage (mostly located in northern and eastern parts of the country) and mountainous regions with glaciers (particularly in the west) were identified as the main source regions of diffuse P emissions. Out of these two, the first type of region (hilly agricultural areas) is the problematic one, because here high P emissions are associated with significant eutrophication problems in local water bodies. One of these regions is the Upper-Austrian territory, where a remarkable number of the sub-catchments showed high rates of P emissions and risk of failing good water quality because of high P-levels. Therefore, a new project (STOBIMO-OÖ, Zessner *et al.*, 2011c) has recently commenced, focusing on the analysis of the Upper-Austrian nutrient fluxes to provide a sound basis for strategic decisions and river basin management plans.

The Federal State of Upper-Austria is located in the middle-northern part of the county (Fig. 6.1). Its administrative area is 11 980 km^2, however, its natural watershed extends beyond its administrative boundaries (17 430 km^2). The whole watershed consists of 85 sub-catchments, 64 of them lie within the administrative area. The river Danube crosses the region in the northern part, while the river Inn flows and joins the Danube at the northwestern border of the area (the upstream sub-catchments of these rivers were not considered as study areas). Other important rivers are the Traun and the Enns. The topography of the region is heterogeneous: the landscape is mountainous in the south, hilly to flat in the middle and hilly again in the north. The average slope is 8%, varying from 1% to 31% among the sub-catchments. Dominant physical soil types are sandy and loamy textures. Natural landscape forms (wood and shrub land) have the highest area proportion (54%), however they are particularly dominant in the southern mountainous areas. Agriculture is an important sector in the region covering 36% of the area (arable land: 17%, pasture: 19%). The mean accumulated P surplus of the agricultural topsoils was 400 kg P ha^{-1} (until 2006), with minima of 140 kg P ha^{-1} and maxima of 730 kg P ha^{-1}. Annual rainfall amount for the period 2001-2006 was 1210 mm a^{-1} (minimum: 840 mm a^{-1}, maximum: 1950 mm a^{-1}), whilst the mean area-specific discharge was 710 mm a^{-1}, ranging from 260 mm a^{-1} and 2030 mm a^{-1}. According to data from the period 2001-2006, 22 of 58 monitoring stations (38%) show a

clear exceedance of the bioregion-related Environmental Quality Standard (EQS) value of the orthophosphate concentration (0.02-0.10 g P m^{-3}, as 90th percentiles, BMLFUW, 2010). Available subsidized management practices in the frame of the ÖPUL Program with relevance to P emission reduction in Upper-Austria are the winter crop growing and the grassy buffer zone establishment (ÖPUL, BMLFUW, 2007). Winter crop planting has already been implemented on 34% of the arable fields (on 11% mulching is also applied). This is already more than two thirds of the areas where these types of measures potentially can be applied. However, implementation of buffer zones is very rare, only 0.2% of the possible fields have buffer strips (wpa, 2009).

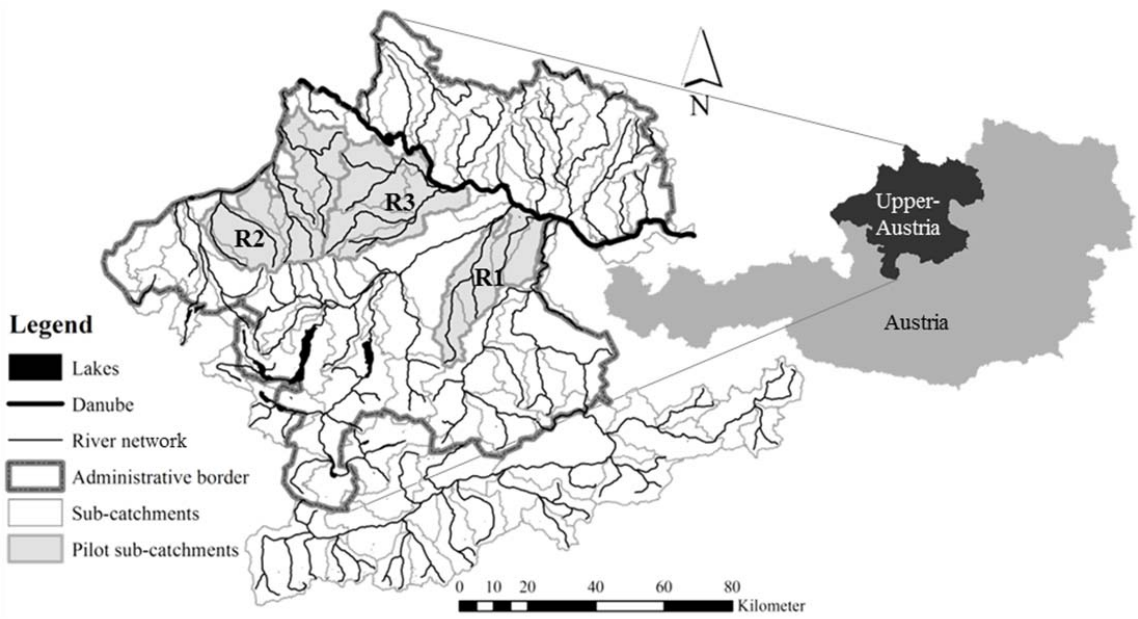

Fig. 6.1 Location and hydrography of the Upper-Austrian territory. Test regions: Krems-Ipfbach (R1), Pram-Antiesen (R2), Trattnach-Aschach (R3).

6.3 Methods

The lumped parameter MONERIS model (Behrendt *et al.*, 1999, Venohr *et al.*, 2011) and the distributed parameter PhosFate model (Kovács *et al.*, 2008, Kovács *et al.*, 2012b) were applied to calculate the actual P emissions and river loads and to evaluate the impact of different management scenarios on P river loads.

6.3.1 MONERIS model

The MONERIS model has been developed to calculate nutrient (nitrogen and P) emissions entering river systems at the medium to large watershed scale (catchment area larger than 100 km^2). It is a lumped parameter model for the estimation of long-term averages based on mostly empirical relationships. The application of the model requires detailed statistical, sampling and literature data, default parameters and digital maps about various characteristics of the watershed. It provides long-term average amount of water balance components, nutrient emissions and river loads at the main sub-catchment outlets. It separates seven different pathways, which result in the total amount of P emissions. Six of these are diffuse sources: atmospheric deposition, overland flow, erosion, tile drainage, groundwater and urban systems. The seventh component is the contamination from point sources (waste water treatment plants and industrial dischargers). For each pathway the appropriate water balance component (in the case of erosion, the sediment flux) is computed empirically and then P concentrations are determined for the water (sediment) flows. Soil P concentration is estimated based on long-term P balance calculations for the agricultural areas. Additionally possible field retention is taken into account along the pathways (*e.g.* sediment deposition on the surface). Finally, from the total emission values of each sub-catchment, total P (TP) river loads are computed using an empirical in-stream retention model. Different retention efficiency is taken into account for the tributaries, main channels and outlet lakes. The model was applied to calculate the nutrient emissions of large sub-catchments into the Danube River and its main tributaries for the period 1998–2000 in the frame of the daNUbs research project (Schreiber *et al.*, 2005, Kroiss *et al.*, 2006). An enhanced version was developed and applied for the alpine catchments of Austria (Zessner *et al.*, 2011a). This extended version also contains separated river load calculations for the dissolved and particulate P forms.

6.3.2 PhosFate model

The catchment-scale P emission and transport model PhosFate was developed for watershed management purposes. It was originally planned to evaluate the point/non-point ratio of the P emissions and to assess the efficiency of different management scenarios in comparison to

the present state based on the critical area concept. PhosFate is a semi-empirical, long-term average, distributed parameter model. Its spatial units are raster cells (with a size of for example 50 x 50 m), the time scale is one year or more. The model computes the main elements of the hydrologic cycle (water balance modeling and flow routing), soil erosion, local P emissions, suspended solids (SS) and P transport in the terrestrial areas and throughout the stream network including the impacts of point sources and reservoirs. An optimization algorithm is added to reveal the critical source and transfer areas of the catchment. The overall model concept is to build up the catchment from elementary cells to represent the spatial heterogeneity of the watershed. Sub-grid variability is conceptualized by either assuming no variability in the cells or applying effective parameters. Hydrology, soil loss rates and P emissions are computed for every single cell independently according to their own properties. Then the individual cells are connected by the flow tree and cumulative transport is calculated with an explicit routing using mass balance equations. SS and P retention is calculated for every cell as a function of the residence time of surface runoff in the cell. Main inputs to the model are digital maps (elevation, soil type, land use and humus content), statistical data (agricultural P surplus), meteorological data (rainfall records) and reservoir data (location, operation volume). Results of the calculations are the spatial distribution of the hydrological properties, the soil loss and P emissions, the SS and P load values at any arbitrary point within the catchment, the SS and P retention patterns of the catchment and the cell residence time and travel time values to the outlet. PhosFate has been applied in several European test-catchments (Hungary, Albania, Austria; Honti *et al.*, 2010, Kovács *et al.*, 2012a, Kovács *et al.*, 2012b).

PhosFate's description of erosion and particulate phosphorous (PP) transport is based on Kovács *et al.*, 2012b, with several enhancements. The constant slope length (100 m in Kovács *et al.*, 2012b) of the USLE-equation has been changed to a more realistic value that is related to the upstream catchment area (or the flow accumulation) of a specific cell. For complex slopes, the impact of surface runoff on local soil loss can be better represented by the upstream (contributing) catchment area rather than by a distance (slope length). The approach presented by (Desmet and Govers, 1996, Eq. (A.18) in Appendix A) has been utilized for PhosFate, which considers soil loss differences along the slope from the top to the bottom. Enrichment during overland transport was originally calculated with a constant local

enrichment ratio. A transport-related enrichment ratio has been additionally incorporated into the exponential term of the transport equation (Eq. (A.58) in Appendix A), which expresses a gradual enrichment of P attached to the finer particles as the travel distance increases (Novotny, 2003).

6.3.3 Model application and scenario analysis

The MONERIS model was applied to the whole Upper-Austrian territory for the period 2001-2006. Since the model was re-calibrated for the Austrian conditions (Zessner *et al.*, 2011a), no subsequent change in the parameter values has been made. However, several input data were collected from the federal authority in order to improve the basis for calculations. These included crop planting and soil loss data at the plot scale, hydrogeological and tile drainage maps, statistical data on agricultural production, sewer system and wastewater discharge data at the municipality level. Based on the results of the MONERIS application, the PhosFate model was applied for the same period but only for some selected pilot sub-catchments of Upper-Austria, which showed a clear P pollution problem caused by soil erosion. This modeling step focused on the PP fluxes of the test areas only (Fig. 6.1). For these areas a detailed digital elevation model and land use map (Hollaus and Suppan, 2003) were henceforward used. Model parameters were calibrated against the measured PP loads at the most downstream gauges. Subsequent validation was done for the upstream gauges.

In order to reduce P emissions via soil erosion, six targeted management intervention scenarios have been devised in this study in accordance to the Agri-environmental Programme of Austria (ÖPUL, BMLFUW, 2007).

i) S1: Intensification of the winter crop planting from 34% of the arable lands (present state) to 50%, plus mulching and direct sowing (where possible) from 11% of the arable lands (present state) to 20%, based on crop data at the municipality level, differentiated among five slope classes (0-1%, 1-2%, 2-4%, 4-8%, >8%).

ii) S2: restricted crop rotation on arable lands with a slope higher than 8% (wheat instead of maize, clover instead of silo maize).

iii) S3: erosion protection via grassland establishment on 7% of the arable lands with the steepest slopes (land use transformation on 7% of the arable fields is concerned as possible change by ÖPUL).

iv) S4: erosion protection via pasture establishment on 7% of the arable land (critical source areas), which have the most remarkable contribution to the river loads.

v) S5: establishment of buffer zones (50 m wide vegetative filter strips) along the water bodies, where the mass transfer to the rivers is significant (critical transmission areas).

vi) SB: hypothetical background condition assuming pristine forest throughout the catchment.

S1-S3 intervention scenarios are variants to reduce local soil erosion by ensuring better soil coverage (crop coverage instead of bare soil in winter, close grown crops instead of row crops, grass instead of crop) in comparison to the actual arable conditions. The aim of S4 is similar (crop is substituted by grass) but is targeted on the critical source areas. S5 is a transport control measure designed to intercept runoff and retain soil particles. SB represents full soil protection with intense vegetative coverage and corresponding sediment retention. Each scenario was simulated by the PhosFate model at high spatial resolution. The scenarios were represented in the model by changing the CM (crop management) factor value of the USLE equation and the Manning´s roughness parameter in the transport algorithm. Scenarios S4 and S5 could directly be executed with the model by analyzing the source load and transfer load values of the cells (Kovács *et al.*, 2012b).

Despite the targeted spatial localization of the scenarios, they have still some shortcomings. S1-S3 scenarios concentrate on the significant source areas to reduce the local emissions, but they do not take the transport efficiency of the mobilized P fluxes. S4 scenario does not consider that an intervention in a cell affects the load reduction potential of all other cells in its hydraulic hierarchy. Thus, a management action in a cell can significantly reduce the importance of other cells, which show a high potential to reduce river loads on their own. Consequently, not all the effective sources need a management action, impacts of some source cells can be switched off. Scenario S5 focuses on the transport control by establishing retentive zones, however, it does not manage other, upstream located source areas. Even though a buffer zone has been implemented, these source areas could transport P to the river

network if the retention in the buffer zone is not efficient enough (*e.g.* on higher slopes or at higher passing runoff rates). To overcome these problems, the optimization algorithm presented in Kovács *et al.* (2012b) was additionally applied. This iterative approach determines a priority list of the catchment´s cells based on their load reduction efficiency. Load reduction can be caused in a cell by the decreasing local emissions or the increasing retention. The algorithm monitors step by step the achievable load reduction (as a sum of the two reduction functions) at each cell by a specific intervention and assigns always the cell with the highest load reduction value for improved management practice. Thus, implementing a highly effective management practice at particular locations (effective hot-spots) in the catchment, significant river load reduction can be achieved at low area demand.

The optimization algorithm originally implements one particular management practice (*e.g.* afforestation or grassland establishment) with the same costs everywhere. This procedure has been improved by considering different management options at different costs within the catchment. At each location (cell) the most preferable management practice was chosen to be applied if the given location had been selected as effective hot-spot cell. Determination of preferable practices simply depends on the actual land use and the distance to a receiving water body. Three variants of cropland management were examined. The first option assumes full protection of the soils by afforestation. The second variant considers erosion protection in arable lands using restricted crop rotation, whilst the third one replaces arable fields with meadow or pasture. Grassland is converted to forest in all options. Agriculture is excluded in the riparian areas by implementing buffer zones (forest in the first option, mixed natural land in the others). The variants of the optimization are the following:

i) OPT1: afforestation everywhere;

ii) OPT2: restricted crop rotation applied in arable lands, afforestation in grasslands and vegetative buffer zone (mixture of grassland, shrub land and woodland) established in the riparian zones;

iii) OPT3: pasture/meadow established in arable lands, afforestation in grasslands and vegetative buffer zone (mixture of grassland, shrub land and woodland) established in the riparian zones.

Total annual costs were assigned to the practices. The costs include implementation costs, maintenance and operation costs and profit losses due to the management practice change. Cost elements of each management action were derived from the literature (BMLFUW, 2008; wpa, 2009; AWI, 2013). To estimate profit losses, an average distribution of crop types in the Upper-Austrian territory (15% maize, 10% silo maize, 15% wheat, 20% barley, 20% fodder crop, 20% other arable crops) over the arable lands was assumed and from the average area-specific annual profits (contribution margins) of the various crop types a weighted average profit per hectare arable land was calculated. For restricted crop rotation, the average annual profits per hectare were adjusted by removing maize and silo maize and replacing them with wheat and clover in the weighted mean. No profit was assumed for afforestation and buffer zone implementation. Profit losses were calculated as a profit difference between the actual and the preferred situation. Total implementation costs were equally distributed over a 10 year period. Costs of the management actions were calculated by summation of the annual profit losses, intervention and maintenance costs. Table 6.1 shows the area-specific annual total costs (€ ha^{-1} a^{-1}) for each management intervention. In the situation that restricted crop rotation is implemented on a homogeneous maize field, the annual total cost would be 180 € ha^{-1} a^{-1}, however, assuming an average crop distribution in all arable fields has decreased this value to 50 € ha^{-1} a^{-1}. Potential relative emission reductions (based on the change of the CM-factor) and their specific costs per percent, hectare and year are also reported, whereas the latter values were computed as the ratio of the total annual costs and the potential reduction rates.

Table 6.1 Preferred land use types, their costs and their potential emission reductions.

Actual landuse	Preferred landuse	Annual total area-specific costs (€ ha^{-1} a^{-1})	Potential reduction of the PP emissions (%)	Costs of the PP emission reduction (€ $\%^{-1}$ ha^{-1} a^{-1})
Cropland	Woodland	570	99	5.7
Cropland	Cropland with restricted rotation	50	40	1.3
Cropland	Pasture/meadow	260	96	2.7
Pasture/meadow	Woodland	340	80	4.3
Cropland in riparian zone (< 25 m)	Vegetative buffer zone	360	98	3.7
Pasture/meadow in riparian zone (< 25 m)	Vegetative buffer zone	110	40	2.8

6.3.4 River load estimations and water quality target for the PP loads

Observed river loads were calculated for both model performances from measured discharge and P concentration data. Annual TP and PP loads were computed using the ICPDR-method (ICPDR, 2005). In case of the PhosFate model, from the total PP loads, event PP loads were determined. Event PP loads are considered as erosion induced PP river loads that occur during high rainfall events and they can be calculated as the difference between the total and the base PP loads. Base PP loads are either fluxes generated by the channel flow via resuspension of the sediment or fluxes from point sources or algae biomass. Base loads were calculated at each gauge as the product of the mean base flow rate and the mean PP concentration during low flow periods.

Since there is no EQS value for neither TP nor PP concentration in the Austrian regulations (BMLFUW, 2010), an assumption of possible PP concentration limit was necessary to define management targets. Even though the PP pool is not directly available for the algae, a considerable part of the PP settled to the sediment can reenter the water column as dissolved P via desorption or diffusion. Orthophosphate EQS value is 0.05 g P m^{-3} (as 90th percentile) for the concerned regions. To determine a similar value for the PP it was assumed that half of the orthophosphate EQS is related to the reentering fraction and one-third of the transported PP load could be retained in the channel system and can potentially be reentered as dissolved P. Thus, a PP target concentration value of 0.075 g P m^{-3} was assumed for the 90th percentile PP concentrations (transformed to mean value it is 0.05 g P m^{-3}). Multiplying the mean value with the mean stream flow rate, target values for the total PP loads were determined. Assuming that the catchment management actions affect the event loads only, base PP loads were subtracted from the total target values, resulting in target values for the PP event loads.

6.4 Results and discussion

6.4.1 MONERIS results at sub-catchment scale

Fig. 6.2 left shows the comparison of the calculated and observed long-term average (2001-2006) total P loads at the outlets of several sub-catchments. The majority of the computed loads have a deviation from the measured values less than 30%, however, a significant

number (16 of the 38 outlet gauges) of the sub-catchments shows higher inaccuracy. Even though input data were improved, the river loads in many sub-catchments have been overestimated. The majority of the gauges with higher errors belong to the sub-catchments so called Traun-Enns Platte (a region between the rivers Traun and Enns), the others are single smaller streams. One possible reason for this is that no subsequent calibration was done for Upper-Austria after calibrating the model for the whole Austrian territory. Additionally, river retention of P is empirically related to the hydraulic properties of the catchment (hydraulic load and specific runoff) and the calculated retention rates might be underestimated. Finally, the observed loads have been determined from biweekly or monthly data, which can be highly uncertain. Nevertheless, the model fit is reasonable, however, there are some inaccuracies, especially for the Traun-Enns Platte, which should be clarified using detailed monitoring data.

Total P emissions of the Upper-Austrian water bodies for the period 2001-2006 were 758 tons P per year or 606 g P ha^{-1} a^{-1}. Thirty-five percent of the emissions (265 tons per year) were retained in the channel network, lakes and reservoirs mainly via settling, resulting in a P export of 493 tons per year. Soil erosion was found to be the most important pathway contributing to the total emissions with a proportion of 40% (mainly coming from agricultural fields). Diffuse sources are clearly dominant (78% of the total emissions). The remaining 22% comes from point sources. Besides erosion, groundwater flow and urban runoff are other significant pathways that contribute 18% and 12% respectively. Fig. 6.2 right presents the spatial distribution of the area-specific P emissions into the surface waters via soil erosion at the sub-catchment scale. The values range between 35 and 872 g P ha^{-1} a^{-1}, the average for Upper-Austria is 243 g P ha^{-1} a^{-1} (or 304 tons P per year, out of which 255 tons P per year were emitted from the agricultural fields). The middle hilly region has the highest emission values (dark grey color) and here soil erosion is the dominant pathway (pie diagrams in Fig. 6.2). Since 90th percentiles of the measured concentrations exceed the EQS values for most of the water bodies in this region (indicated by continuous lines in Fig. 6.2), these sub-catchments were suitable pilot areas for further modeling at higher spatial resolution and to assess various management scenarios to reduce PP emissions and/or transport. Totally 16 sub-catchments of three medium-sized regions (R1: Krems-Ipfbach, R2:

Pram-Antiesen and R3: Trattnach-Aschach, Fig. 6.1) were selected for smaller scale investigations.

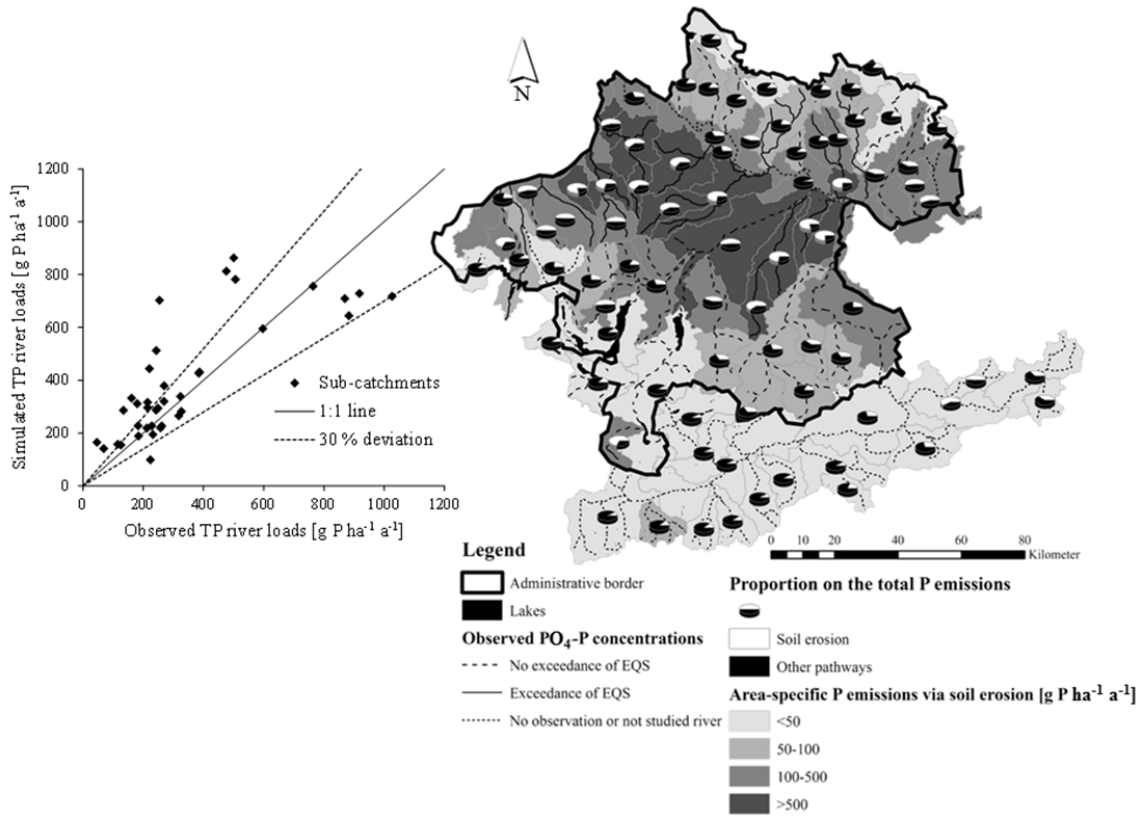

Fig. 6.2 Observed versus simulated long-term average (2001-2006) total P loads of the gauged Upper-Austrian sub-catchment outlets (left); spatial distribution of the long-term average (2001-2006) P emissions of the water bodies via soil erosion in Upper-Austria, pie diagrams illustrate the relative contribution of the soil erosion to the total P emissions, whilst the lines indicate the exceedance of the EQS for PO_4-P (right).

6.4.2 PhosFate results at local (cell) scale

Observed versus modeled PP event river loads are demonstrated in Fig. 6.3 left, where event river loads are considered as soil erosion-generated fluxes. Since only 16 selected sub-catchments were subsequently modeled with PhosFate, upstream gauges other than the outlet ones have been used for the validation (in total 34 gauges). Even though the calibration for the region´s main outlets provided almost perfect fit to the measured values, the validation

stations show some inaccuracies. Similarly to the MONERIS results, the model mostly overestimates the observed values. Higher inaccuracies can be realized at the smaller tributaries or at the upstream gauges, where the local conditions and the process dynamics have a strong influence on the river loads. Thus, both the modeling approach (averages over the time, scale issues) and the inappropriate sampling frequency can cause the computation errors. About 60% of the gauges have a deviation less than 30%, whilst only 20% of the stations show an error higher than 50%.

In the three test-regions (R1-R3), the mean area-specific local PP emission rate is 5.2 kg P ha^{-1} a^{-1}, 4.6 kg P ha^{-1} a^{-1} and 5.4 kg P ha^{-1} a^{-1}, respectively. The range of the emissions among the sub-catchments of the regions is between 1.9 kg P ha^{-1} a^{-1} and 7.6 kg P ha^{-1} a^{-1} (Fig. 6.3 right). Since an intensive retention takes place via settling along the transport pathways between the point of origin and the river channels, only a small part of the local cell emissions can reach the water bodies, as it is obvious from the significant difference (order of magnitude) between the local emission rates and the measured river loads. Emissions entering the river network are for the main catchments 320 g P ha^{-1} a^{-1}, 570 g P ha^{-1} a^{-1} and 680 g P ha^{-1} a^{-1}, respectively, which are significantly above the Upper-Austrian average value (243 g P ha^{-1} a^{-1}). Remarkable variations can be found among the sub-catchments (values can be found between 140 g P ha^{-1} a^{-1} and 1000 g P ha^{-1} a^{-1}, Fig. 6.3 right, gray triangles). Comparing these values to the MONERIS-results, in R1 the emission rates are significantly lower, whilst R2 and R3 have similar values.

The exported PP fluxes are 280 g P ha^{-1} a^{-1}, 430 g P ha^{-1} a^{-1} and 540 g P ha^{-1} a^{-1}, indicating 14%, 25% and 21% relative in-stream retention, respectively. The retention values among the catchments (differences between the gray triangles and diamonds) vary between 7% and 27%. They are usually lower than the MONERIS values and show higher variability. Similar local emissions can produce differing river emissions and loads. This could be a consequence of the different spatial placement of the various land use forms within the sub-catchments (*e.g.* various distances to the river network, existence of buffer zones or flat sedimentation zones, *etc.*), which can be resulted in different retention patterns. However, remarkable differences between the local emissions and emissions of the river network are visible in region R1, where a higher value of the retention parameter was necessary to achieve

reasonable fit to the observations than that of the other catchments. That means, either the observed values are underestimated or the model computes inaccurate values for the emissions and/or for the river retention. Measured water quality data at higher frequency could improve the calculations. Fig. 6.3 right also contains the target event load values for each sub-catchment (light gray dots), which have a range between 120 g P ha^{-1} a^{-1} and 260 g P ha^{-1} a^{-1}. Excluding one sub-catchment in region R1, all of the studied sub-catchments need a significant river load reduction to meet the target load values. The necessary load declines are between 20% and 80% amongst the sub-catchments, the average value is 60%. For the regions (R1-R3), the required export reductions are 40%, 65% and 75%, respectively.

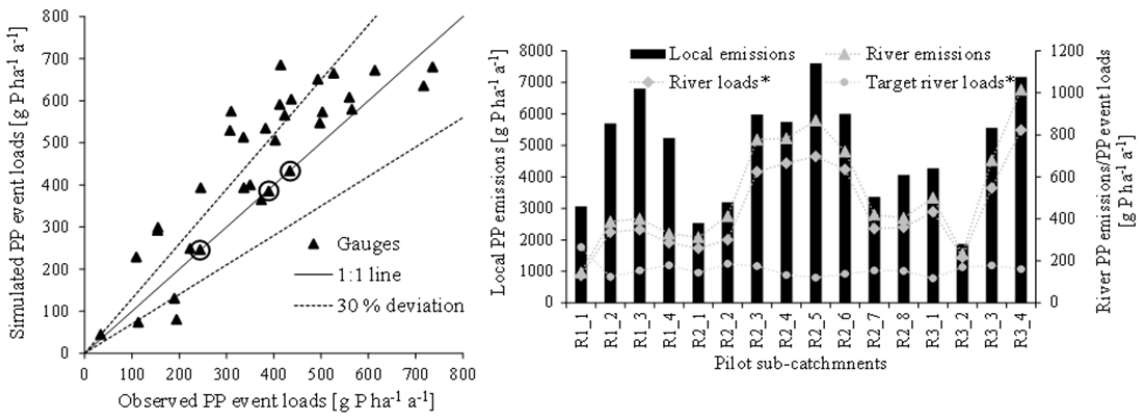

Fig. 6.3 Observed versus modeled long-term average (2001-2006) PP event loads at gauges in the case study sub-catchments (left, circles indicate the gauges used for calibration); local emissions of PP, emissions into the river network and river loads of the case study sub-catchments (right, *: transported local emissions only, not cumulated river loads).

Fig. 6.4 top presents the local PP emission rates caused by the mobilization of the soil particles (gross soil erosion). Due to the relatively high share of the arable lands lying on moderate or steep slopes, significant parts of the catchments produce high emission rates (medium to dark gray spots in Fig. 6.4 top). A spatial statistical analysis shows that a relatively low proportion of the catchment area is responsible for the majority of the emissions. In R1, 15% of the catchment area produces 70% of the total emissions (emission rates over 10 kg P ha^{-1} a^{-1}), whilst 50% of the area generates 98% of the locally mobilized P (emission rates over 1 kg P ha^{-1} a^{-1}). In R2 and R3, these numbers are 13%-78% and 16%-79% for the higher threshold, whilst 36%-97% and 41%-98% for the lower threshold,

respectively. These highly erosive slopes could be priority targets of any local source-control measures to avoid accelerated soil and P losses from the arable soils.

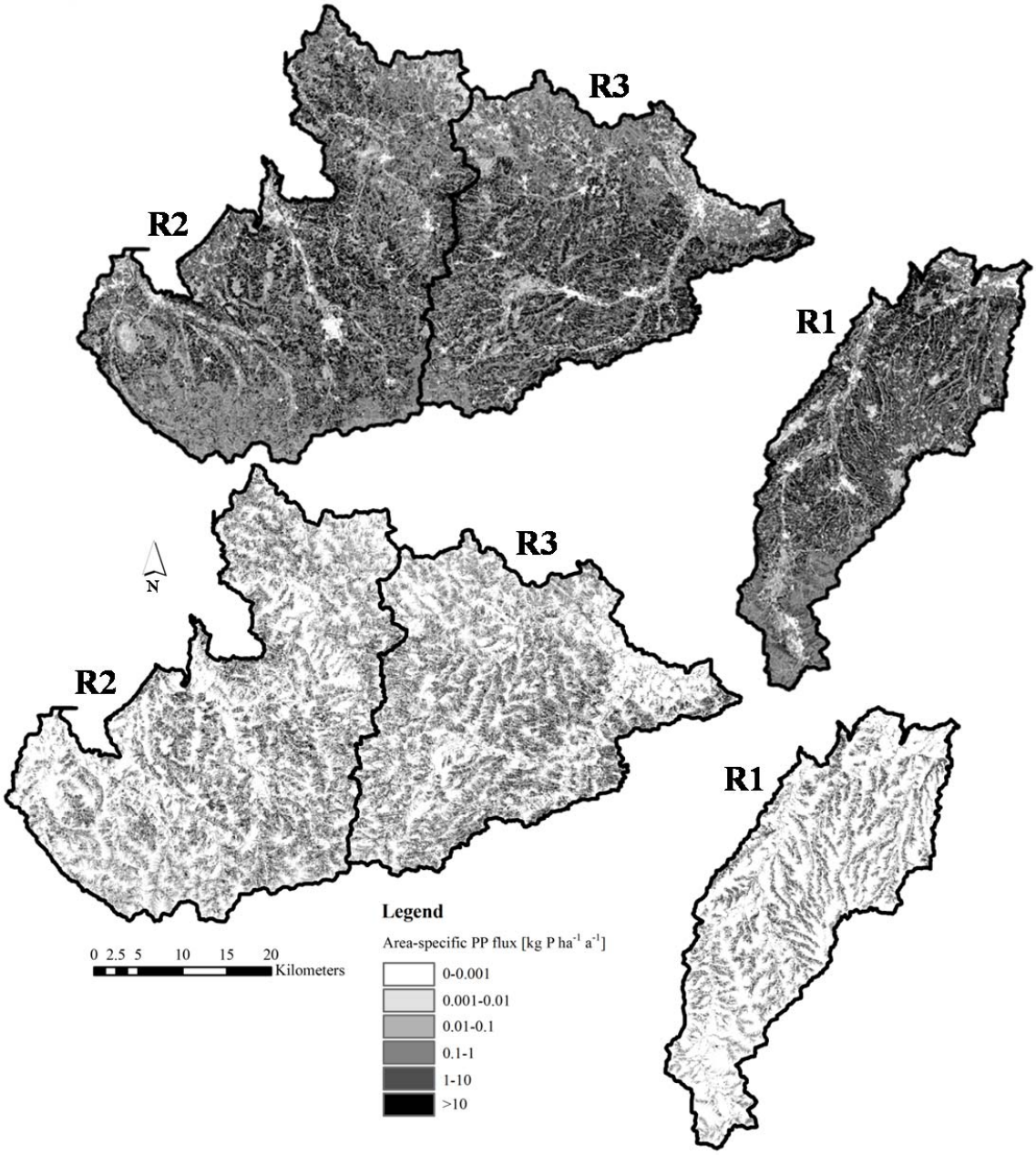

Fig. 6.4 Spatial distribution of the long-term average (2001-2006) local PP emissions (top) and PP cell loads (bottom).

Fig 6.4. bottom shows the contribution of each cell to the river loads that can be transported to the outlet. The pattern of the cell loads is much brighter than that of the local emissions,

indicating that fewer cells can be considered as effective sources that contribute significant loads to the river network. A very low proportion of the catchment area (5% in R1, 7% in R2 and 9% in R3) generates about 85% of the total PP loads generated by erosion in all the three test regions. The source areas are located either in the vicinity of a channel where shorter path lengths between the field and the water body mean there is a low capacity for soil retention and the transmission is high, or on highly erosive slopes (steep fields, sparse vegetation) directly connected to the water body (with limited deposition areas at the bottom of the slope), in some cases even far from the water body. Best management practices intended to protect water quality could primarily be located in these regions of the catchments. Similarly to Meals *et al.* (2008) and Ghebremichael *et al.* (2013), areas with high risk of P export are not uniformly distributed across the catchments or even within a particular land use and a relatively low area proportion is responsible for the majority of the P loads.

6.4.3 Targeted management scenarios

Fig. 6.5 left presents the specific PP event river load values caused by soil erosion at the regional scale (R1-R3) according to the six defined intervention scenarios. Out of them only S4 (pasture establishment on critical source areas) and S5 (implementation of buffer zones on the critical transmission areas) have significant potential to reduce P loads (*e.g.* in R2, the emissions move from 430 g P ha^{-1} a^{-1} under the actual land use, to 160 g P ha^{-1} a^{-1} under S4 and 230 g P ha^{-1} a^{-1} under S5), whilst the others have only limited potential. Even though scenarios S1-S3 can significantly reduce local erosion rates, their intervention area is limited (*e.g.* 7% of the arable land). Additionally, they do not consider the connectivity between the source areas and recipient waters and the transmissibility of the surface pathways. They focus on reducing the local mobilization of P without considering linkages to the water bodies. However, this is considered by S4 and S5 (intervention is located on critical areas), therefore they are more effective. Performance of S4 is the best because it intervenes in the most significant source areas that can be also located in the riparian zones, whilst S5 establishes a riverside retentive buffer zone without managing other source areas. Assumed pristine conditions with fully forest coverage on the catchments remarkably decrease the PP loads (scenario SB). Only 2-3% of the actual river loads would arise under this hypothetic scenario.

Even though this scenario is completely unrealistic, it provides information on the natural background loads from undisturbed lands, which clearly show how significant the human impact on the PP loads is.

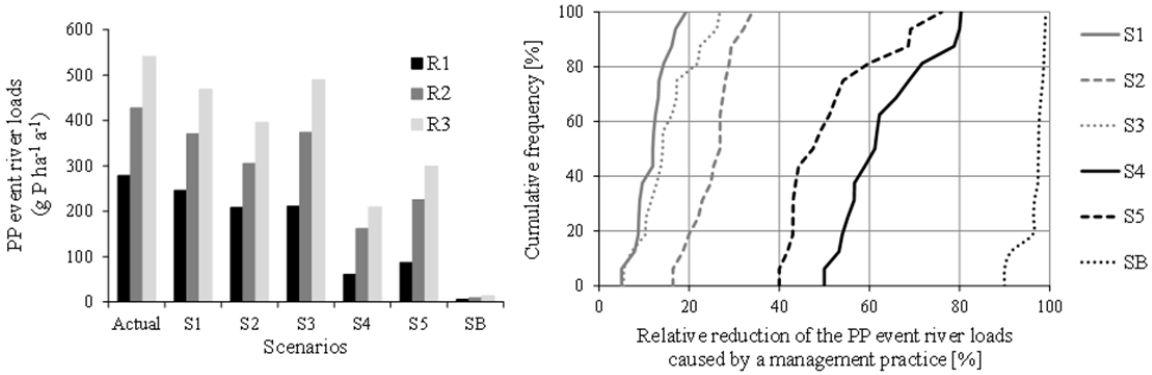

Fig. 6.5 PP event river loads of the test regions according to the different scenarios (left); relative cumulative frequency curves of the relative PP river load reductions and the necessary load reductions (right).

Fig. 6.5 right shows the cumulative relative frequencies of the PP river load reduction values via different scenarios at the sub-catchment scale. The graphs show the proportion of the studied sub-catchments, which have a relative PP load reduction caused by an intervention equal to or less than a given reduction value. Intervention scenarios S1-S3 are only effective in a few sub-catchments. When S2 is applied, 20% of the sub-catchments have a PP load reduction of more than 30%, whilst for S1 and S3 no sub-catchment achieves this reduction rate (20% of the sub-catchments can reach 15% and 20% reduction, respectively). The variability of the reductions is quite low among the sub-catchments for these scenarios, *e.g.* 90% of the sub-catchments have a reduction value higher than 20% in case of S2. In contrast, S4 and S5 can significantly reduce loads at the sub-catchment scale, *e.g.* 40% of the sub-catchments have a reduction value higher than 60% under S4 and 50% under S5, and they vary in a broader range up to 80% and 75% respectively. The reported efficiency of the vegetative filter strips falls in the range of 30-90% for 10-60 m wide strips (Daniels and Gilliam, 1996; Dosskey *et al.*, 2008), depending on the width, slope and vegetation type of the strip, and the slope and slope length, storm intensity, vegetation and soil type of the upslope fields. The model considers that the potentially high efficiency of the buffer zones can be reduced if the local slope or the inflowing runoff rate (slope length) rises. Average

slope and flow accumulation for the buffer zones is *ca.* 7.5-9.5% and 15-20 cells, respectively. That is why the Scenario S4 shows limited reduction capability (40-75%) at the catchment scale (in accordance to the literature data). Another aspect that affects the reduction potential of the practices is the calibrated constant retention parameters of the transport equation. Since they are strongly related to the presented efficiencies, the uncertainties in the observed loads used as basis for the calibration can lead to inaccurate retention rates. This emphasizes how important the accurate annual river load estimation is.

Table 6.2 demonstrates the annual total costs of the scenarios for the regions. S1 and SB scenarios were not evaluated, because costs and benefits of S1 are supposed to be equal, whilst SB as hypothetic scenario would have too large charges due to the complete afforestation. In all regions, the restricted crop rotation has the lowest total costs, whilst buffer zone establishment is the most expensive version. However, the specific cost per unit reduction is the lowest for the scenario S4 and the highest for S3. Efficiency difference between S3 and S4 is significant, even though they have the same total costs. This clearly underlines how important the proper localization of the measures is within a catchment to achieve cost efficiency. Values for S2 and S5 are close to each other in R3 region. S2 is more cost-effective in R2 region than S5, whilst in R1 region it is the opposite. Thus, pasture establishment on the critical source areas is the most cost-effective solution, followed by the restricted crop rotation on slopes higher than 8% and the buffer zone establishment.

Table 6.2 Annual total costs and load reductions of the targeted scenarios.

	Region	S2	S3	S4	S5
Total costs (€ a^{-1})	R1	330 000	570 000	570 000	820 000
	R2	520 000	600 000	600 000	1 080 000
	R3	500 000	540 000	540 000	850 000
Cost of the PP load reduction (€ kg^{-1})	R1	75	134	42	69
	R2	39	103	21	49
	R3	41	125	19	42
PP load reduction (%)	R1	25	24	78	69
	R2	29	12	62	47
	R3	27	10	61	45

Table 6.2 also contains the achievable load reductions through the scenarios. The numbers indicate that scenarios S2 and S3 cannot achieve the required load reductions and the selected

practices for S4 and S5 (pasture or buffer zone establishment) also might not always be sufficient on their own to meet the desired decline values (for R1-R3 40%, 65% and 75%, respectively).

6.4.4 Cost-effective optimized management under different management situations

Fig. 6.6 presents the results of the optimization algorithm in the three main regions according to different management plans. Three optimized management options are considered for specific locations where the highest river load reductions can be achieved: afforestation (OPT1), restricted crop rotation (OPT2) and replacement of arable land with meadows or pastures (OPT3). OPT2 and OPT3 also include afforestation in pastures and buffer zone establishment at riverside locations (at 25 m width). Load reduction curves are saturation-type functions, the specific reductions decrease as the total costs rise because interventions in the most cost-effective cells are applied firstly. Area demand curves have a moderate gradient for the pasture establishment (OPT3) and afforestation (OPT1), whilst they rise strongly for the restricted rotation (OPT2) alternative. Considerable load reductions can be achieved if the effective hot-spots are covered with forest only (OPT1). Managing only a few (3-6% of the agricultural land), but properly selected cells with a highly effective ideal measure (such as forest with low emission but high retention rate), leads to expected load declines of 80%. However, the expenses of afforestation are quite high due to high implementation costs and failing profit, resulting in a mean specific cost of approximately 550 € ha^{-1} annually. Even though only a small proportion of the agricultural areas would need intervention, the annual total costs of OPT1 variant for 80% load reduction would range between 0.6-1.5 million € among the regions.

Appling combined management actions (OPT2, OPT3) based on some simple rules how to locate them in the catchment would bring lower PP load reduction, but also lower total costs compared to the afforestation. OPT2 implemented on 3-6% of the agricultural area would lower PP load by *ca.* 50% and costs 150-250 000 € per year, while OPT3 on the same size of area would lower P load by *ca.* 70% and costs 300-700 000 €, respectively. Even though afforestation reduces the local emissions and necessarily the source loads to a greater extent

than the other alternatives, due to its significant total costs the specific costs of the load reduction is highest for afforestation (it is the opposite for the restricted rotation, Table 6.1).

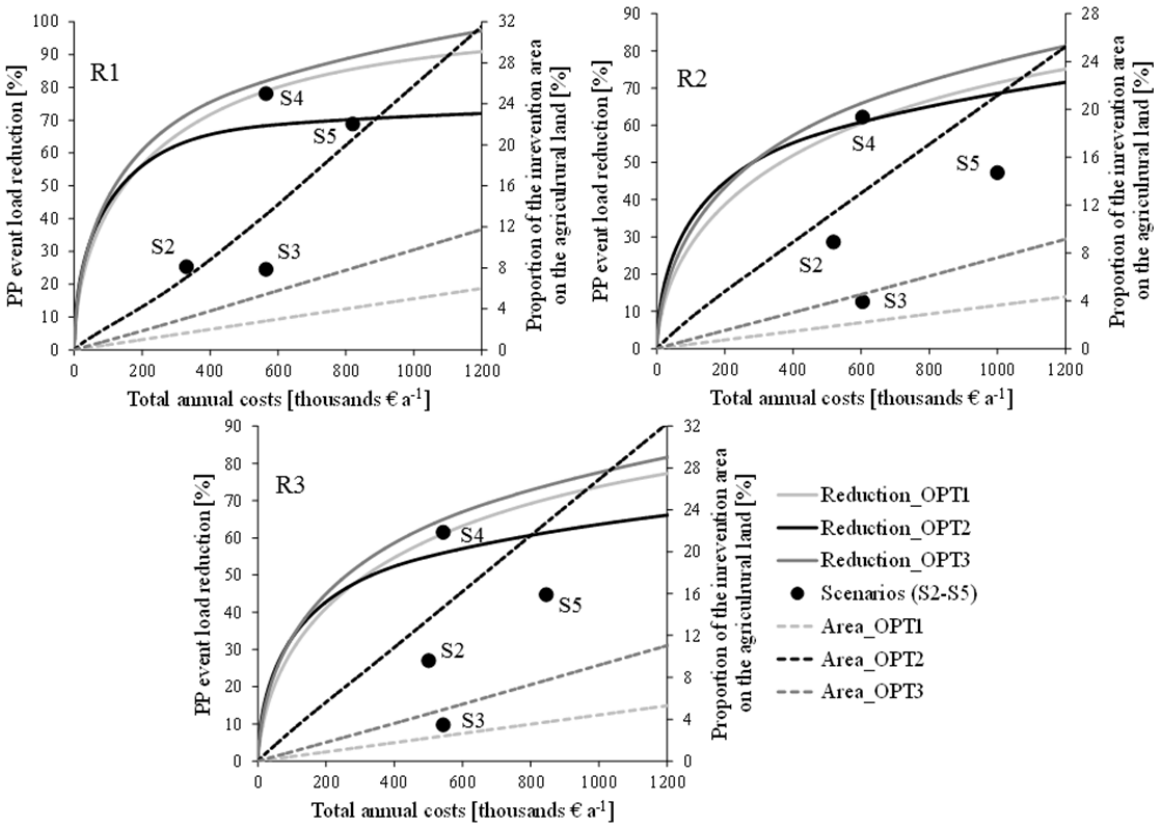

Fig. 6.6 PP event load reductions and intervention areas versus total costs according to different optimization alternatives: OPT1-afforestation, OPT2-restricted crop rotation plus buffer zone, OPT3-meadow or pasture establishment plus buffer zone.

This is partially compensated in the algorithm by considering the transmissivity of the fields, as forestry provides a strong buffer for the passing mass fluxes leading to high transfer load reduction, thus the total load reduction increases. In OPT2 and OPT3, the most effective source areas are always managed first, followed by some buffer zone cells. Due to the lower costs of the interventions of OPT2 and OPT3, at lower load reduction rates afforestation has the highest costs. As the most important sources and buffer zones have been managed, intervention on other source areas is required, but their impact on the water quality is less significant due to the longer travel distances or the established downstream retentive zones. Thus, interventions with lower emission reduction would need higher implementation area to

achieve the reduction targets than that of the others with high reduction. This is the reason behind the crossing of the costs-reduction curves in Fig. 6.6, cost-efficiency of the cheapest but technically less effective restricted rotation is very good in the first 30-50% reduction rates, but it drops rapidly as the reduction further increases. As a consequence of the different load reductions and total costs, in the range of low reduction rates (under 40-50%) restricted crop rotation has the highest financial efficiency. It turns, however, as the reduction demand increases, pasture establishment and later also afforestation becomes more cost-effective and restricted rotation is less favorable due to its high area demand (high number of source areas to be managed). Optimized management actions in R1 are highly effective, which is a consequence of the high retention parameter calibrated. In case of R2 and R3, higher costs and area proportions are needed to meet a particular load reduction value.

Black dots in Fig. 6.6 demonstrate the total annual costs and the possible load reduction of the targeted scenarios (S2-S5). The source controlling options (S2 and S3) have clearly less economic efficiency in respect to emission reduction into the river system, the corresponding optimized management versions (OPT2 and OPT3) have much higher reduction rate at the same costs. It is due to the missing buffer zone establishment and missing linkages between the managed fields and the water bodies. Transport controlling scenario S5 shows relatively high reduction rates, but it still provides less financially effective solution. That means buffer zones on their own are not sufficiently effective measures. Management of the effective sources (S4) can produce similar technical and economic effectiveness than that of OPT2 and OPT3, because it concentrates on the cells that have higher activity to transport P to the river network. This can be improved by implementing a vegetative buffer zone to intensify riverside retention and by considering the downstream-upstream feedbacks of the interventions on the other cells.

Table 6.3 indicates the costs and area demand of the necessary PP load reductions for the regions. For R1, a reduction of PP river loads of about 40% would be needed to achieve the required target of an average in stream concentration of 0.05 g PP m^{-3}. This is easily achievable with a very small proportion of the agricultural area. Afforestation (OPT1) has the lowest area demand, however its costs are the highest. Pasture establishment (OPT3) and restricted rotation (OPT2) with protection of the riparian zone provide the most economically

effective solution (70 000 € and 75 000 € annual costs) concerning 0.7% and 1.8% of the agricultural land, respectively. Change in crop rotation on this 2% of the arable land would result in a minor modification of the cropping system (maize is grown on approximately 25% of the arable fields, so only 0.5% of the fields would actually require intervention. Reduction of maize production by 2% over the region (assuming the same productivity throughout) would not cause serious management problems in the region. In R2 and R3, where 65% and 75% load reduction is needed to achieve sufficient water quality protection, crop rotation would require a substantial implementation area, especially in R3, where 59% of the agricultural fields would need management change. In these cases the decrease of the maize production would be significant as well, which could lead problems in other sectors, such as animal feeding. This is even more apparent if a more rigorous PP target concentration value is considered (*e.g.* 0.05 g m^{-3} as 90th percentile), which cannot be achieved with restricted crop rotation with reasonable costs and area demand. Afforestation and pasture implementation would need less area (3-8% of agricultural land) to meet the required load reductions in R2 and R3 and the costs of the latter one are the lowest (R2: 580 000 €, R3: 890 000 € annually).

Finally it can be seen that for achievement of the required reduction targets, cost efficiency is the highest for OPT3 (pasture establishment) in all cases, whereas load reduction costs range between 10 and 26 € per kg P reduction. OPT1 (afforestation) is the least effective in R1, OPT2 (restricted rotation) is the worst in R2 and R3. Increase of the specific reduction costs in R2 and R3 compared to R1 indicates that the cost efficiency decreases as higher load reduction is required.

Fig. 6.7 shows the location of the cells selected for intervention through the example of OPT3 variant in R3 region. Ninety percent of the intervention areas concern arable fields, while the rest concerns pastures. Twenty-three percent of the selected cells are located in the direct vicinity of a channel, whilst an additional 17% lie between 25 and 50 m distance. Thus, management of the riparian zones is very important to establish protective zones that can reduce the necessity of intervention in a large proportion of the catchment. However, 60% of the cells screened by the optimization are still source areas with an average river load contribution (source load) of 9 kg P ha^{-1} a^{-1}.

Table 6.3 Costs, area demand and cost-specific PP event load reductions according to different optimization alternatives.

		Unit	R1	R2	R3
Load reduction target		%	40	65	75
Costs	OPT1	€ a^{-1}	88 000	740 000	1 070 000
	OPT2	€ a^{-1}	75 000	800 000	2 180 000
	OPT3	€ a^{-1}	70 000	580 000	890 000
Area demand	OPT1	%	0.44	2.7	4.7
	OPT2	%	1.8	17.0	58.6
	OPT3	%	0.65	4.3	8.1
Load reduction cost	OPT1	€ kg^{-1}	13	24	31
	OPT2	€ kg^{-1}	11	26	64
	OPT3	€ kg^{-1}	10	19	26

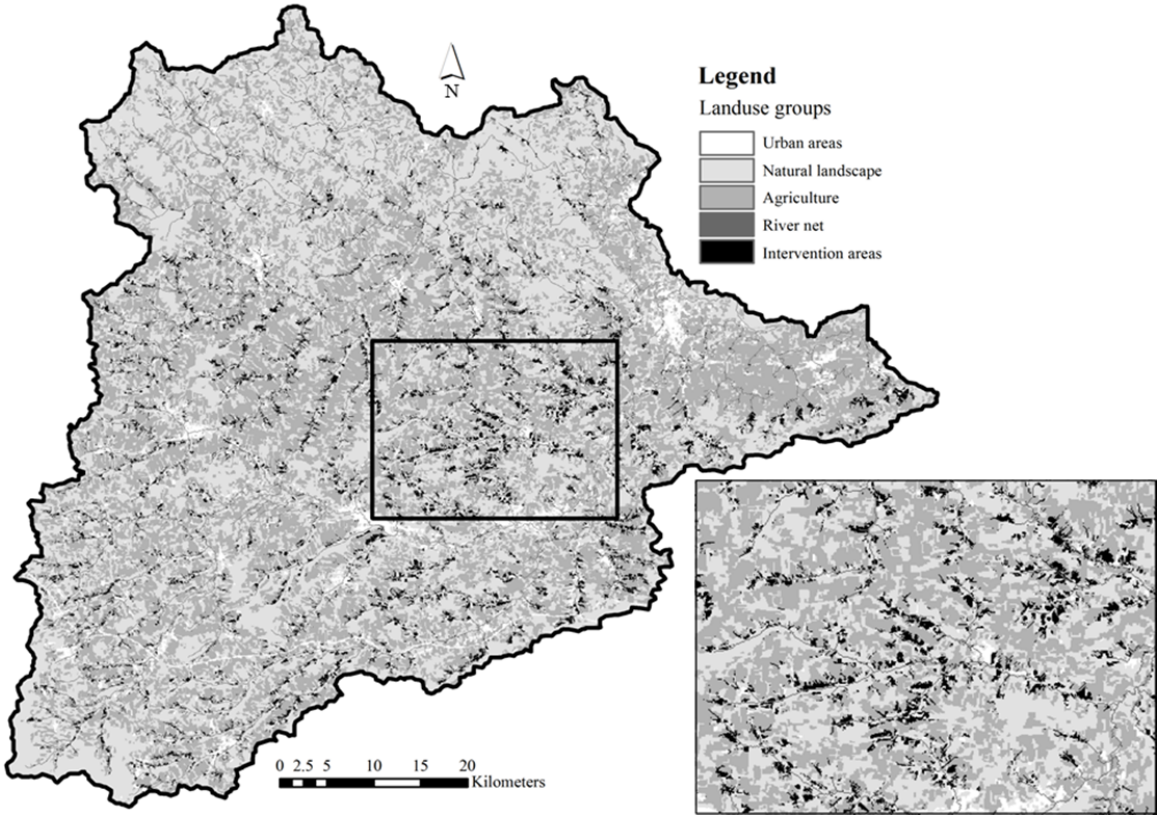

Fig. 6.7 Location of the intervention areas in R3 region.

6.4.5 Discussion

It was shown in Kovács *et al.*, 2012b that the PhosFate model has several uncertainties, which are mainly caused by scale issues (inaccurate or missing spatial information, aggregated sub-grid processes and parameters). Therefore, the model is considered as a screening method for the sub-catchment level that can recognize P hot-spots, which could be of interest for local practical investigations. Similarly, MONERIS ignores the spatial variability of the parameters within a sub-catchment and can only uncertainly be applied, especially beyond its calibration range (*e.g.* medium-sized catchments, Central-European climate conditions). Therefore it is suggested that both models are applied at scale they were designed to operate. MONERIS can be used as a pre-screening approach in a larger region (large river basin, medium to large catchments, country, federal state) to reveal the relevance of different emission pathways in the main sub-catchments of the region. This leads to identification of sub-catchments with P pollution problem caused by agricultural soil erosion. General scenario analyses can be also performed and requirements for emission reduction via different pathways (including soil erosion) can be assessed. After selecting the problematic sub-catchments where the focus is on reduction of emissions into surface water via soil erosion, PhosFate can henceforward analyze the spatial distribution of the emissions and loads at the small or medium sub-catchment scale. It can show where the hot-spots are approximately and where any practical management action should focus. Single BMPs can be localized (targeted) in space and their impacts on water quality evaluated. Optimization of the interventions can radically reduce the intervention area by focusing on the cells with the strongest potential to decrease river loads. Consequently we consider the approach presented as a two-step screening method to find the hot-spots of the catchments in an administrative region or river basin, which are likely to be potential targets for practical and cost efficient management programs to control P transfer into water bodies.

Costs of the measures are roughly determined in this study. An average crop distribution was assumed at all cropland cells to calculate income losses and an average profit per hectare arable land has been applied. This was mainly done to show the potential of the method and less to have as realistic as possible cost estimations. Supposing average crop distribution can lead to inaccuracies. For example, the model can suggest interventions that are not

appropriate for the actual land use (*e.g.* restricted crop rotation on arable lands where maize is not grown in the reality). In the opposite situation, when maize is actually grown on 100% of a plot, the real intervention costs would be higher. Detailed information on the actual distribution of the crop types (for example that held in the Integrated Administration and Control System, EC AGRI) would help overcome these challenges and substantially improve the performance of the model. For meadow or pasture establishment it was assumed that only a smaller part of the harvested hay is sold on the market and majority is used for feeding the farm´s livestock, but there is no information on whether the farm, to which a particular cell belongs, has animal husbandry. Calculation of the profit loss for meadow or pasture does not contain the income gains of the livestock sector due to the established grassland as a feed source. Afforestation and vegetative buffer zone establishment considers a general composition of the plant species and mean implementation and maintenance cost values only. No profit was assumed for forestry due to the considerable time delay to harvest timber. Any additional agricultural issues encountered by farmers in response to management interventions that can cause resistance or low willingness at the farmer´s side to participate have not been taken into account and would be valuable for future work. Despite the possible inaccuracies in the cost calculations, the refined optimization algorithm is able to compare different management alternatives in terms of their cost efficiency and it is feasible to evaluate combined management plans with spatially differentiated practices at differing costs.

Even though the optimization algorithm of PhosFate is not able to simultaneously handle a complete range of management practices compared to the methods with simple genetic algorithm or (Srivastava *et al.*, 2002; Gitau *et al.*, 2004; Veith *et al.*, 2004) or multi-objective algorithm (Bekele and Nicklow, 2005; Maringanti *et al.*, 2009) it is an appropriate tool to find and optimize the hot-spots in the catchment applying a simpler iterative selection (optimization) approach. Applying a wide variety of the BMP solutions can be successful at the farm or small catchment scale (Srivastava *et al.*, 2002; Gitau *et al.*, 2004; Veith *et al.*, 2004; Bekele and Nicklow, 2005; Qui and Altinakar, 2010), but in medium sized or larger catchments due to the complexity of the catchment properties, farm structures and the farmer`s interests it might be uncertain and also computationally challenging with long model runs. PhosFate is suggested to be applied for general evaluations of cost-effectiveness

at the catchment scale including a few main (preferred) BMP solutions at reasonable computation resources. The screened critical areas could be either implementation locations of specially targeted strategies or could be further analyzed by the optimization method to find the most cost-effective placement of the measures, whereas spatial differentiation of the favorable management practices and their costs is possible on cell basis. For any management plan at the catchment scale a few feasible, localized measures can provide useful information on the cost efficiency rather than a complicated pattern of many possible practices. In the situation if more alternatives were suitable for the preferred management action, the optimization can be easily reproduced. Also, cost-effective management solutions can be demonstrated for different water quality targets. Explicit routing and full parameter distribution can lead to a better capture of the spatial interactions amongst the fields and consequently can provide more specific localization of the measures in comparison to the approaches having aggregated spatial units or implicit routing (Gitau *et al.*, 2004; Bekele and Nicklow, 2005; Maringanti *et al.*, 2009). Comparison of all targeted interventions (scenarios S2-S5) to the optimized solutions shows a similar result to Veith *et al.* (2004), optimization can provide higher cost efficiency than targeting. Additionally, considerable number of riparian cells that have limited emissions and source loads had been found by the optimization where targeting did not implement any measure. Significant advantage of the optimization over targeting is that optimization is able to show for any particular load reduction requirement the most cost-effective management combination and spatial placement, whilst targeting can predict the achievable load reduction for some specific localization of measures without finding cost optimum.

6.5 Conclusions

A two-step screening approach has been presented by coupling two P emission models at different scale and spatial resolution. The first, lumped parameter model is appropriate to pre-filter those sub-catchments in a larger region (river basin, administrative area) that show high contributions to the P river loads via emissions generated by agricultural erosion. This is followed in the filtered sub-catchments by a distributed parameter model to find the hot-spot regions, which succeed to send the highest P fluxes into the surface waters. Ranking the cells according their load reduction potential using an optimization algorithm, a highly effective

localization of the measures can be demonstrated, which could provide a basis for any practical interventions to reduce P loads.

Management strategy optimization has been enhanced by incorporating costs of the measures. Cost calculations were performed including profit losses, implementation and maintenance costs and different management scenarios were allocated to each unit cell of the catchments. The optimization approach was modified by calculating the load reduction potential per € of the cells that ensures the delineation of the fields where the most cost-effective management could be achieved. Involving cost considerations, the method gives policy makers some idea on the value of economic support/subsidies needed to reduce P pollution in waterways.

In the situation if minor load reduction is required, the classic arable management actions (*e.g.* restricted crop rotation) supported by riparian buffer zones can cost-effectively reduce P loads. However, if significant load reduction is necessary to achieve water quality targets, land use conversions (pasture establishment, afforestation) provide more financially effective solutions. Placement of the interventions shows a heterogeneous distribution concentrating on both riparian zones and effective source areas. The essential outcome of the method is that it is able to designate the potential regions in the catchments, where a highly cost-effective management strategy on catchment-scale water quality improvement can be likely developed without a massive realignment of the actual agricultural system. The localization can help for the practical implementation of the management plans by radically decreasing the number of fields that could be real potential candidates for particular management actions.

7 Summary and conclusions

This Thesis presents the catchment-scale, distributed parameter, long-term average and semi-empirical P emission and transport model PhosFate. It was tested in various hilly, medium-sized catchments with significant agricultural coverage. Even though the model does not specifically address the dynamics of the mass fluxes, it is able to reasonably simulate the annual SS and PP loads. Cross-validation for several upstream gauges was also acceptably executed that indicates the applicability of retention parameters calibrated for the outlet in the entire catchment, though slightly different values of the factors among the test-catchments had to be set. Model results are likely sensitive to the accuracy of the input data. Data inaccuracies and low resolution of some of the input data as well as uncertainties in the model structure can lead to uncertainties in runoff pathways, emission rates and consequently, retention parameter values. These can result in uncertain load reduction efficiencies and hot-spot identification. In addition, the scale problem may confound the results as many of the processes occur at the sub-grid scale. Representation of the sub-grid variability by either assuming zero variability or applying effective parameter values is also uncertain. Despite its uncertainties, the model is an appropriate tool for critical area screening in catchments in respect to P pollution of the surface water bodies.

PhosFate is able to reveal the significant sources of local emissions by spatially distributed emission modeling. Identification of emission source areas is essential for any resource management effort to reduce local soil and P loss from the agricultural fields. Targeting management practices on the highly erosive regions of a catchment, substantial P amounts can be retained on the fields. It contributes to a better utilization efficiency of P. Through applying an explicit P transport model, the responsibility of each cell in respect to water quality degradation can be assessed. Despite the higher proportion of emission source areas, only a few percent of the total area is responsible for the majority of the river loads. This small proportion can be further reduced if the most important transfer areas are revealed as well. Interventions that aim to improve water quality should focus on these effective source and transfer zones. The area demand of the interventions can be minimized by managing those parts with the strongest possibility to reduce river loads (either source or transfer

areas). That means if intervention measures are concentrated on the highly contributive areas, highly effective management can be achieved without having to transform the overall land use practice in the catchment. Introducing specific, P emission or transport control BMPs on a carefully selected few percent of the total area can significantly cut the total amount of emissions and also the transported material fluxes. Placement of the interventions shows a heterogeneous distribution concentrating on both riparian zones and effective source areas. By combining source controlling with the optimization algorithm the goals of both soil nutrient and water quality management can be simultaneously fulfilled intervening in a reasonable proportion of the catchment area.

By involving cost considerations the method is able to provide policy makers with some idea on the value of economic support/subsidies needed to reduce P pollution in waterways. In the situation that minor load reduction is required the classic arable management actions (*e.g.* restricted crop rotation) supported by riparian buffer zones can cost-effectively reduce P loads. However, if significant load reduction is necessary to achieve water quality targets, land use conversions (pasture establishment, afforestation) provide more financially effective solutions. The essential outcome of the method is that it is able to designate the potential regions in the catchments, where a highly cost-effective management strategy on catchment-scale water quality improvement can be likely developed without a massive realignment of the actual agricultural system. Despite the possible inaccuracies in the cost calculations, the optimization algorithm extended with cost considerations is able to compare different management alternatives in terms of their cost efficiency and it is feasible to evaluate combined management plans with spatially differentiated practices at differing costs. The optimization is also able to show for any particular load reduction requirement the most cost-effective management combination and spatial placement.

PhosFate model is considered as a screening procedure at the catchment scale. The model is able to identify the possible hot-spots where improved management activities may be of interest. In a next step it may be beneficial to perform more detailed analyses (field scale modeling and field experiments) to determine the precise management options necessary at the local scale. Nevertheless, screening procedures can effectively support national or basin scale management programs, which can concern many smaller water bodies with limited financial funds, by determining priority areas for the management actions. By coupling

PhosFate with a large scale emission model, basin- or state-wide strategies for P management can be designed. The large-scale lumped parameter model is appropriate to pre-filter those sub-catchments in a region (river basin, administrative area) that show high contribution via erosion to the P river loads. This can be followed in the filtered sub-catchments by the distributed parameter model PhosFate to find the hot-spot regions that send the highest P fluxes via erosion into the surface waters. The localization can help with the practical implementation of the management plans by radically decreasing the number of fields that could be real potential candidates for particular management actions.

8 References

AMA. Homepage of the Agrarmarkt Austria (AMA), http://www.ama.at.

Amorea E, Modicaa C, Nearingb MA, Santoroa VC. Scale effect in USLE and WEPP application for soil erosion computation from three Sicilian basins. Journal of Hydrology 2004; 293: 100–114.

Ángyán J, Buttner G, Németh T, Podmaniczky LA. Természetvédelem és a mezőgazdálkodas összehangolásának EU-konform rendszere (System for harmonization of nature protection and agriculture in conformity with EU). Budapest: Budapest University of Economic Sciences; 1997.

Arnold JG, Allen PM, Muttiah R, Bernhard G. Automated base flow separation and recession analysis techniques. Ground Water 1995; Vol. 33 No. 6: 1010-1018.

Aurousseau P, Gascuel-Odoux C, Squividant H, Trepos R, Tortrat F, Cordier MO. A plot drainage network as a conceptual tool for the spatial representation of surface flow pathways in agricultural catchments. Computers &Geosciences 2009; 35: 276–288.

AWI. Deckungsbeiträge und Kalkulationsdaten (Contribution margins and calculation data). Vienna: Austrian Federal Institute of Agricultural Economics (AWI); 2013.

Batelaan O, DeSmedt F. WetSpass: GIS-based recharge estimation by coupling surface–subsurface water balances. Journal of Hydrology 2007; 337: 337–355.

Batelaan O, Woldeamlak ST. ArcView interface for WetSpass, User manual, version 19-5-2004. Brussels: Vrije Universiteit Brussel; 2004.

Bechmann ME, Stalnacke P, Kvaerno SH. Testing the Norwegian phosphorus index at the field and subcatchment scale. Agriculture, Ecosystems and Environment 2007; 120: 117–128.

Behrendt H, Huber P, Opitz D, Schmoll O, Scholz G, Uebe R. Nährstoffbilanzierung der Flussgebiete Deutschlands (Nutrient emissions into river basins of Germany), Research report UBA-FB Ref. No. 296 25 515. Berlin: Leibnitz-Institute of Freshwater Ecology and Inland Fisheries; 1999.

Bekele EG, Nicklow JW. Multiobjective management of ecosystem services by integrative watershed modeling and evolutionary algorithms. Water Resour. Res. 2005; 41 W10406: 1-10.

Bingner RL, Theurer FD. AnnAGNPS Technical processes, version 3.3. Oxford: National Sedimentation Laboratory, USDA-ARS; 2003.

Blöschl G, Sivapalan M. Scale issues in hydrological modeling: a review. Hydrological processes 1995; Vol. 9: 251-290.

BMLFUW. Österreichische Programm zur Förderung einer umweltgerechten, extensiven und den natürlichen Lebensraum schützenden Landwirtschaft, ÖPUL (The Austrian Agri-environmental Programme). Vienna: Austrian Federal Ministry of Agriculture, Forestry, Environment and Water Management (BMLFUW); 2007.

BMLFUW. Deckungsbeiträge und Daten für die Betriebsplanung (Contribution margins and data for operation planning) Vienna: Austrian Federal Ministry of Agriculture, Forestry, Environment and Water Management (BMLFUW); 2008.

BMLFUW. Nationaler Gewässerbewirtschaftungsplan 2009 (National River Basin Management Plan 2009). Vienna: Austrian Federal Ministry of Agriculture, Forestry, Environment and Water Management (BMLFUW); 2009.

BMLFUW. Qualitätszielverordnung Ökologie Oberflächengewässer – QZV Ökologie OG 32000L0060 (Regulation on the water quality targets: freshwater ecology). Vienna: Austrian Federal Ministry of Agriculture, Forestry, Environment and Water Management (BMLFUW); 2010.

Bockheim JG. Study of the economic and environmental benefits of reducing soil erosion in Albania, Report. Wisconsin: Terra Institute, Ltd; 2001.

Borah DK, Bera M. Watershed-scale hydrologic and nonpoint-source pollution models. Review of mathematical bases. Trans. ASAE 2003; 46(6): 1553–1566.

Borselli L, Cassi P, Torri D. Prolegomena to sediment and flow connectivity in the landscape: A GIS and field numerical assessment. Catena 2008; 75: 268-277.

Bouraoui F, Dillaha TA. ANSWERS-2000: Non-point source nutrient planning model. Journal of Environmental Engineering 2000; Vol. 126 No. 11: 1045-1055.

Bruci E, Mucaj L, Kovaci V. Climate and erosion in the Ohrid – Prespa zone, Report. Tirana: Hydrometeorological Institute; 2003.

Campbell N, D'Arcy B, Frost A, Novotny V, Sansom A. Diffuse pollution: an introduction to the problems and solutions. London: IWA Publishing; 2004.

Campbell KL, Edwards DL. Phosphorus and water quality impacts. In: Ritter WF, Shirmohammadi A, editors. Agricultural nonpoint source pollution. Boca Raton: Lewis Publishers; 2001. p. 91-111.

Collins K, Blackmore C, Morris D, Watson D. A systemic approach to managing multiple perspectives and stakeholding in water catchments: some findings from three UK case studies. Environmental Science and Policy 2007; 10: 564-574.

Daniels RB, Gilliam JW. Sediment and chemical load reduction by grass and riparian filters. Soil Sci. Soc. Am. J. 1996; 60: 246-251.

Desmet PJJ, Govers G. A GIS procedure for automatically calculating the USLE LS factor on topographically complex landscape units. J. Soil and Water Cons. 1996; 51: 427-433.

de Vente J, Poesen J, Verstraeten G, Van Rompaey A, Govers G. Spatially distributed modelling of soil erosion and sediment yield at regional scales in Spain. Global and Planetary Change 2008; 60: 393–415.

Donigian A, Huber C. Modelling of nonpoint source water quality in urban and non-urban areas, Report No. 68-03-3513. Athens: US Environmental Protection Agency; 1991.

Dosskey MG, Helmers MJ, Eisenhauer DE. A design aid for determining width of filter strips. Journal of Soil and Water Conservation 2008; 63 4: 232-240.

Drewry JJ, Newhama LTH, Greene RSB. Index models to evaluate the risk of phosphorus and nitrogen loss at catchment scales. Journal of Environmental Management 2011; 92: 639-649.

EEA. Homepage of the European Environment Agency (EEA), http://www.eea.europa.eu/.

EC AGRI. Homepage of the Directorate-General for Agriculture and Rural Development of the European Commission (EC AGRI), http://ec.europa.eu/agriculture/index_en.htm.

EC JRC. Homepage of the European Soil Portal, European Commission - Joint Research Centre Institute for Environment and Sustainability (EC JRC), http://eusoils.jrc.ec.europa.eu/.

Flanagan DC, Livingston SJ. Water erosion prediction project (WEPP), version 95.7, User summary, NSERL Report No. 11. West Lafayette: National Soil Erosion Research Laboratory, USDA-ARS; 1995.

Foster GR, Yoder DC, Weesies GA, McCool DK, McGregor KC, Bingner RL. Revised Universal Soil Loss Equation, User´s Guide, Version 2. Washington: USDA-Agricultural Research Service; 2003.

Fread DL. Flow routing. In: Maidment DR, editor. Handbook of hydrology. New York: McGraw-Hill, Inc.; 1993. p. 10.1-36.

Fryirs KA, Brierley GJ, Preston NJ, Spencer J. Catchment-scale (dis)connectivity in sediment flux in the upper Hunter catchment, New South Wales, Australia. Geomorphology 2007; 84: 297–316.

Ghebremichael LT, Veith, TL, Hamlett JM. Integrated watershed- and farm-scale modeling framework for targeting critical source areas while maintaining farm economic viability. Journal of Environmental Management 2013; 114: 381-394.

Giri S, Nejadhashemi AP, Woznicki SA. Evaluation of targeting methods for implementation of best management practices in the Saginaw River Watershed. Journal of Environmental Management 2012; 103: 24-40

Gitau MW, Veith TL. Quantifying the effects of phosphorus control best management practices. In: Radcliffe DE, Cabrera ML, editors. Modeling phosphorus in the environment. Boca Raton: CLC Press; 2007. p. 351-383.

Gitau MW, Veith TL, Gburek WJ. Farm–level optimization of bmp placement for cost–effective pollution reduction. Transactions of the ASAE 2004; Vol. 47(6): 1923−1931.

Grayson R, Blöschl G. Spatial modelling and catchment dynamics. In: Grayson R, Blöschl G, editors. Spatial patterns in catchment hydrology. Cambridge: Cambridge University Press; 2000. p. 51-81.

Hollaus M, Suppan F. SINUS: Landbedeckungsdatensatz aus der Kulturlandschaftsforschung (Land cover recording from landscape research), Report. Vienna: University of Natural Resources and Life Sciences, Vienna; 2003.

Honti M, Istvánovics V, Kovács Á. Balancing between retention and flushing in river networks – optimizing nutrient management to improve trophic state. Science of the Total Environment 2010; 408: 4712-4721.

ICPDR. Water quality in the Danube River Basin – 2005, TNMN Yearbook. Vienna: International Commission for the Protection of the Danube River (ICPDR); 2005.

ICPDR. Danube River Basin Management Plan, Document IC/151. Vienna: International Commission for the Protection of the Danube River (ICPDR); 2009.

Jolánkai G, Panuska J, Rast W. Modelling of nonpoint source pollutant loads. In: Thornton JA, Rast W, Holland MM, Jolánkai G Ryding SO, editors. Assessment and control of nonpoint source pollution of aquatic ecosystems. Pearl River: The Parthenon Publishing Group; 1999, p. 291–338.

Knisel WG. A field scale model for chemical, runoff and erosion from agricultural management systems. Conservation Service Report 26. Washington: U. S. Department of Agriculture; 1980.

Kovács Á, Fülöp B, Honti M. Detection of hot spots of soil erosion and reservoir siltation in ungauged Mediterranean catchments. Energy Procedia 2012a; 18:934-943.

Kovács Á, Honti M. Estimation of diffuse phosphorus emissions at small catchment scale by GIS-based pollution potential analysis. Desalination 2008; 226: 72-80.

Kovács Á, Honti M, Clement A. Design of best management practice applications for diffuse phosphorus pollution using interactive GIS. Water Science and Technology 2008; Vol. 57.11: 1727-1733.

Kovács Á, Honti M, Zessner M, Eder A, Clement A, Blöschl G. Identification of phosphorus emission hotspots in agricultural catchments. Science of the Total Environment 2012b; 433:74-88.

Kroiss H. Nutrient Management in the Danube Basin and its Impact on the Black Sea (DANUBS) Final Report EVK1-CT-2000-00051. Vienna: Institute for Water Quality and Waste Management, Vienna University of Technology; 2005.

Kroiss H, Zessner M, Lampert C. daNUbs: Lessons learned for nutrient management in the Danube Basin and its relation to Black Sea eutrophication. Chemistry and Ecology 2006; 22 (5): 347-357.

Leonea A, Ripaa MN, Bocciab L, Lo Portoc A. Phosphorus export from agricultural land: a simple approach. Biosystems engineering 2008; 101: 270–280

Liu YB, De Smedt F. WetSpa extension: A GIS-based hydrologic model for flood prediction and watershed management, User manual. Brussels: Vrije Universiteit Brussel; 2004.

Löwgren, M. The Water Framework Directive: Stakeholder preferences and catchment management strategies – Are they reconcilable? Ambio 2005; 34 (7): 501-506.

Lowrance R, Altier LS, Williams RG, Inamdar SP, Sheridan JM, Bosch DD, Hubbard RK, Thomas DL. REMM: The Riparian Ecosystem Management Model. Journal of Soil and Water Conservation 2000; 55(1): 27-34.

Maringanti C, Chaubey I, Popp J. Development of a multi-objective optimization tool for the selection and placement of best management practices for nonpoint source pollution control Water Resour. Res. 2009; 45 W06406: 1-15.

Meals DW, Cassell EA, Hughell D, Wood L, Jokela WE, Parsons R. Dynamic spatially explicit mass-balance modeling for targeted watershed phosphorus management, II. Model application. Agriculture, Ecosystems and Environment 2008; 127: 223–233.

Molnar P, Ramirez JA. Energy dissipation theories and optimal channel characteristics of river networks. Water Resources Research 1998; Vol. 34 No. 7: 1809–1818.

Morgan RPC. Soil Erosion and Conservation. Malden: Blackwell Publishing; 2005.

Morgan RPC, Quinton JN, Smith RE, Govers G, Poesen JWA, Auerswald K, Chischi G, Torri D, Styczen ME. The European Soil Erosion Model (EUROSEM): a dynamic approach for predicting sediment transport from fields and small catchments. Earth Surface Processes and Landforms 1998; 23: 527–544.

Mostaghimi S, Brannan KM, Dillaha TA, Bruggeman AC. Best management practices for nonpoint source pollution control: selection and assessment. In: Ritter WF, Shirmohammadi A, editors. Agricultural nonpoint source pollution. Boca Raton: Lewis Publishers; 2001. p. 257-305.

Mostaghimi S, Park SW, Cooke RA, Wang SY. Assessment of management alternatives on a small agricultural watershed. Water Research 1997; Vol. 31 No. 8: 1867-1878.

Muñoz-Carpena R, Parsons JE, Gillian JW. Modeling hydrology and sediment transport in vegetative filter strips. Journal of Hydrology 1999; 214: 111-129.

Nearing MA, Norton LD, Zhang X. Soil erosion and sedimentation. In: Ritter WF, Shirmohammadi A, editors. Agricultural nonpoint source pollution. Boca Raton: Lewis Publishers; 2001. p. 29-58.

Neitsch SL, Arnold JG, Kiniry JR, Williams JR, King KW. Soil and Water Assessment Tool, Theoretical documentation, version 2000, TWRI Report TR-191. College Station: Texas Water Resources Institute; 2002.

Németh T. Talajaink szervesanyag-tartalma és nitrogénforgalma (Organic matter and nitrogen cycle of soils). Budapest: Hungarian Academy of Science; 1996.

Novotny V. Diffuse Pollution and Watershed Management. Hoboken: John Wiley and Sons, Inc.; 2003.

O'Callaghan JF, Mark DM. The extraction of drainage networks from digital elevation data. Computer Vision Graphics and Image Processing 1984; 28: 328–344.

OJEC. Directive 2000/60/EC of the European Parliament and of the Council of 23 October 2000 establishing a framework for Community action in the field of water policy. Official Journal of the European Communities (OJEC) 2000; L 327/1.

Ouyang D, Bartholic J. Predicting sediment delivery ratio in Saginaw Bay watershed. In: Book of proceedings of the 22nd National Association of Environmental Professionals Conference, May 19–23, 1997. Collingswood: National Association of Environmental Professionals; 1997. p. 659–671.

Pano N, Frasheri A, Avdyli B, Haska H. Impact of climate change on erosion process in the Albanian hydrographic river network. In: Book of proceedings of the 9th International Symposium on River Sedimentation (ISRS), 18-21 Oct. 2004. Beijing: Ministry of Water Resources, People's Republic of China; 2004.

Parker JS, Moore R, Weaver M. Developing participatory models of watershed management in the Sugar Creek watershed (Ohio, USA). Water Alternatives 2009; 2(1): 82-100.

Pierzynski GM. Phosphorus sources for agriculture: production and characteristics. In: Sims JT, Sharpley AN, editors. Phosphorus: agriculture and the environment. Madison: American Society of Agronomy, Inc; 2005. p. 1-51.

Poulos SE, Collins MB. Fluviatile sediment fluxes to the Mediterranean Sea: a quantitative approach and the influence of dams. In: Jones SJ, Frostick, LE, editors. Sediment flux to basins: causes, controls and consequences. London: Geological Society, Vol. 5 Issue 191; 2002.

Qi H, Altinakar MS. A conceptual framework of agricultural land use planning with BMP for integrated watershed management Journal of Environmental Management 2011; 92: 149-155.

Radcliffe DE, Cabrera ML, editors. Modeling Phosphorus in the Environment. Boca Raton: CLC Press; 2007.

Randle TJ, Yang CT, Daraio J. Erosion and reservoir sedimentation. In: U. S. Department of the Interior Bureau of Reclamation: Erosion and sedimentation manual. Denver: Bureau of Reclamation; 2006. p. 2.1-2.94.

Rao NS, Easton ZM, Schneiderman EM, Zion MS, Lee DR, Steenhuis T. Modeling watershed-scale effectiveness of agricultural best management practices to reduce phosphorus loading. Journal of Environmental Management 2009; 90: 1385–1395.

Rawls WJ, Ahuja LR, Brakensiek DL, Shirmohammadi A. Infiltration and soil water movement. In: Maidment DR, editor. Handbook of hydrology. New York: McGraw-Hill, Inc.; 1993. p. 5.1–5.51.

Renard KG, Foster GR, Weesies GA, McCool DK, Yoder DC. Predicting Soil Erosion by Water: A Guide to Conservation Planning with the Revised Universal Soil Loss Equation (RUSLE). Agricultural Handbook 703. Washington: U.S. Department of Agriculture; 1997.

Ritter WF, Shirmohammadi A, editors. Agricultural Nonpoint Source Pollution. Boca Raton: CRC Press LLC; 2001.

Salamin P. Erózió elleni küzdelem és környezetvédelem (Erosion control and environmental protection). Budapest: Budapest University of Technology; 1982.

Schilling C, Zessner M, Kovács Á, Hochedlinger G, Windhofer G, Gabriel O, Thaler S, Parajka J, Natho S. Stickstoff- und Phosphorbelastungen der Fliessgewässer Österreichs und Möglichkeiten zu deren Reduktion (Nitrogen and phosphorus emissions to Austria's rivers and their reduction possibilities). Österreichische Wasser- und Abfallwirtschaft 2011; 63: 105-116.

Schneiderman EM, Steenhuis TS, Thongs DJ, Easton ZM, Zion MS, Mendoza GF, Walter MT, Neal AC. Incorporating variable source area hydrology into curve number based watershed loading functions. Hydrol. Proc. 2007; 21 (25): 3420–3430.

Schreiber H, Constantinescu LT, Cvitanic I, Drumea D, Jabucar D, Juran S, Pataki B, Snishko S, Zessner M, Behrendt H. Harmonized inventory of point and diffuse emissions of nitrogen and phosphorus for a transboundary river basin, Delivery 5.5 of the daNUbs Project (EVK1-CT- 2000-00051). Berlin: Institute of Freshwater Ecology and Inland Fisheries; 2003.

Schröder JJ, Cordell D, Smit AL, Rosemarin A. Sustainable use of phosphorus, Report 357, EU Tender ENV.B.1./ETU/2009/0025. Wageningen: Wageningen University and Research Centre; 2010.

Shirmohammadi A, Montas HJ, Bergstrom L, Knisel WG Jr. Water quality models. In: Ritter WF, Shirmohammadi A, editors. Agricultural nonpoint source pollution. Boca Raton: Lewis Publishers; 2001. p. 233-256.

Somlyódy L, Buzás K, Clement A, Licskó I. Települési vízgazdálkodás (Urban water management) In: Somlyódy L, editor. A hazai vízgazdálkodás stratégiai kérdései (Strategic issues of the Hungarian water resources management). Budapest: Hungarian Academy of Science; 2002. p. 277–318.

Somlyódy L, Hock B. Vízminőség és szabályozása (Water quality and its management), In: Somlyódy L, editor. A hazai vízgazdálkodás stratégiai kérdései (Strategic issues of the Hungarian water resources management). Budapest: Hungarian Academy of Science; 2002. p. 139–176.

Somlyódy L, Van Straten G, editors. Modelling and managing shallow lake eutrophication. With application to Lake Balaton. Berlin: Springer-Verlag, 1986.

Srivastava P, Hamlett JM, Robillard PD, Day RL. Watershed optimization of best management practices using AnnAGNPS and a genetic algorithm. Water Resources Research 2002; Volume 38 Issue 3: 3.1–3.14

Strauss P, Auerswald K, Klaghofer E, Blum WEH. Erosivität von Niederschlägen: ein Vergleich Österreich-Bayern (Rainfall erosivity: a comparison of Austria-Bavaria). Zeitung für Kulturtechnik und Landentwicklung 1995; 36: 304-308.

Tar F. Payment calculation schemes for the planning of agro-environmental measures. Budapest: Ministry for Agriculture and Rural Development; 2006.

Tetzlaff B, Friedrich K, Vorderbrügge T, Vereecken H, Wendland F. Distributed modelling of mean annual soil erosion and sediment delivery rates to surface waters. Catena 2013; Volume 102: 13–20.

Ulén B, Djodjic F, Etana A, Johansson G, Lindström J. The need for an improved risk index for phosphorus losses to water from tile-drained agricultural land. Journal of Hydrology 2011; 400: 234–243.

USGS. Mineral commodity summaries, Report. Reston: U.S. Geological Survey; 2012.

Vache KB, Eilers JM, Santelmann MV. Water quality modeling of alternative agricultural scenarios in the U.S. corn belt. Journal of the American Water Resources Association 2002; 38 (3): 773-787.

Van Rompaey AJJ, Verstraeten G, Van Oost K, Govers G, Poesen J. Modelling mean annual sediment yield using a distributed approach. Earth Surface Processes and Landforms 2001; 26: 1221–36.

Van Vuuren DP, Bouwmana AF, Beusen AHW. Phosphorus demand for the 1970–2100 period: A scenario analysis of resource depletion. Global Environmental Change 2010; 20: 428–439.

Veith TL, Wolfe ML, Heatwole CD. Cost−effective bmp placement: optimization versus targeting. Transactions of the ASAE 2004; Vol. 47 (5): 1585−1594.

Venohr M, Hirt U, Hofmann J, Opitz D, Gericke A, Wetzig A, Natho S, Neumann F, Hürdler J, Matranga M, Mahnkopf J, Gadegast M, Behrendt H. Modelling of Nutrient Emissions in River Systems – MONERIS – Methods and Background. International Review of Hydrobiology 2011; 96 Issue 5: 435–483.

Vigiak O, Rattray D, McInnes J, Newham LTH, Roberts AM. Modelling catchment management impact on in-stream phosphorus loads in northern Victoria. Journal of Environmental Management 2012; 110: 215-225.

VM. 10/2010. (VIII. 18.) VM rendelet a felszíni víz vízszennyezettségi határértékeiről és azok alkalmazásának szabályairól (Regulation on the water quality standard values of the surface waters and their application rules). Budapest: Hungarian Ministry of Rural Development (VM); 2010.

Vollenweider RA, Kerekes J. Eutrophication of waters. Monitoring, assessment and control, OECD Cooperative programme on monitoring of inland waters (Eutrophication control). Paris: OECD; 1982.

WB. Homepage of the world data bank of the World Bank, http://databank.worldbank.org/data/home.aspx.

Westermann DT. Phosphorus reaction and cycling in soils. In: Sims JT, Sharpley AN, Editors. Phosphorus: agriculture and the environment. Madison: American Society of Agronomy, Inc; 2005. p. 1-51.

White MJ, Storm DE, Busteed PR, Smolen MD, Zhang H, Fox GA. A quantitative phosphorus loss assessment tool for agricultural fields. Environmental Modelling and Software 2010; 25: 1121-1129.

Williams JR, Dyke PT, Jones CA. EPIC: a model for assessing the effect of erosion on soil productivity. In: Lauenroth WK, editor. Analysis of ecological systems: State of the art in ecological modeling. Amsterdam: Elsevier; 1983.

Wischmeier WH, Smith DD. Predicting Rainfall Erosion Losses: a guide to conservation planning. Washington: U. S. Government Printing Office; 1978.

wpa. Effektivität von Gewässerrandstreifen zum Schutz von Oberflächengewässern (Efficiency of buffer strips for protection of surface waters), Bericht BMLFUW-UW.3.2.2/0003-VII 1/2009. Vienna: wpa Beratende Ingenieure; 2009.

Zessner M, Gabriel O, Kovács Á, Kuderna M, Schilling C, Hochedlinger G, Windhofer G. Nährstoffströme Oberösterreich: Analyse der Nährstoffströme in oberösterreichischen Einzugsgebieten nach unterschiedlichen Eintragspfaden für strategische Planungen (Nutrient fluxes of Upper-Austria: Catchment-scale nutrient flux analysis according to different pathways for strategic planning in Upper-Austria), Report WPLO-2010-290023/1-Stu/Mö. Vienna: Institute for Water Quality and Waste Management, Vienna University of Technology; 2011c.

Zessner M, Gabriel O, Kovács Á, Thaler S, Schilling C, Hochedlinger G, Windhofer G. STOBIMO-Nährstoffe: Stoffbilanzmodellierung für Nährstoffe auf Einzugsgebietsebene als Grundlage für Bewirtschaftungspläne und Maßnahmenprogramme (STOBIMO-Nutrients: Catchment-scale nutrient balance modeling as a basis of management programs), Report BMLFUW-UW.3.1.2/0029-VII/1/2008. Vienna: Institute for Water Quality and Waste Management, Vienna University of Technology; 2011b.

Zessner M, Kovács Á, Schilling C, Hochedlinger G, Gabriel O, Thaler S, Natho S, Windhofer G. Enhancement of the MONERIS model for application in alpine catchments in Austria. International Review of Hydrobiology 2011a; Vol. 96 No. 5: 541-60.

Zessner M, Postolache C, Clement A, Kovács Á, Strauss P. Considerations on the influence of extreme events on the phosphorus transport from river catchments to the sea. Water Science and Technology 2005; Vol. 51 No. 11: 193–204.

Zhang X, Drake NA, Wainwright J. Scaling issues in environmental modeling. Wainwright J, Mulligan M. editors. In: Environmental modelling: Finding simplicity in complexity. Chichester: John Wiley & Sons Ltd.; 2004. p. 319-334.

Appendix A: The PhosFate model

A.1 Hydrology

Hydrology is modeled by the adapted version of the long-term, distributed parameter water balance model WetSpass (Water and Energy Transfer between Soil, Plants and Atmosphere under quasi-Steady State, Batelaan and Woldeamlak, 2004; Batelaan and DeSmedt, 2007). The water balance components of vegetated, bare soil, impervious and open water surfaces in a particular cell are summed up to calculate the total water balance of a raster cell. Water balance is calculated for the summer and winter seasons. The seasonal water balance equation is:

$$P_i = I_i + SR_i + T_{a,i} + E_{a,i} + RCH_i \tag{A.1}$$

where P_i is the rainfall amount of cell i [mm a^{-1}], I_i is the amount of intercepted rainfall of cell i [mm a^{-1}], SR_i is the surface runoff of cell i [mm a^{-1}], $T_{a,i}$ is the actual transpiration of cell i [mm a^{-1}], $E_{a,i}$ is the actual evaporation of cell i [mm a^{-1}], RCH_i is the groundwater recharge of cell i [mm a^{-1}] and i is the cell index [-].

The interception is depending on the type of vegetation using a constant intercepted fraction for the vegetated surfaces:

$$I_i = P_i \cdot \frac{i_i}{100} \cdot a_{veg,i} \tag{A.2}$$

i_i is the interception ratio of cell i [%], $a_{veg,i}$ is the rate of vegetated surfaces of cell i [-].

The surface runoff is calculated in relation to precipitation amount, precipitation intensity, and soil infiltration capacity:

$$SR_i = P_i \cdot c_{Rpot,i} \cdot c_{Peff,i} \tag{A.3}$$

where $c_{Rpot,i}$ is the potential runoff coefficient of cell i [-], $c_{Peff,i}$ is the ratio of the effective to the total precipitation of cell i [-].

The runoff coefficient is a function of vegetation, soil type and slope and it is weighted according to the vegetated, bare soil, impervious and open water surfaces in a cell, whereas interception loss is considered for the vegetated surfaces:

$$c_{pot,i} = c_{pot,veg,i} \cdot \left(1 - \frac{i_i}{100}\right) \cdot a_{veg,i} + c_{pot,bare,i} \cdot a_{bare,i} + c_{pot,imp,i} \cdot a_{imp,i} + c_{pot,wat,i} \cdot a_{wat,i} \tag{A.4}$$

where $c_{pot,veg,i}$ is the potential runoff coefficient for the vegetated surfaces of cell i [-], $c_{pot,bare,i}$ is the potential runoff coefficient for the bare soil surfaces of cell i [-], $a_{bare,i}$ is the rate of bare soil surfaces of cell i [-], $c_{pot,imp,i}$ is the potential runoff coefficient for the impervious surfaces of cell i [-], $a_{imp,i}$ is the rate of impervious surfaces of cell i [-], $c_{pot,wat,i}$ is the potential runoff coefficient for the open water surfaces of cell i [-], $a_{wat,i}$ is the rate of open water surfaces of cell i [-].

Reference transpiration is obtained from open-water evaporation and a vegetation coefficient:

$$T_{r.i} = PET_i \cdot c_{pen,veg,i} \tag{A.5}$$

where $T_{r,i}$ is the reference transpiration of cell i [mm a^{-1}], PET is the potential open water evaporation of cell i [mm a^{-1}] $c_{pen,veg}$ is the Penman vegetation coefficient of cell i [-].

The Penman vegetation coefficient can be calculated as the ratio of reference vegetation transpiration as given by the Penman-Monteith equation to the potential open-water evaporation, as given by the Penman equation:

$$c_i = \frac{1 + \frac{\gamma_p}{\Delta_i}}{1 + \frac{\gamma_p}{\Delta_i} \cdot \left(1 + \frac{r_{c.i}}{r_{a,i}}\right)} \tag{A.6}$$

where γ_p is the psychometric constant [kPa °C^{-1}], Δ_i is the gradient of the saturated vapor pressure curve of cell i [kPa °C^{-1}], $r_{c,i}$ is the canopy resistance of cell i [s m^{-1}], $r_{a,i}$ is the aerodynamic resistance of cell i [s m^{-1}].

The Penman vapor pressure coefficient can be obtained from the air temperature:

$$\frac{\gamma_p}{\Delta_i} = 1.5411 \cdot exp\left(-0.0575 \cdot TEMP_i\right) \tag{A.7}$$

where $TEMP_i$ is the average air temperature of cell i [°C].

The canopy resistance is a function of the stomata resistance and the leaf area index:

$$r_{c,i} = \frac{r_{l,i}}{LAI_i} \tag{A.8}$$

where r_l is the minimum stomata resistance of cell i [s m^{-1}], LAI is the leaf area index of cell i [-], both depending on the vegetation type.

The aerodynamic resistance is computed by:

$$r_{a,i} = \frac{1}{c_{vK}^{\ 2} \cdot u_i} \cdot \left(ln\left(\frac{h_{c,i} + z_{m,i} - d_i}{0.123 \cdot h_{c,i}} \right) \right)^2 \tag{A.9}$$

where c_{vK}: is the von Karman constant [-], u_i is the wind speed of cell i [m s^{-1}], $h_{veg,i}$ is the vegetation height of cell i, depending on the vegetation type [m], $z_{m,i}$ is the height of meteorological measurement above the vegetation top of cell i [m], d_i is the displacement height of the wind profile of cell i [m].

The displacement height of the wind profile is the following:

$$d_i = 0.67 \cdot h_{c,i} \tag{A.10}$$

The actual transpiration is calculated from the potential value considering the soil water content with the function below (assuming groundwater level below the root zone):

$$T_{a,i} = T_{r,i} \cdot \left(1 - c_{text,i} \frac{P_i + N_m \cdot \left(\Theta_{fc,i} - \Theta_{wp,i}\right) z_{root,i}}{T_{r,i}} \right) \cdot a_{veg,i} \tag{A.11}$$

where $c_{text,i}$ is a calibrated parameter related to the soil texture of cell i, depending on the soil type [-], N_m: is the number of months in the season [-], $\theta_{fc,i}$ is the water content of the soil at

field capacity of cell i, depending on the soil type [-], $\theta_{wp,i}$ is the water content of the soil at permanent wilting point of cell i, depending on the soil type [-], $z_{root,i}$ is the depth of the root zone of cell i depending on the vegetation type [mm].

The actual soil/impervious surface/open water evaporation:

$$E_{a,i} = \left(PET_i - I_i - T_{a,i}\right) \cdot \left[\left(1 - c_{text,i} \frac{P_i + N_m \cdot \left(\Theta_{fc,i} - \Theta_{wp,i}\right) z_{evap,i}}{PET_i}\right) \cdot \left(a_{veg,i} + a_{bare,i}\right) + a_{imp,i} + a_{wat,i}\right] \quad \text{(A.12)}$$

where $z_{evap,i}$ is the evaporation depth of cell i [mm].

The groundwater recharge is calculated as a residual term of the water balance:

$$RCH_i = P_i - I_i - SR_i - T_{a,i} - E_{a,i} \quad \text{(A.13)}$$

Annual surface runoff is calculated as a sum of the summer and winter values:

$$SR_{a,i} = SR_{s,i} + SR_{w,i} \quad \text{(A.14)}$$

where $SR_{a,i}$ is the annual surface runoff of cell i [mm a^{-1}], $SR_{s,i}$ is the summer half yearly surface runoff of cell i [mm a^{-1}], $SR_{w,i}$ is the winter half yearly surface runoff of cell i [mm a^{-1}].

Annual recharge is calculated as a sum of the summer and winter values if they are positive:

$$RCH_{a,i} = RCH_{s,i}(>0) + RCH_{w,i}(>0) \quad \text{(A.15)}$$

where $RCH_{a,i}$ is the annual recharge of cell i [mm a^{-1}], $RCH_{s,i}(>0)$ is the summer half yearly positive recharge of cell i [mm a^{-1}], $RCH_{w,i}(>0)$ is the winter half yearly positive recharge of cell i [mm a^{-1}].

A.2 Soil erosion

Gross soil loss is estimated using an adapted version of the USLE approach:

$$SL_i = R_i \cdot K_i \cdot L_i \cdot S_i \cdot CM_i \cdot SP_i \quad \text{(A.16)}$$

where SL_i is the annual gross soil loss rate of cell i [t SS ha^{-1} a^{-1}], R_i is the annual rainfall energy factor of cell i [MJ mm ha^{-1} h^{-1} a^{-1}], K_i is the soil erodibility factor of cell i [t SS ha h ha^{-1} MJ^{-1} mm^{-1}], L_i is the slope-length factor of cell i [-], S_i is the slope factor of cell i [-], CM_i is the crop management factor of cell i [-], SP_i is the erosion protection factor of cell i [-].

Parameters of USLE can be derived from meteorological data and various digital maps of catchment properties (elevation, soil, land use). The parameter values are set according to the literature (Novotny, 2003; Randle *et al.*, 2006). The soil erodibility factor is a function of the physical topsoil type, the humus content of the topsoil and the slope. The crop management factors are assigned to the land use classes. Finally, the erosion protection factor is related to the applied management practice and the slope.

The rainfall energy factor is calculated according to Foster *et al.* (2003):

$$R_i = \sum_{s=1}^{m} \left\{ \sum_{f=1}^{n_s} \left[\left(0.29 - 0.209 \cdot exp\left(-0.082 \cdot i_{f,s,i} \right) \right) \cdot h_{f,s,i} \right] \cdot i_{30max,s,i} \right\} \tag{A.17}$$

where $i_{f,s,i}$ is the rainfall intensity f during the storm s in cell i [mm h^{-1}], $h_{f,s,i}$ is the rainfall height of the intensity f during the storm s in cell i [mm], $i_{30max,s,i}$ is the maximum half-hourly rainfall intensity during the storm s in cell i [mm h^{-1}], s is the storm index [-], m is the number of the storm events in the year [-], f is the period index [-], n_s is the number of the periods with constant intensity during the storm s [-].

The slope-length factor is adopted from Desmet and Glovers (1996):

$$L_i = \frac{\left(Flowacc \cdot L_{cell} \right)^{1+m} - \left(\left(Flowacc - 1 \right) \cdot L_{cell} \right)^{1+m}}{L_{cell} \cdot 22.13^m} \tag{A.18}$$

where $Flowacc$ is the flow accumulation (in cells) for cell i [-], L_{cell} is the cell size [m], m is the rill erodibility parameter of cell i.

The rill erodibility parameter is according to Renard *et al.* (1997):

$$m = \frac{b}{1+b} \tag{A.19}$$

where b is the ratio the rill to interrill erosion of cell i [-].

The ratio the rill to interrill erosion is (Renard *et al.*, 1997):

$$b = \frac{\sin S_{cell}}{0.0896 \cdot \left(3 \cdot \left(\sin S_{cell}\right)^{0.8} + 0.56\right)} \tag{A.20}$$

where S_{cell} is the cell slope angle of cell i [°].

The slope factor is (Renard *et al.*, 1997):

$$S_i = \begin{Bmatrix} 10 \cdot \sin S_{cell} + 0.03 & S_{cell} < 9\% \\ 16.8 \cdot \sin S_{cell} - 0.5 & S_{cell} \geq 9\% \end{Bmatrix} \tag{A.21}$$

A.3 Soil P forms

The model considers two pathways of diffuse P emission. Particulate P (PP) and a fraction of dissolved P (DP) reach the recipient waters via surface runoff and soil erosion. Another fraction of DP enters stream channels with base flow. PP emission represents the bulk of the diffuse total P output from the catchment.

PP content of the topsoil consists of three different pools in the model:

$$C_{PPtot,i} = C_{PP,act,i} + C_{PP,org,i} + C_{PP,sta,i} \tag{A.22}$$

where $C_{PPtot,i}$ is the total PP content of the topsoil at cell i [µg P g^{-1}], $C_{PP,act,i}$ is the active (labile) inorganic PP concentration of the topsoil at cell i [µg P g^{-1}], $C_{PP,org,i}$ is the organic PP concentration of the topsoil (mainly in the humus layer) at cell i [µg P g^{-1}] and $C_{PP,sta,i}$ is the stable inorganic PP concentration of the topsoil at cell i [µg P g^{-1}].

The stabile inorganic phase is related to the clay content of the soil (Behrendt *et al.*, 1999):

$$C_{PP,sta,i} = 10.2 \cdot C_{clay,i} \tag{A.23}$$

where $C_{clay,i}$ is the clay content of the topsoil in cell i, depending on the soil type [%].

The organic phase is calculated from the humus content assuming fixed organic material-organic carbon and organic carbon-organic P ratios (Neitsch *et al.*, 2002):

$$C_{PP,org,i} = \frac{C_{hum,i}}{100} \cdot c_{OM-C} \cdot c_{C-P} \tag{A.24}$$

where $C_{hum,i}$ is the humus content of the topsoil in cell i [%], c_{OM-C} is the organic matter-carbon ratio [-], c_{C-P} is the carbon-P ratio [-].

In non-agricultural cells, the stable phase maintains an equilibrium dissolved P (DP) concentration. The equilibrium is according to a Langmuir-type isotherm:

$$C_{PP,sta,i} = \frac{Q_{0,i} \cdot b_i \cdot C_{DP,0,i}}{1 + b_i \cdot C_{DP,0,i}} \tag{A.25}$$

where $Q_{0,i}$ is the adsorption maximum at cell i [µg P g^{-1}] and b_i is the adsorption energy coefficient at cell i [L μg^{-1}], $C_{DP,0,i}$ is the DP concentration of the topsoil pore water at cell i under natural conditions [µg P L^{-1}]. Resolving the equation to the DP concentration yields:

$$C_{DP,0,i} = \frac{C_{PP,sta,i}}{b_i \cdot \left(Q_{0,i} - C_{PP,sta,i}\right)} \tag{A.26}$$

Parameters of the isotherm (adsorption maximum and energy coefficient) are related to soil features (clay and humus content, pH value) according to Novotny (2003).

The maximum of the adsorbed P is:

$$Q_{0,i} = -3.5 + 10.7 \cdot C_{Clay,i} + 49.5 \cdot C_{Hum,i} \cdot R_{OM-C} \tag{A.27}$$

The energy coefficient of adsorption is:

$$b_i = \left(0.061 + 170 \cdot 10^{-pH_i} + 0.027 \cdot C_{Clay,i} + 0.076 \cdot C_{Hum,i} \cdot R_{OM-C}\right) \cdot 10^{-3} \tag{A.28}$$

where pH is the pH value of the topsoil in cell i [-].

The total natural inorganic P content of the soil is:

$$C_{P,0,i} = C_{PP,sta,i} \cdot \rho_S \cdot \left(1 - \Theta_{S,i}\right) + C_{DP,0,i} \cdot \Theta_{S,i} \tag{A.29}$$

where $C_{P,0,i}$ is the total inorganic P concentration of the topsoil at cell i under natural conditions [µg P L^{-1}], ρ_S is the soil particle density [kg m^{-3}], $\Theta_{S,i}$ is the porosity of the topsoil layer at cell i, depending on the soil type [m^3 m^{-3}].

The active inorganic pool is related to the soil P surpluses and determined from the long-term agricultural P surplus and the cultivated soil depth. Agricultural surplus is a direct modeling input, it can be calculated using statistical data on the amounts of applied fertilizer and manure, added crop residue and waste water (as inputs) and the harvested crops (as outputs) over the last 40-50 years. Atmospheric deposition and humus mineralization can also be taken into account. P surplus is then divided to DP and PP phases using a partition function. Again, Langmuir-type adsorption equation is used for the partitioning. If agricultural surplus exists, the total soil inorganic P concentration is:

$$C_{P,agr,i} = \frac{SUR_{P,i} \cdot 10^2}{z_{soil}} + C_{P,0,i} \tag{A.30}$$

where $C_{P,agr,i}$ is the total inorganic P concentration of the topsoil at cell i under agricultural conditions [µg P L^{-1}], $SUR_{P,i}$ is the long-term accumulated agricultural P surplus of the topsoil at cell i [kg P ha^{-1}], z_{soil} is the depth of the cultivated soil [m].

The partitioning between the phases is:

$$C_{P,agr,i} = C_{PP,agr,i} \cdot \rho_S \cdot \left(1 - \Theta_{S,i}\right) + C_{DP,i} \cdot \Theta_{S,i} = \frac{Q_{0,i} \cdot b_i \cdot C_{DP,i}}{1 + b_i \cdot C_{DP,i}} \cdot \rho_S \cdot \left(1 - \Theta_{S,i}\right) + C_{DP,i} \cdot \Theta_{S,i} \tag{A.31}$$

where $C_{PP,agr,i}$ is the total inorganic PP concentration of the topsoil at cell i under agricultural conditions [µg P kg^{-1}], $C_{DP,i}$ is the DP concentration of the topsoil pore water at cell i under agricultural conditions [µg P L^{-1}].

Solving Eq. (A.31) for the inorganic DP content of the soil yields:

$$C_{DP,i} = -\frac{\rho_S \cdot (1-\Theta_{S,i}) \cdot Q_{0,i} \cdot b_i - \Theta_{S,i} + C_{P,act,i} \cdot b_i}{2 \cdot \Theta_{S,i} \cdot b_i} + \\ + \frac{\sqrt{(\rho_S \cdot (1-\Theta_{S,i}) \cdot Q_{0,i} \cdot b_i + \Theta_{S,i} - C_{P,act,i} \cdot b_i)^2 + 4 \cdot \Theta_{S,i} \cdot b_i \cdot C_{P,act,i}}}{2 \cdot \Theta_{S,i} \cdot b_i} \quad \text{(A.32)}$$

The total inorganic PP content of the soil from the isotherm is:

$$C_{PP,agr,i} = \frac{Q_{0,i} \cdot b_i \cdot C_{DP,i}}{1 + b_i \cdot C_{DP,i}} \quad \text{(A.33)}$$

The active inorganic PP content of the soil is:

$$C_{PP,act,i} = C_{PP,agr,i} - C_{PP,sta,i} \quad \text{(A.34)}$$

Kinetics of the sorption processes is ignored, because surface exchange reactions may be completed within minutes, while the second phase of desorption from subsurface horizons within the interior of particles is too slow (days to months) to significantly influence the dissolved concentrations.

A.4 P emissions

Emissions are calculated for surface runoff, erosion and recharge as a product of the corresponding flow (soil loss) rate and soil P concentration value. For urban areas, average concentration values of urban runoff were assigned depending on the urban land use form (Novotny, 2003).

DP emissions via surface runoff:

$$E_{SR,i} = SR_{a,i} \cdot A_{cell} \cdot C_{DP,i} \cdot c_{wash} \cdot 10^{-5} \quad \text{(A.35)}$$

where $E_{SR,i}$ is the DP emissions via surface runoff at cell i [kg P a^{-1}], A_{cell} is the cell area [ha], c_{wash} is the ratio of P concentration in surface runoff to soil pore water [-].

PP emissions via urban runoff (in urban cells only):

$$E_{SR,urb,i} = SR_{a,i} \cdot A_{cell} \cdot C_{DP,urb,i} \cdot 10^{-2} \quad \text{(A.36)}$$

$E_{SR,urb,i}$ is the annual DP emission via urban runoff at cell i [kg P a^{-1}], $C_{DP,urb}$ is the DP concentration of the urban surface runoff at cell i [mg P l^{-1}].

PP emissions via soil erosion:

$$E_{ER,i} = SL_i \cdot A_{cell} \cdot C_{PP,i} \cdot c_{enr,i} \cdot 10^{-3} \quad \text{(A.37)}$$

where $E_{ER,i}$ is the annual PP emission via soil erosion at cell i [kg P a^{-1}], $c_{enr,i}$ is the local enrichment ratio at cell i [-].

The local enrichment ratio represents the particle sorting of the erosion, *i.e.* fine particles are more erodible. It is related to the clay content of the soil and adjusted to the clay content of each cell:

$$c_{enr,i} = 1 + \frac{C_{clay,i}}{100} \quad \text{(A.38)}$$

Since total PP pool in the topsoils is subject to erosion, while the organic and the stable PP pools are assumed to be time-invariant, a supply mechanism is needed to close the mass balance. Humification during the decomposition of terrestrial organic matter may provide the supply of the organic PP pool. In the case of the stable PP pool, weathering of the parent rocks and deposition of airborne particles can be considered. These supply mechanisms are not modeled, it is assumed that they equalize the losses via erosion or the changes are negligible.

PP emissions via urban runoff (in urban cells only):

$$E_{ER,urb,i} = SR_{a,i} \cdot A_{cell} \cdot C_{PP,urb,i} \cdot 10^{-2} \quad \text{(A.39)}$$

where $E_{ER,urb,i}$ is the annual PP emission via urban runoff at cell i [kg P a^{-1}] $C_{PP,urb}$ is the PP concentration of the urban surface runoff at cell i [mg P l^{-1}].

PP emissions via recharge:

$$E_{RCH,i} = RCH_{a,i} \cdot A_{cell} \cdot C_{DP,i} \cdot c_{leach} \cdot 10^{-5} \tag{A.40}$$

where $E_{RCH,i}$ is the DP emissions via recharge at cell i [kg P a^{-1}], c_{leach} is the ratio of P concentration in leachate to soil pore water [-].

Emissions via runoff and recharge can cause a decrease in the soil DP concentration. This is compensated via P desorption from the active PP pool, resulting in lower PP concentration in the soil. This change is neglected in the model because impact of the agricultural surplus as input on the soil P level is much higher than the influence of the dissolved losses, especially at long-term scale.

A.4 Flow routing

Flow routing is computed by connecting the individual cells to each other. The routing within the catchment is cumulative according to the flow tree. Flow tree is determined from the slope map using the classic D8 routing scheme (O'Callaghan and Mark, 1984). It conveys the water flow from each cell always to only one of the eight neighborings, to which the given cell has the highest elevation gradient (slope). Each cell is characterized as either field or channel cell. Distinction is based on a threshold value of upstream located cells along the flow paths directed to a given cell, which is minimally necessary to form a channel. Flow components are separately routed and then they are summed up to obtain river discharge.

Surface runoff routing on the field:

$$OUT_{SR,f,i} = IN_{SR,f,i} + \frac{SR_{a,i} \cdot A_{cell} \cdot 10^{-1}}{365 \cdot 86400} \tag{A.41}$$

where $OUT_{SR,f,i}$ is the outflowing surface runoff at field cell i [m^3 s^{-1}], $IN_{SR,f,i}$ is the inflowing surface runoff at field cell i [m^3 s^{-1}].

Surface runoff routing in the channel:

$$OUT_{SR,ch,i} = IN_{SR,ch,i} \tag{A.42}$$

where $OUT_{SR,ch,i}$ is the outflowing surface runoff at channel cell i [m^3 s^{-1}], $IN_{SR,ch,i}$ is the inflowing surface runoff at channel cell i [m^3 s^{-1}], arriving from both the adjacent terrestrial cells and the upstream channel cells.

Base flow is routed in the channel only. In the lack of information on the composition of subsurface soil horizons, bedrock and groundwater table, the flow paths of groundwater are considered to follow surface flow paths, but groundwater flow is represented in the channel cells only as base flow amount from the upstream contributing area:

$$OUT_{BF,ch,i} = \frac{\sum_{j=1}^{n_i} \left(RCH_{a,upstr,j} \right) \cdot A_{cell} \cdot 10^{-1}}{365 \cdot 86400} \tag{A.43}$$

where $OUT_{BF,ch,i}$ is the outflowing base flow at channel cell i [m^3 s^{-1}], $RCH_{a,upstr,j}$ is the recharge at the upstream field cell j [mm a^{-1}], j is the upstream cell index [-], n_i is the number of the upstream cells of cell i [-].

Stream flow routing in the channel:

$$OUT_{Q,i} = OUT_{SR,ch,i} + OUT_{BF,i} + Q_{PS} \tag{A.44}$$

where $OUT_{Q,i}$ is the outflowing river flow at channel cell i [m^3 s^{-1}], $Q_{PS,i}$ is the point source discharge at channel cell i [m^3 s^{-1}].

A.5 Sediment transport

Similarly to the flow, transport modeling of the local mass fluxes within the catchment is also cumulative. The channel cells have dual function, they simultaneously represent the stream channel and the interface between terrestrial and aquatic ecosystems. They route flow and mass fluxes downstream as parts of a watercourse (channel function) and also convey loads coming from their neighboring field cells through riparian zone (field function). The interface, which is a part of the riparian zone, may significantly modify terrestrial inputs to the water. For example, arable land is prone to high erosion, particularly when it is situated in narrow and steep valleys of medium-sized rivers or streams. At the typical spatial resolution of the model inputs, arable fields often extend down to the channel. It is, however, unlikely

that a narrow, frequently inundated stream-side interface would be cultivated. As elements of the riparian interface, channel cells retain mass flux received from the terrestrial cells. The field function of channel cells is not identical with the terrestrial cells: they retain but do not release mass fluxes. This assumption reflects the efficient retention of material fluxes observed in the riparian zones of rivers. As a low-erosion, high-retention land-use type, the interface is supposed to be covered by grass.

Mass balance equation is solved at each cell. The outflowing suspended solids (SS) flux in a field cell is the sum of the inflowing flux, the gross soil loss and the sediment retention via settling (negative value):

$$OUT_{SS,f,i} = IN_{SS,f,i} + SL_i \cdot A_{cell} - RET_{SS,f,i} \tag{A.45}$$

where $OUT_{SS,f,i}$ is the outflowing sediment load of field cell i [t SS a^{-1}], $IN_{SS,f,i}$ is the inflowing sediment load of field cell i [t SS a^{-1}] and $RET_{SS,f,i}$ is the sediment deposition at field cell i [t SS a^{-1}].

Sediment deposition is computed from the inflowing load and local soil loss values with an exponential function of the cell residence time:

$$RET_{SS,f,i} = IN_{SS,f,i} \cdot \left[1 - exp\left(-k_{SS,f} \cdot t^*_{cell,f,i}\right)\right] + SL_i \cdot A_{cell} \cdot \left[1 - exp\left(-k_{SS,f} \cdot t^*_{cell,f,i} \cdot 0.5\right)\right] \tag{A.46}$$

where $k_{SS,f}$ is the sediment field deposition rate [s^{-1}], $t^*_{cell,f,i}$ is the residence time of overland flow at field cell i [s].

The passing SS flux is experiencing full-scale retention during its travel through the cell. Residence time depends on the average flow velocity and the flow path length. For each cell two flow path lengths are considered: one for the inflowing fluxes and one for the local emissions. Flow path length is identical to the cell size for the inflowing SS fluxes, whilst mean local soil loss from an elementary cell can be conceptualized to occur in the middle of the cell, *i.e.* the half of the cell size is set for the local emissions (hence the factor of 0.5 in the second part of the equation above). In channel cells, flow path length is equal to cell size for the channel function. For the field function, half of the cell size is set as terrestrial flow path length (width of the riparian zone) for the inflowing fluxes assuming that the channel is

located on the cell centerline and the water surface covers negligible proportion of the cell size.

The residence time for both overland and channel flow is:

$$t^{*}_{cell,i} = \frac{FPL_{cell,i}}{v_i} \tag{A.47}$$

where $FPL_{cell,i}$ is the flow path length in cell i [m], v_i is the average flow velocity [m s^{-1}].

The average flow velocity is calculated for both overland and channel flow with the Manning´s equation (Liu and DeSmedt, 2004):

$$v = \frac{1}{n_i} \cdot HR_i^{\frac{2}{3}} \cdot S_i^{\frac{1}{2}} \tag{A.48}$$

where n_i is the Manning´s roughness coefficient at cell i [$m^{-1/3}$ s], HR_i is the average hydraulic radius at cell i [m] and S_i the slope at cell i [m m^{-1}].

The average hydraulic radius is estimated for both overland and channel flow with a power function of the upstream catchment area of the given cell (Molnar and Ramirez, 1998; Liu and DeSmedt, 2004):

$$HR_i = a_P \cdot A_{drain,i}^{b_P} \tag{A.49}$$

where $A_{drain,i}$ is the total drained area upstream of the cell i [km^2] and a_P, b_P are model parameters related to the discharge frequency [-].

The Manning´s roughness parameter vales are related to the land use classes (Fread, 1993; Liu and DeSmedt, 2004).

The outflowing flux in a channel cell is:

$$OUT_{SS,ch,i} = IN_{SS,ch,i} - RET_{SS,ch,i} \tag{A.50}$$

where $OUT_{SS,ch,i}$ is the outflowing sediment load of channel cell i [t SS a^{-1}], $IN_{SS,ch,i}$ is the inflowing sediment load of channel cell i [t SS a^{-1}], arriving from both the adjacent terrestrial

cells and the upstream channel cells, $RET_{SS,ch,i}$ is the sediment deposition at channel cell i [t SS a^{-1}].

Different deposition parameters are used for the terrestrial and in-stream transport, whereas the latter represents net deposition rate. SS fluxes via resuspension from the bottom sediment are neglected. In channel cells, sediment resuspension is neglected. SS load is the outcome of gross resuspension and gross in-stream retention and thus, an infinite number of combinations of these two processes would result in the same net retention and SS delivery. To avoid this identification problem, the model simulates net in-stream retention of SS. Thus, the sediment load can be calibrated with two adjustable parameters (field and in-stream retention parameters), which should be adapted to local conditions. The channel retention is:

$$RET_{SS,ch,i} = IN^{f}_{SS,ch,i} \cdot \left[1 - exp\left(-k_{SS,f} \cdot t^{*f}_{cell,ch,i}\right)\right] + IN^{ch}_{SS,ch,i} \cdot \left[1 - exp\left(-k_{SS,ch} \cdot t^{*ch}_{cell,ch,i}\right)\right] \qquad \text{(A.51)}$$

where $IN^{f}_{SS,ch,i}$ is the inflowing sediment load of channel cell i from the adjacent terrestrial cells [t SS a^{-1}], $IN^{ch}_{SS,ch,i}$ is the inflowing sediment load of channel cell i from the upstream channel cell [t SS a^{-1}], $t^{*f}_{cell,ch,i}$ is the residence time of overland flow at channel cell i [s], $k_{SS,ch}$ is the sediment channel deposition rate [s^{-1}], $t^{*ch}_{cell,ch,i}$ is the residence time of channel flow at channel cell i [s].

Reservoirs are considered for the channel transport as well (using the latter equation), whereas reservoir residence time is calculated from the outflowing discharge and the operation volume.

The residence time in lake or reservoir cells is:

$$t^{*}_{res,i} = \frac{V_i}{OUT_{Q,i}} \qquad \text{(A.52)}$$

where $t^{*}_{res,i}$ is the residence time of the reservoir assigned to the cell i [s], V_i is the operation volume of the of the reservoir assigned to the cell i [m^3].

A.6 DP transport

DP transport is simply calculated by accumulation of the DP emissions. The recent version considers retention for DP during the channel transport only.

The outflowing surface flux in a field cell is (subsurface emissions are routed in the channel only):

$$OUT_{DP,f,i} = IN_{DP,f,i} + E_{SR,i} + E_{SR,urb,i} \tag{A.53}$$

where $OUT_{DP,f,i}$ is the outflowing DP load of field cell i [kg P a^{-1}], $IN_{DP,f,i}$ is the inflowing DP load of field cell i [kg P a^{-1}].

The outflowing flux in a channel cell is:

$$OUT_{DP,ch.,i} = IN_{DP,ch,i} + \sum_{j=1}^{n_i} E_{RCH,upstr,j} + E_{PS,DP,i} - RET_{DP,ch,i} \tag{A.54}$$

where $OUT_{DP,ch,i}$ is the outflowing DP load of channel cell i [kg P a^{-1}], $IN_{DP,ch,i}$ is the inflowing DP load of channel cell i [kg P a^{-1}], arriving from both the adjacent terrestrial cells and the upstream channel cells, $E_{RCH,upstr,j}$ is the emission via recharge at the upstream field cell j [kg P a^{-1}], $E_{PS,DP,i}$ is the DP emission from point sources at channel cell i [kg P a^{-1}], $RET_{DP,ch,i}$ is the DP retention at channel cell i [kg P a^{-1}].

Point emissions of DP are introduced into the water (channel cells) according to information on the location of waste water treatment plants, industrial discharges and large livestock farms. Kinetics of organic P decomposition and P adsorption are neglected.

DP is subject to uptake by phytoplankton and in-stream retention. Retention mechanisms may include adsorption and biotic uptake in the bottom deposits. An overall rate of DP loss is used that is assumed to be constant along the channel.

The channel retention for DP is:

$$RET_{DP,ch,i} = IN^{ch}_{DP,ch,i} \cdot \left[1 - exp\left(-k_{DP,ch} \cdot t^{*ch}_{cell,ch,i}\right)\right] \tag{A.55}$$

where $IN^{ch}_{DP,ch,i}$ is the inflowing DP load of channel cell i from the upstream channel cell [t SS a^{-1}], $k_{DP,ch}$ is the DP channel retention rate [s^{-1}].

The DP retention of the reservoirs is:

$$RET_{DP,res,i} = IN^{ch}_{DP,ch,i} \cdot \left[1 - exp\left(-k_{DP,res} \cdot t^{*}_{res,i}\right)\right] \tag{A.56}$$

where $RET_{DP,res,i}$ is the PP retention in the reservoir assigned to cell i [kg P a^{-1}], $k_{DP,res}$ is the DP retention factor in the reservoirs [-].

A.7 PP transport

The PP transport is described similarly to that of the SS substituting the gross soil loss with the PP emission. Retention parameters applied for the SS transport are utilized without any change. The single but remarkable difference is the introduction of the enrichment ratio during the overland transport. The overall enrichment factor is the ratio of the PP concentration of the suspended sediment to that of the parent soil. This enrichment is a consequence of the selective sediment transport, *i.e.* the fine particles have higher proportion in the SS than that of the coarse ones. Since fine particles usually have high adsorption capacity (specific surface), the selective transport is accompanied with an enrichment of the P. PhosFate considers two enrichment factors. The local factor related to the soil clay content caused by the erosion (Eq. (A.38)) considers the selective particle detachment. An additional overland transport-related factor is defined as well to consider the selective transport of the fine particles due to their slower settling compared to that of the coarser ones. No further enrichment is assumed in the channel. Since in the recent version, there is no direct transformation between the dissolved and particulate phases after separating them in the topsoil, these processes are indirectly aggregated into the enrichment parameters as well.

The mass balance for PP is:

$$OUT_{PP,i} = IN_{PP,f,i} + E_{ER,i} - RET_{PP,f,i} \tag{A.57}$$

where $OUT_{PP,f,i}$ is the outflowing PP load of field cell i [kg P a^{-1}], $IN_{PP,f,i}$ is the inflowing PP load of field cell i [kg P a^{-1}], $RET_{PP,f,i}$ is the PP deposition at field cell i [kg P a^{-1}].

PP point source emissions are similarly defined than that of DP. Decomposition of the organic pool is not modeled.

The PP field retention is the following:

$$RET_{PP,f,i} = IN_{PP,f,i} \cdot \left[1 - exp\left(-\frac{k_{SS,f}}{k_{enr,f}} \cdot t^{*}_{cell,f,i}\right)\right] + E_{ER,i} \cdot \left[1 - exp\left(-\frac{k_{SS,f}}{k_{enr,f}} \cdot t^{*}_{cell,f,i} \cdot 0.5\right)\right] \quad (A.58)$$

where $k_{enr,f}$ is the PP enrichment factor related to the overland transport [-].

The outflowing PP flux in a channel cell is:

$$OUT_{PP,ch,i} = IN_{PP,ch,i} + E_{PS,PP,i} - RET_{PP,ch,i} \quad (A.59)$$

where $OUT_{PP,ch,i}$ is the outflowing PP load of channel cell i [kg P a^{-1}], $IN_{PP,ch,i}$ is the inflowing PP load of channel cell i [kg P a^{-1}], arriving from both the adjacent terrestrial cells and the upstream channel cells, $E_{PS,PP,i}$ is the PP emission from point sources at channel cell i [kg P a^{-1}], $RET_{PP,ch,i}$ is the PP deposition at channel cell i [kg P a^{-1}].

The channel retention for PP is:

$$RET_{PP,ch,i} = IN^{f}_{PP,ch,i} \cdot \left[1 - exp\left(-\frac{k_{SS,f}}{k_{enr,f}} \cdot t^{*f}_{cell,ch,i}\right)\right] + IN^{ch}_{PP,ch,i} \cdot \left[1 - exp\left(-k_{SS,ch} \cdot t^{*ch}_{cell,ch,i}\right)\right] \quad (A.60)$$

where $IN^{f}_{PP,ch,i}$ is the inflowing PP load of channel cell i from the adjacent terrestrial cells [t P a^{-1}], $IN^{ch}_{PP,ch,i}$ is the inflowing PP load of channel cell i from the upstream channel cell [t P a^{-1}].

PP retention of the reservoirs is approximated with the Vollenweider model (Vollenweider and Kerekes, 1982):

$$RET_{PP,res,i} = IN^{f}_{PP,ch,i} \cdot \left[1 - exp\left(-\frac{k_{SS,f}}{k_{enr,f}} \cdot t^{*f}_{cell,ch,i}\right)\right] + IN^{ch}_{PP,ch,i} \cdot \left(1 - \frac{1}{1 + k_{PP,res,i} \cdot \sqrt{\frac{t^{*}_{res,i}}{86400 \cdot 365}}}\right) \quad (A.61)$$

where $RET_{PP,res,i}$ is the PP retention in the reservoir assigned to cell i [kg P a^{-1}], $k_{PP,res}$ is the PP retention factor in the reservoirs [-].

Appendix B: Authorship

Chapter 2 of this Thesis is based on the publication "Estimation of diffuse phosphorus emissions at small catchment scale by GIS-based pollution potential analysis" by Ádám Kovács and Márk Honti, Desalination 226 (2008), 72-80.

The contribution of Ádám Kovács to this paper was:

- concept and method development (potential analysis);
- data preparation in GIS;
- model simulations and evaluation of the results;
- paper writing.

Chapter 3 of this Thesis is based on the publication "Design of best management practice applications for diffuse phosphorus pollution using interactive GIS" by Ádám Kovács, Márk Honti and Adrienne Clement, Water Science and Technology 57(11) 2008, 1727–1733.

The contribution of Ádám Kovács to this paper was:

- concept and model development (PhosFate model);
- data preparation in GIS, scenario development (BMP options);
- model simulations and evaluation of the results;
- paper writing.

Chapter 4 of this Thesis is based on the publication "Detection of hot spots of soil erosion and reservoir siltation in ungauged Mediterranean catchments" by Ádám Kovács, Bence Fülöp and Márk Honti, Energy Procedia 18 2012, 934–943.

The contribution of Ádám Kovács to this paper was:

- concept formulation and model development (optimization algorithm);
- data preparation in GIS, scenario development (BMP options);
- model simulations and evaluation of the results;
- paper writing.

Chapter 5 of this Thesis is based on the publication "Identification of phosphorus emission hotspots in agricultural catchments" by Ádám Kovács, Márk Honti, Matthias Zessner, Alexander Eder, Adrienne Clement and Günter Blöschl, Science of the Total Environment 433 (2012) 74–88.

The contribution of Ádám Kovács to this paper was:

- concept development and model improvement (PhosFate model);
- data preparation in GIS;
- model simulations and evaluation of the results;
- paper writing.

Chapter 6 of this Thesis is based on the publication "From the regional towards the local scale: a coupled modeling approach to manage phosphorus emissions into surface water bodies of Upper-Austria" by Ádám Kovács, Gemma Carr, Simon Thaler, Márk Honti, Adrienne Clement and Matthias Zessner, submitted to Journal of Environmental Management.

The contribution of Ádám Kovács to this paper was:

- concept development and model improvement (PhosFate model, optimization algorithm);
- data preparation in GIS, scenario development (targeting and optimization options);
- model simulations and evaluation of the results;
- paper writing.